ESA Climate Change Initiative

Aerosol_cci+

PRODUCT VALIDATION AND INTERCOMPARISON REPORT

Version 1.2

Document reference: Aerosol_cci+_PVIR_v1.2.doc

DOCUMENT STATUS SHEET

	FUNCTION	NAME	DATE	SIGNATURE
contributing authors	Editors	T. Popp	10.03.2020	
Evalaution team	Contributing authors	L. Sogacheva T. Popp	15.07.2020	
reviewed by	Science leader	T. Popp	28.07.2020 28.08.2020	
approved by	Technical officer (ESA)	S. Pinnock		
issued by	Project manager	T. Popp		

EXECUTIVE SUMMARY

This document evaluates the first set of test datasets within the ESA Climate Change Initiative extensions project Aerosol_cci+. The test datasets have been developed and processed by Swansea university with their mature algorithm and cover all four sensors from the dual view sensor line: ATSR-2 (1998), AATSR (2008), SLSTR onboard Sentinel3-A and Sentinel3-B (2019). For each sensor the contractual coverage of the initial dataset is for four months in all seasons (March, June, September, December).

The evaluations are first done with level2 10x10km orbit projection datasets for the main variable Aerosol Optical Depth (AOD) and the Fine Mode AOD (FM-AOD. Reference data-sets are from the AERONET sun photometer network which measure AOD with a typical uncertainty of 0.01 (Eck, et al., 1999). Secondly, inter-comparisons to other satellite aerosol datasets are made (MODIS, MISR, POLDER) which constitute the "state of the art" for satellite retrievals, but are not the independent truth since those other satellite retrievals do also have their own uncertainties.

The differences for AOD to AERONET show good agreement for ATSR-2 and AATSR but larger noise and a significant positive bias for both SLSTR. More detailed analysis for different stations / regions and differentiating between low (<0.2) and high (>0.2) AOD ranges reveal detailed issues which should be targeted by further algorithm improvements. For Fine Mode AOD an additional positive bias for all sensors can be observed, with similar geographical patterns as for AOD.

The comparisons to other satellites reveal that in year 2008 the AOD difference between AATSR and GRASP over land, ocean and globally, is within the accepted difference (estimated by the total uncertainty based on uncorrelated GCOS accuracy requirements for both datasets). AATSR AOD is higher than MISR AOD over land and lower than MODIS AOD over ocean; both differences are slightly above the accepted difference. Differences between AATSR and MISR over ocean and AATSR and MODIS over land are within the accepted difference. Regional analysis shows a considerable difference between the products.
Positive offsets between S3 (S3A and S3B) and MODIS/MISR AOD products are observed in 2019 over land. Over ocean, the difference between S3 and MODIS and MISR is, with only few exceptions, within the accepted difference. Globally, differences between S3A and MODIS and MISR are within the accepted difference. The difference between S3B and MODIS is within the accepted difference, while the difference with MISR is slightly higher. Regional analysis shows a considerable difference between the products also in year 2019. Differences between S3A and S3B AOD are within the accepted value, with one exception in March for the Atlantic region influenced by the Saharan dust transport.

In addition to the validation of AOD and FM-AOD, this report also does a thorough validation of the pixel-level uncertainties provided for AOD within the product files. This is done by comparing them statistically to estimates of the true error represented by the differences of retrieved AOD to AERONET AOD. This means that such an assessment can only cover the conditions contained in the AERONET measurements, i.e. cloud-filtered observations

measured at land, shore and few island stations with significant gaps in some remote regions and the Southern hemisphere.

In the next iteration of this validation and inter-comparison report, a new updated version of all datasets will be assessed together with a second dataset from another retrieval algorithm (CISAR by Rayference) which relies in parts on different mathematical concepts. Furthermore, also ship cruise reference data over oceans from the MAN database will be used and inter-comparisons to daily datasets from MODIS, MISR and POLDER are planned.

This report starts with definitions (sec. 1), a brief overview of the reference data (sec. 2) and the test data to be evaluated (sec. 3) before summarizing results of the level2 validation (sec. 4), the prognostic uncertainty validation (sec. 5) and the inter-comparisons to other satellite AOD data (sec. 6). It concludes with a summary of findings (sec. 7), references (sec. 8) and detailed listings of station statistics (Annex).

Document change record

Issue	Date	Modified Items / Reason for Change
0.9	10.03.2020	issue of the template
1.0	15.07.2020	Contributions by evaluation partners
1.1	28.07.2020	Review by science lead, final layout and editing
1.2	28.08.2020	Correction of minor RIDs raised by ESA Further elaboration of quantitative agreement between different satellite datasets in section 6

LIST OF TABLES

LIST OF FIGURES

TABLE OF CONTENTS

1 DEFINITIONS AND ABBREVIATIONS

This section summarizes the major definitions relevant for the validation report.

AAOD (Absorption Aerosol Optical Depth) is the vertically normalized atmospheric column integrated aerosol absorption at a certain wavelength (usually at 550 nm, the reference wavelength in global modelling) [note, AAOD = AOD*(1-SSA)]

AERONET represents a federated network of globally distributed ground-based CIMEL sun-/sky-photometers, which is maintained (calibration facility, data processing and aerosol and water vapor products access) by NASA (National Aeronautics and Space Administration) and PHOTONS (PHOtométrie pour le Traitement Opérationnel de Normalisation Satellitaire)

ANG (Ångström exponent), a parameter which describes the logarithmic wavelength dependence of AOD. It can be interpreted as a measure of the aerosol particle size for mono-modal aerosol size distributions (AND~0 means large; ANG~2 means small particles)

AOD (Aerosol Optical Depth) is the vertically normalized atmospheric column integrated aerosol extinction at a certain wavelength or waveband (usually at 550nm, the reference wavelength in modelling). AOD is also often referred to as Aerosol Optical Thickness (AOT).

AODdu (Dust Aerosol Optical Depth) is the component of total AOD due to dust particles.

AODf of **FM-AOD** (Fine Mode Aerosol Optical Depth) is the component of total AOD due to fine particles (usually with radius < 0.5 µm).

AODc (Coarse Mode Aerosol Optical Depth) is the component of total AOD due to coarse particles (usually with radius < 0.5 µm).
ATSR (Along Track Scanning Radiometer) was a multi-channel imaging radiometer (with dual view capabilities in the visible and near-IR solar spectrum). Two versions are used for aerosol retrieval: ATSR-2 on board of the European Space Agency's ERS-2 satellite (1995-2002) and the advanced ATSR (AATSR) on ESA's ENVISAT satellite (2002-2012).

ECV (Essential Climate Variables) are geo-physical quantities of the Earth-Atmosphere-System that are technically and economically feasible for systematic (climate) observations.

ENVISAT ("Environmental Satellite") is a now inoperative ESA polar-orbiting (ca 10am local overpass) satellite, which supplied between 2002 and 2012 atmospheric data, including for aerosol remote sensing relevant AATSR, MERIS and GOMOS sensor data.

FCDR (Fundamental Climate Data Records or simply **CDR**) represent long-term records of measurements or retrieved physical quantities from remote sensing. FCDRs require consistency across multiple platforms with respect to (1) calibration, (2) algorithms, (3) spatial and temporal resolution, (4) quantification of errors and biases and (5) data format. FCDRs also need to manifest applied ancillary data.

FMF (Fine Mode Fraction) is the fraction of the total AOD which is contributed by aerosol particles smaller than 1μm in diameter. Due to their smaller size these aerosol particles are referred to as fine-mode aerosol, in contrast to larger or coarse model aerosol particles.

GCOS (Global Climate Observing System), located at WMO in Geneve, is intended to be a long-term, user-driven operational system capable of providing the comprehensive observations required for (1) monitoring the climate system, (2) detecting and attributing climate change, (3) assessing impacts of, and supporting adaptation to, climate variability and change, (4) application to national economic development and (5) research to improve understanding, modelling and prediction of the climate system.

MAN (Marine Aerosol Network) is the ocean branch of the AERONET network, based on handheld solar attenuation measurements with calibrated MICROTOPS-II sun-photometers.

MISR (Multi-angle Imaging Spectro-Radiometer) is a multi-spectral sensor on NASA's EOS Terra platform with (9) multi-directional view capabilities.

MODIS (Moderate Resolution Imaging Spectro-Radiometer) is a multi-spectral sensor on NASA's EOS Terra and Aqua platforms.

POLDER (POLarization and Directionality of the Earth's Reflectances) is a passive optical imaging radiometer and polarimeter for studies on radiative and microphysical properties of clouds and aerosols on the French CNES PARASOL (Polarization and Anisotropy of Reflectances for Atmospheric Sciences coupled with Observations from a Lidar).

SDA (Spectral De-Convolution Algorithm), exploits AOD at several wavelengths to estiamte the fraction of fine and Coarse Mode AOD; the algorithm divides aerosols into fine and coarse mode fractions in an optical sense (O'Neill, et al., 2003). This parameter differs moderately from a sub-micron fraction which is defined according to a simple microphysical (radius) cutoff.

The **Sentinel** constellation of satellites provides Earth Observations from space as part of the joint ESA and EU Copernicus program, formerly GMES (Global Monitoring for Environment and Security)

SLSTR The SLSTR instrument on Sentinel-3 maintains the continuity with the (A)ATSR series of instruments. The design supports the basic functionality of AATSR, with the addition of a wider swath, new channels dedicated to fire and cirrus cloud detection.

SSA (Single Scattering Albedo) quantifies the likelihood of scattering during an attenuation (or 'extinction') event by an atmospheric particle of given size and shape at a certain wavelength (most important at 550 nm, the reference wavelength in global modeling). The remaining fraction, 1-SSA referred to co-single scattering albedo, quantifies the likelihood of absorption during an attenuation (or extinction) event.

2 REFERENCE DATA

AERONET/MAN offers high quality data on aerosol column properties via measurements of solar radiation at cloud-free conditions. Direct solar attenuation data provide highly accurate data of AOD at different solar wavelengths so that even a mid-visible (550nm) AOD split into super-micron size (coarse-mode) aerosol as by mineral dust and sea-salt and to sub-micron size (fine-mode) aerosol (FM-AOD) as by pollution and wildfires can be assigned. Particular informative are complementary sky-radiance samples (at more than 400 AERONET continental of island sites worldwide) which in combination with direct attenuation data provide detailed information on aerosol size (22 bin size-distributions) and on aerosol composition (refractive indices and thus SSA). While most AERONET sites have good data coverage over all seasons, the site distribution over land is highly uneven and often missing in important regions. This means that not all major global / seasonal aerosol plumes are well covered in the global validation statistics (especially for ATSR-2 / 1998 with much less stations) as can be seen in Fig. 2.1. Furthermore, it is obvious that the statistics are dominated by stations in the US and Europe and by stations with low mean AOD values (<0.2; darker blue in fig. 2.1). To address oceanic references, the MAN dataset will be added which offers data of about 200 research voyages over the last decade.

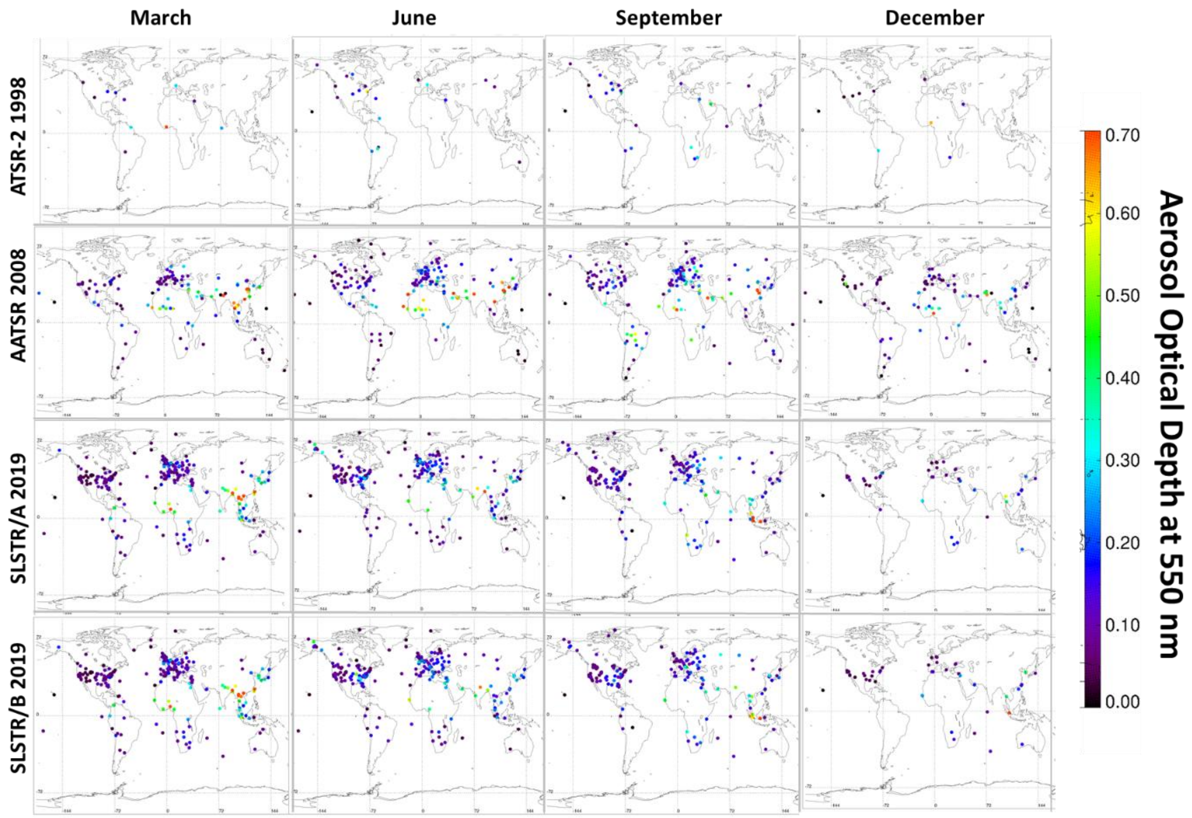

Figure 2.1 *Monthly AOD550 mean maps from AERONET matched to the 4 sensors*

MODIS is the most widely used satellite-sensor based aerosol product data-set (e.g. AOD, fire counts), (1) as global coverage (with at least two daytime overpasses) is among the best (an important element in data assimilations), (2) the retrieval (improved over two decades) has reached a higher level of maturity and (3) its retrieval data can be accessed relatively easy. As retrieval over brighter (land) surfaces remain difficult, there appears (despite of pulling information from two different [deep blue and dark target] approaches) a tendency to overestimate AOD over continents. In this study, MODIS aerosol data of the most recent collection 6.1 (combined DR&DB) processing are applied. As data for AODf in that processing are (officially) only offered over oceans, AODf estimates for MODIS over land were added based on a method by P. Ginoux were added, which also provides AODdu estimates over continents. AODc is simply defined by the difference: AOD minus AODf. Monthly (March, June, September and December) MODIS maps for years 2008 and 2019 mid-visible total AOD are presented in Figure 6.1, fine-mode AOD (AODf), coarse-mode AOD (AODc) and dust AOD (AODdu) will be analyzed in the next version of the report.

MISR offers advanced aerosol retrievals with its multi-spectral and multi-viewing capabilities. In past retrieval comparisons, the older MISR v22 AOD retrieval was a top performer over continents but displayed a strong AOD high bias over oceans. In the new MISR v32 retrieval not only pixel resolution was improved but also the ocean bias was largely removed. Still, MISR has limited spatial daily coverage and its monthly statistics (even at 1x1 degree spatial resolution) is poor compared to polar orbiting satellite sensors with a wider swath. Thus, only larger differences that are consistent over larger regions should be discussed in more detail. AODf is here represented by MISR assigned AOD to small aerosol sizes, AODc represents the MISR assigned AOD to mid and larger aerosol sizes and AODdu refers to MISR assigned AOD to non-spherical aerosol. Monthly (March, June, September and December) MISR maps for years 2008 and 2019 mid-visible total AOD are presented in Figure 6.1, fine-mode AOD (AODf), coarse-mode AOD (AODc) and dust AOD (AODdu) will be analyzed in the next version of the report.

POLDER The POLarization and Directionality of the Earth's Reflectances) is a key sensor dedicated to cloud and aerosol aboard the Parasol satellite, which flies in formation with the A-train formation including Aqua and CALIOP (afternoon daytime overpass). POLDER provides global coverage every one to two days. The retrieved aerosol products are primarily AOD and ANG over oceans. Moreover, polarization capabilities allow estimates of dust AOD over oceans and FM-AOD over continents. This instrument was operated 2005 – 2013 and can thus only be used for comparison with AATSR, not with SLSTR. Monthly (March, June, September and December) POLDER/GRASP maps for years 2008 and 2019 mid-visible total AOD are presented in Figure 6.1.

3 OVERVIEW OF TEST DATA FOR EVALUATION

The test data include 4 months global observations with 10km horizontal resolution for each of the four sensors concerned as shown in Table 3.1. Figures 3.1 – 3.3 show monthly mean maps of AOD at 550 nm, the uncertainty of AOD at 550 nm and the FM-AOD at 550 nm of the four months in each year which will be analysed. The images show similar dominant seasonal patterns (e.g. summer Atlantic desert outbreaks, autumn biomass burning events in the Southern hemisphere, Eastern Asian pollution) and some inter-annual differences. They also reveal the limitations of coverage due to low sun and underlying snow / ice (respective hemisphere winters). Particularly good agreement between the 2 SLSTR maps of the same year (last 2 rows) can be seen as well as the weaker coverage of the earliest sensor ATSR-2 (first lines). Fine-Mode AOD suppresses the large dust outbreaks well but not completely. It appears slightly larger for the 2 SLSTR datasets than for the 2 ATSR datasets. Pixel-level uncertainties show distinctly larger values for SLSTR than for ATSR-2 and AATSR in the Northern hemisphere (except the Sahara) and smaller values in the Southern hemisphere.

***Table 3.1** analysed dataset list*

label	***retrieval version***	***provider***	***period***
ATSR2 SU v4.32	ATSR-2, SU, v4.32 (corrected)	Swansea	1998: 3, 6, 9, 12
AATSR SU v4.32	AATSR, SU, v4.32	Swansea	2008: 3, 6, 9, 12
SLSTRA SU v1.11	SLSTR/S3A, SU, v1.11	Swansea	2019: 3, 6, 9, 12
SLSTRB SU v1.11	SLSTR/S3B, SU, v1.11	Swansea	2019: 3, 6, 9, 12

Note that in the SLSTR SU v1.11 products two variables have been swapped (AAOD and FM-AOD). We rectified this by reading the variable “AAOD” for evaluating FM-AOD.

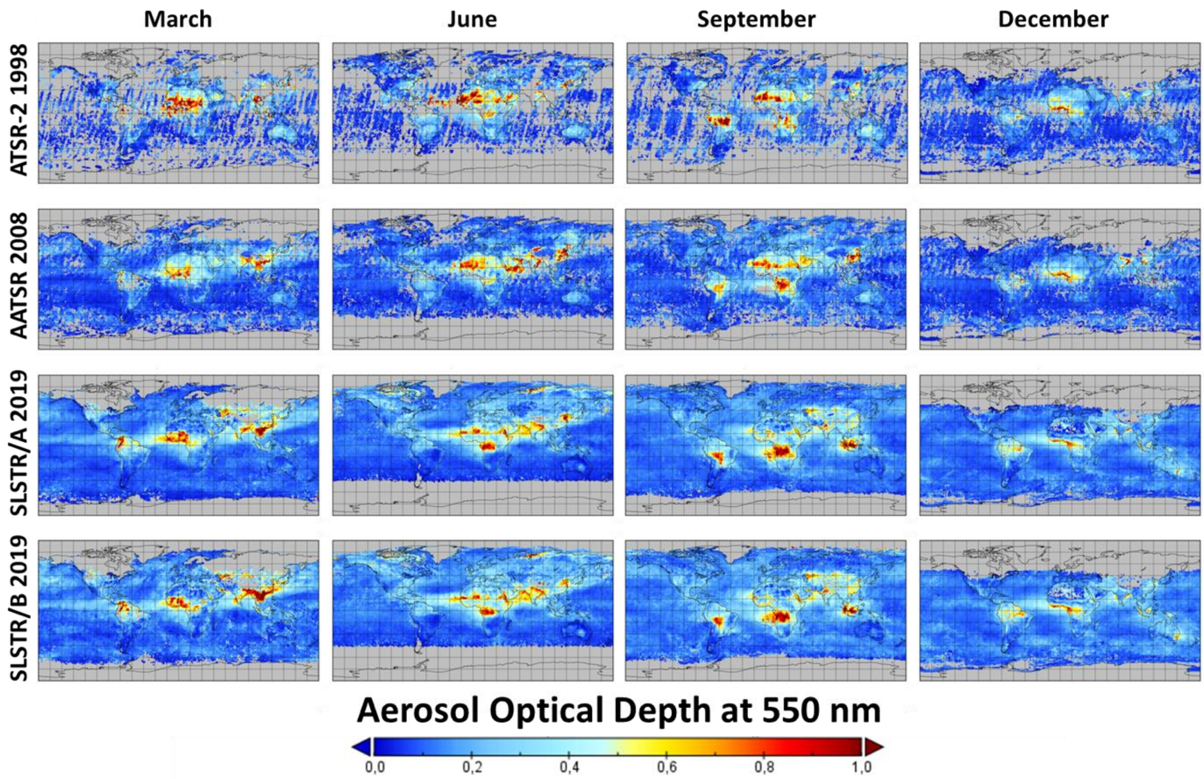

Figure 3.1 *Monthly AOD550 mean maps of the 4 sensor datasets*

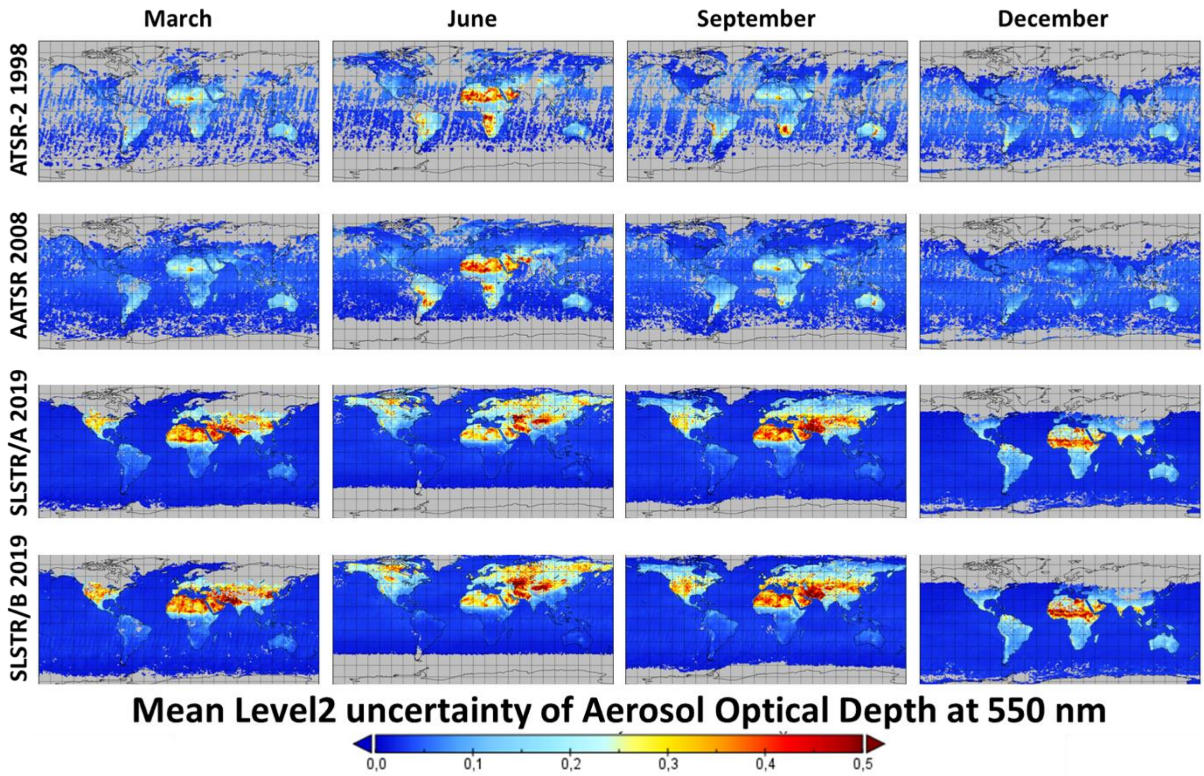

Figure 3.2 *Monthly AOD550 uncertainty mean maps of the 4 sensor datasets (L2 uncertainty mean)*

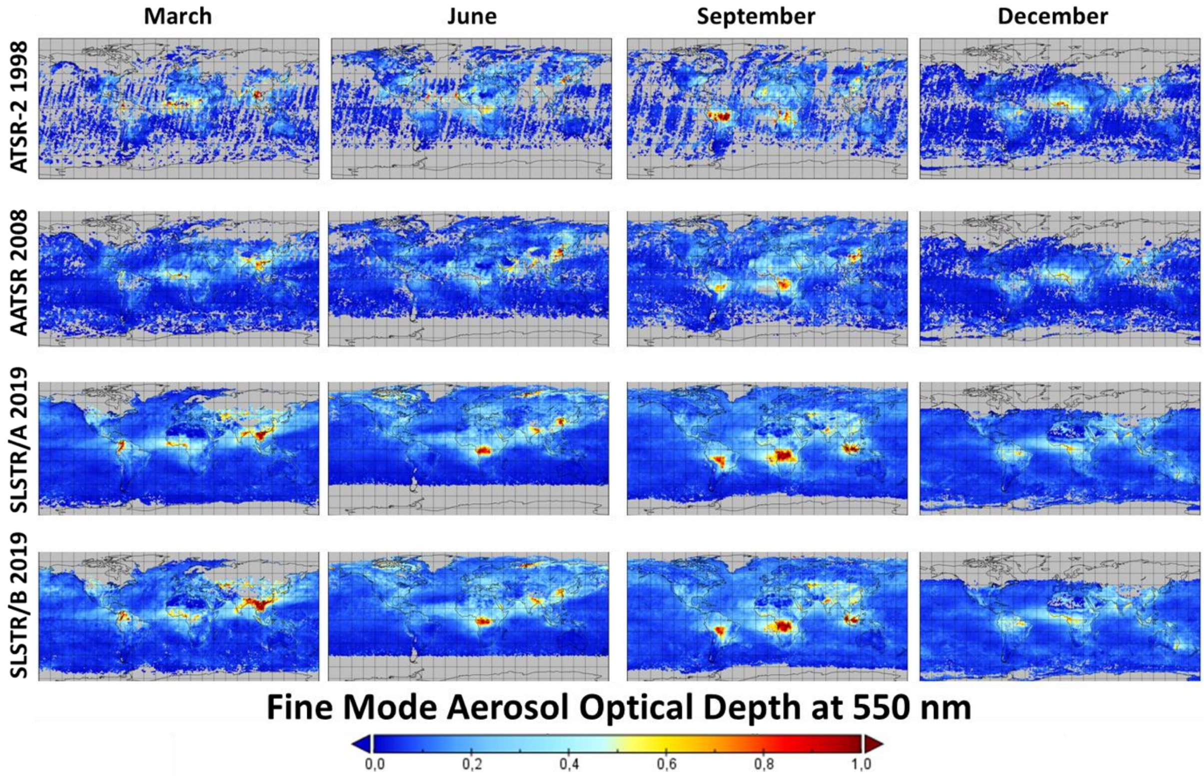

***Figure 3.3** Monthly FM-AOD550 mean maps of the 4 sensor datasets*

4 LEVEL2 EVALUATION AGAINST AERONET

4.1 Validation of AOD550

According to the standard procedure established in the community, the validation is done for the level2 datasets with 10x10 km^2 resolution in orbit projection, which are closest to the retrieval and therefore are able to provide direct insight into their quality. For each dataset version per algorithm and sensor, matching to AERONET (and future MAN) reference measurements is made within ±30 minutes and ±50km. We keep individual satellite pixels (no spatial averaging; in particular to avoid averaging the prognostic uncertainties) which are counted as “Number of sat pixel” in Table 4.1. This means that several satellite pixels may match with the same Aeronet station observation (which we count as “Number1 of stat obs”). We use the newest AERONET version 3 data with better coverage of high AOD cases. In the matching all available AERONET measurements within the time window for one day / location are averaged, while individual satellite pixels are kept to avoid changes due to averaging of the level2 values. We calculate then statistical quantities (**bias, rmse, stdv, Pearson correlation, fraction of pixels within GCOS requirement envelope**) for AOD per station and on global average for all land stations and all coastal / ocean stations. The accuracy requirement for AOD provided by GCOS is represented as a combination of absolute and relative accuracy due to the log-normal AOD distribution with many low values as **max (0.03 or 10%)**. We calculate the fraction of pixels which fall into this envelope (“**GCOS fraction**”) which should be **68%** for a normal distribution of errors. We also calculate a “Bias corrected GCOS fraction” where we subtract the mean bias from all satellite observations for testing the GCOS envelope. Furthermore, we try to iteratively fit the smallest possible envelope which contains 68% of the errors of all pixels (in steps of 0.01 and 3.3% rounded), which we name “Adapted GCOS envelope”.

All statistical quantities are presented per sensor / year separately over land and ocean in Table 4.1. Those values are furthermore presented separately per sensor / year for each station in Table A.1 in the Annex (section 9). It should be noted that the statistics for ATSR-2 (with much less stations operating in the early days of AERONET and less coverage of ATSR-2) and for some stations are of low significance when the number of matching pairs is low (all statistics) or when only low AOD values occur (correlation is of less meaning). The tables in the Annex contain the relevant station information (latitude, longitude, elevation, land / water assignment) and further statistical values (number of matching pairs, mean AOD of AERONET and Satellite, split of bias for all / low / high AOD.

Table 4.1 shows low bias for ATSR-2 and AATSR (0.01 to 0.02) over land, somewhat larger bias for ATSR-2 and AATSR over ocean (0.03 to 0.04), but consistently larger bias for both SLSTR over land and ocean (0.05 to 0.06). Standard deviations (except ATSR-2 with less matching pairs) range from 0.07 or 0.08 over ocean for all sensors to 0.11 over land for AATSR and 0.15 over land for both SLSTR. Correlation coefficients over ocean are similar for all sensors (better than 0.8) and over land range from 0.6 (ATSR-2) to 0.9 (AATSR). GCOS fractions are near 50% for ATSR-2 and

AATSR (and after bias-correction only slightly larger) and below 40% for SLSTR (after bias-correction over ocean increased to about 55%). Adapted GCOS envelopes (not bias-corrected!) range from [0.03 or 29%] for AATSR over ocean to [0.04 or 29%] for AATSR over land and [0.06 or 29%] for SLSTR over ocean and [0.09 or 23%] for SLSTR over land – altogether showing larger noise for large AOD values. In summary, both SLSTR datasets have high bias and stdv (in particular over land) with lower GCOS fractions and wider adapted GCOS envelopes.

Table 4.1 Global validation statistics for AOD at 550nm

year	sensor	alg_version	area	Number of sat pixel	number1 of stat obs	bias	rmse	stdv	Pearson corr	GCOS fraction	Corrected GCOS fraction	Adapted GCOS envelope
1998	ATSR2	SU_v4.32	land	6597	119	0.01	0.20	0.19	0.59	48.8	49.3	max(0.05 or 29%)
1998	ATSR2	SU_v4.32	ocean	1283	42	0.04	0.08	0.07	0.78	45.6	47.5	max(0.07 or 3%)
2008	AATSR	SU_v4.32	land	65636	1302	0.02	0.11	0.11	0.89	52.3	51.0	max(0.04 or 29%)
2008	AATSR	SU_v4.32	ocean	9314	296	0.03	0.12	0.11	0.84	57.0	59.7	max(0.03 or 29%)
2019	SLSTRA	SU_v1.11	land	112397	2925	0.05	0.16	0.15	0.73	35.2	34.6	max(0.09 or 23%)
2019	SLSTRA	SU_v1.11	ocean	55781	1085	0.05	0.10	0.08	0.86	40.3	55.6	max(0.06 or 29%)
2019	SLSTRB	SU_v1.11	land	92417	2300	0.05	0.15	0.15	0.68	34.3	33.7	max(0.09 or 33%)
2019	SLSTRB	SU_v1.11	ocean	44100	850	0.06	0.10	0.08	0.86	33.6	54.4	max(0.07 or 26%)

Suitable for the log-normal AOD distributions we do not calculate linear fits but show as validation summaries for each sensor / year separated over land and ocean box-whisker plots (fig. 4.1 and 4.2) and density scatter plots (Fig. 4.3 and 4.4). Both plot types show the retrieved AOD values against the AERONET reference AOD values. In Fig. 4.1. and 4.2 AOD statistical values are averaged for a suitable number of bins with approximately equal numbers (30 except for ATSR-2 with 15). For each bin the mean and the standard deviation of the AERONET and retrieval AOD values and the 5% / 95% range of the retrievals are shown as asterix, box and vertical line, respectively. With this visualisation AOD bias and spread can be seen as function of the reference AOD value. As additional information those plots also show the GCOS envelope (dashed) and an AOD frequency distribution (to see which range of AOD values will dominate the overall statistics). Furthermore, those plots also show in green boxes the uncertainty values (AERONET set to 0.01 and retrieval averaged from the pixel level uncertainty values in the data files). The plots are rather noisy for ATSR-2 and show for ATSR-2 and AATSR good agreement with some tendency to over-estimate high AOD values and to over-

estimate the lowest AOD bin. Averaged uncertainties for AATSR remain smaller than the standard deviation of AOD values while for ATSR-2 they are a bit larger. For SLSTR the plots show a significant overall bias for low AOD over land (decreasing for larger AOD) and for the whole AOD range over ocean. Averaged uncertainties are smaller than the standard deviations over ocean but clearly larger than the stdv over land and also larger than for AATSR. The density scatter plots (Fig. 4.3 and 4.4) show similar information with SLSTR bias generally higher (in particular over ocean) and also SLSTR scatter larger; for ATSR-2 the statistics are generally weak due to low numbers.
Furthermore, difference histograms over land and ocean are calculated and split for low (<0.2) and high (>0.2) AOD550 ranges per sensor / year (Fig. 4.5 and Fig. 4.6). For AATSR the stdv of high AOD values is larger than for low AOD values while the bias is equally small for all of them (ATSR-2 histograms are noisy but show similar tendencies). For SLSTR over land also stdv is larger for high AOD, but the mean bias is clearly smaller than for low AOD; over ocean a similar tendency can be seen for stdv, but the bias is equal over the whole AOD range.

The maps of mean bias and stdv per station (fig. 4.7 and fig. 4.8) show for the ATSR instruments low bias and stdv (with slightly larger values in Northern tropical latitudes for AATSR), but again a significant positive bias for both SLSTR (a bit lower in the Southern hemisphere, but with less stations) and larger stdv values in the Northern hemisphere over land / mid-latitudes. These findings point to a dependency of retrieval errors to the observing geometry which differs between ATSR and SLSTR instruments with most favourable conditions over the Northern hemisphere for ATSR and the Southern hemisphere for SLSTR.

We also investigated monthly regional bias for each sensor. Those maps are not shown, but we report here a few clear observations of exceptional behaviour (in many other cases there are only one or two stations with exceptional bias or scattered biases between neighbour stations which we do not regard sufficient). For ATSR-2 / 1998 there are too few stations to analyse seasonal and regional behaviour with 4 monhts of data. For AATSR /2008 in March and June the Sahel region has large positive bias, whereas East Asia and Middle East in March and the Atlantic off Africa and South America in June have negative bias. For both SLSTR instruments in 2019 there is a general positive bias in the Northern hemisphere and even larger positive bias in Central North America in Marhc, while negative bias occurs in South Asia and Arabia in March and in Europe in September.

We finally split the validation over the two hemispheres as we are aware of different scattering angle distributions between them. Tab. 4.2 shows the major validation statistics and indicates (but not in all metrics) that for the ATSR instruments AOD retrieval perform less accurately in the South than in the North, while the SLSTR instruments behave in the opposite direction.

Table 4.2 *Validation statistics for AOD at 550nm for Northern / Southern hemispheres*

year	sensor	Algorithm / version	area	Number of sat pixel	Number1 of stat obs	bias	stdv	Pearson corr	GCOS fraction
1998	ATSR2	SU_v4.32	land	6597 4956 1641	119 90 28	0.01 0.00 0.05	0.19 0.21 0.12	0.59 0.59 0.63	48.8 53.9 33.3
1998	ATSR2	SU_v4.32	ocean	1283 2182	42 41	0.04 0.04 -	0.07 0.07 -	0.78 0.78 -	45.6 45.6 -
2008	AATSR	SU_v4.32	land	65636 56962 8674	1302 1119 182	0.02 0.01 0.06	0.11 0.11 0.10	0.89 0.89 0.83	52.3 55.0 34.9
2008	AATSR	SU_v4.32	ocean	9314 8621 693	296 273 22	0.03 0.03 0.02	0.11 0.12 0.03	0.84 0.84 0.73	57.0 56.2 66.7
2019	SLSTRA	SU_v1.11	land	112397 94804 17593	2925 2614 310	0.05 0.05 0.04	0.15 0.14 0.20	0.73 0.77 0.59	35.2 31.3 56.0
2019	SLSTRA	SU_v1.11	ocean	55781 52525 3256	1085 1020 64	0.05 0.05 0.03	0.08 0.09 0.04	0.86 0.86 0.78	40.3 38.5 69.6
2019	SLSTRB	SU_v1.11	land	92417 78279 14138	2300 2059 240	0.05 0.06 0.04	0.15 0.14 0.19	0.68 0.71 0.60	34.3 30.8 53.5
2019	SLSTRB	SU_v1.11	ocean	44100 41478 2622	850 797 52	0.06 0.06 0.03	0.08 0.08 0.04	0.86 0.86 0.62	33.6 31.7 65.0

All North South "South validation is worse" "South validation is better"

Summary for the validation of total AOD

- High positive bias and larger scatter for SLSTR
- decreasing for bias for SLSTR with increasing AOD over land
- constant bias for SLSTR over the whole AOD range over ocean
- SLSTR uncertainties over land significantly larger
- Indication of hemispheric differences in data quality (with less stations in the South), swapped for ATSR and SLSTR

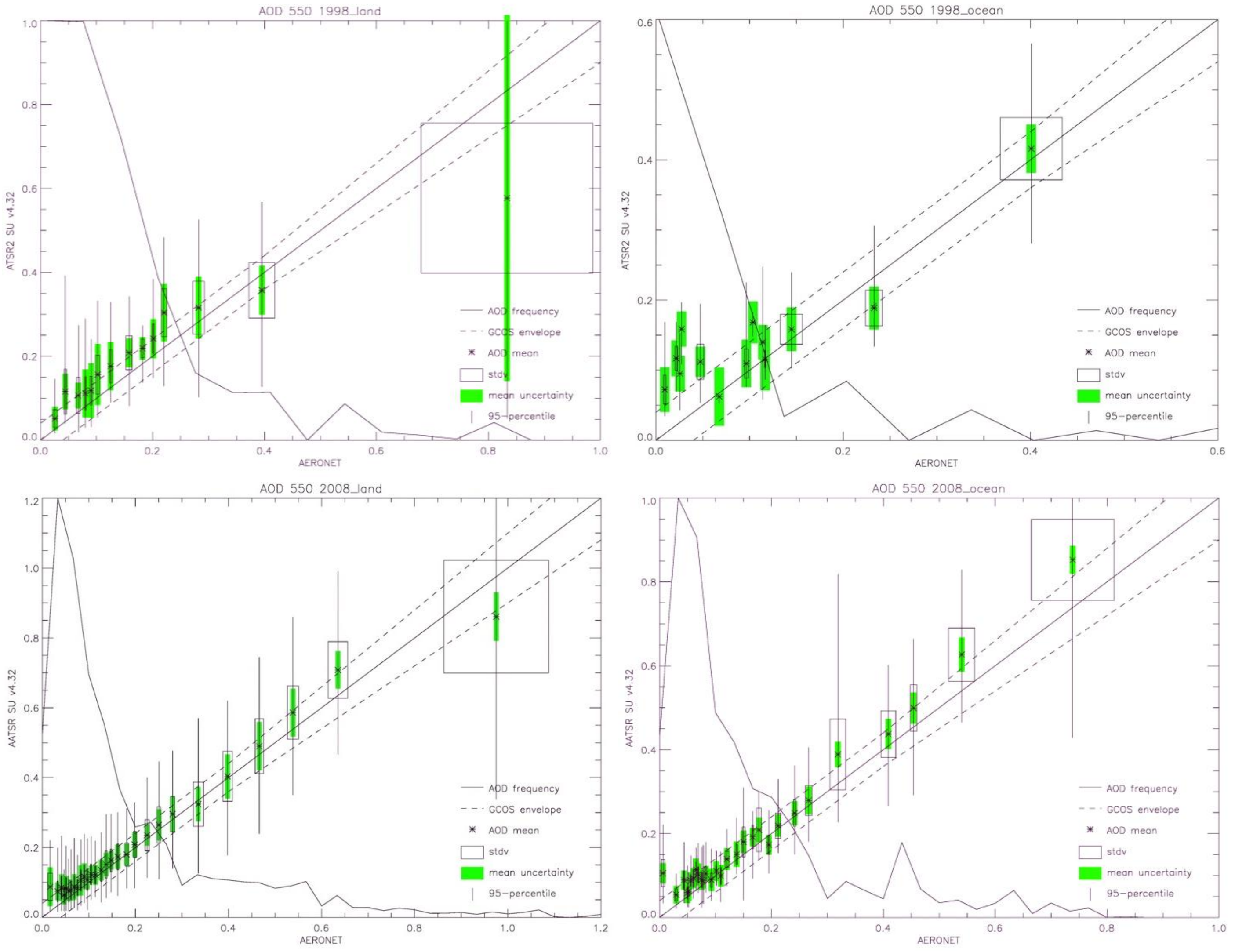

Figure 4.1 *Validation summary plots for ATSR-2 (top) and AATSR (bottom) over land (left) and ocean (right).*

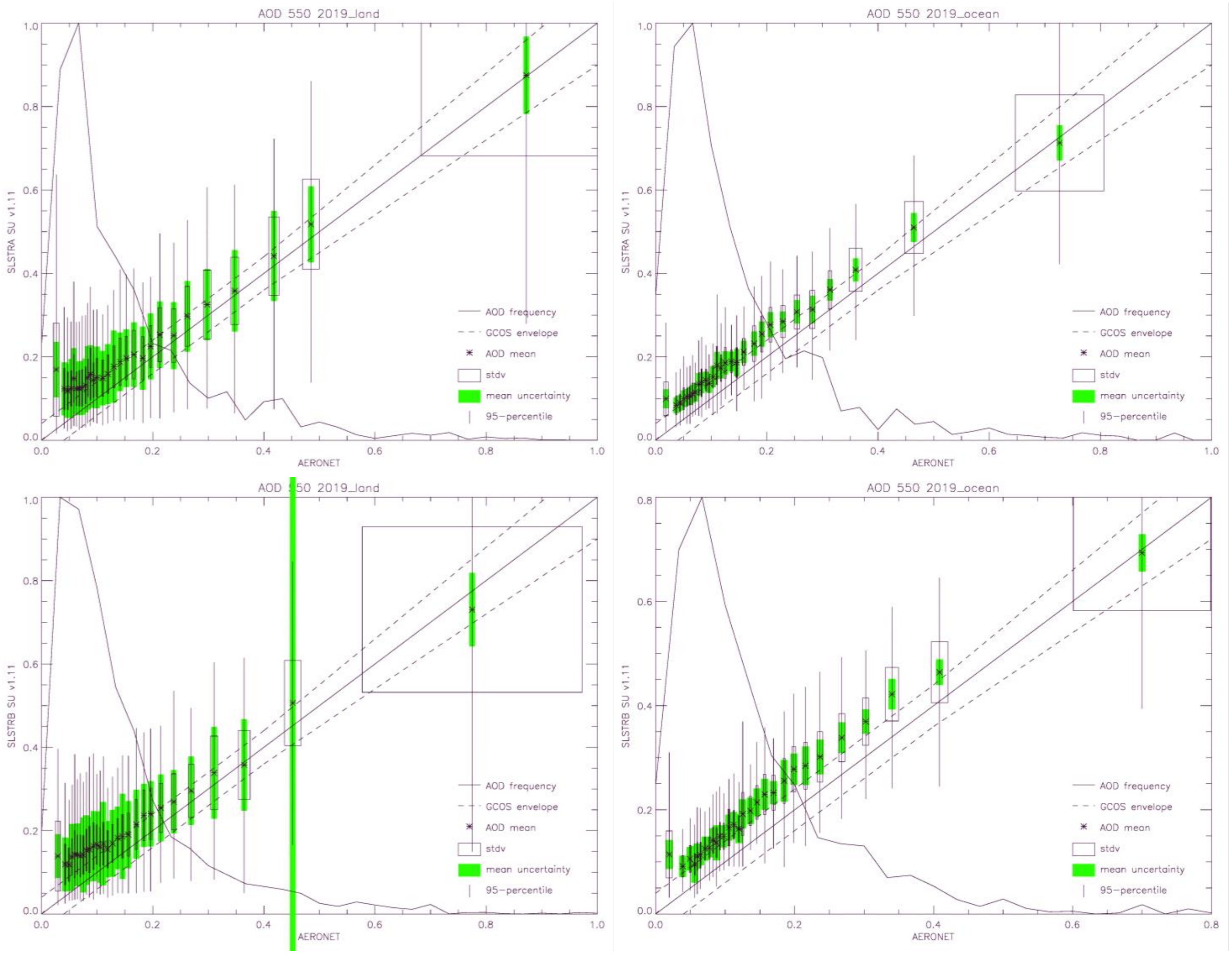

Figure 4.2 *Validation summary plots for SLSTR/3A (top) and SLSTR/3B (bottom) over land (left) and ocean (right).*

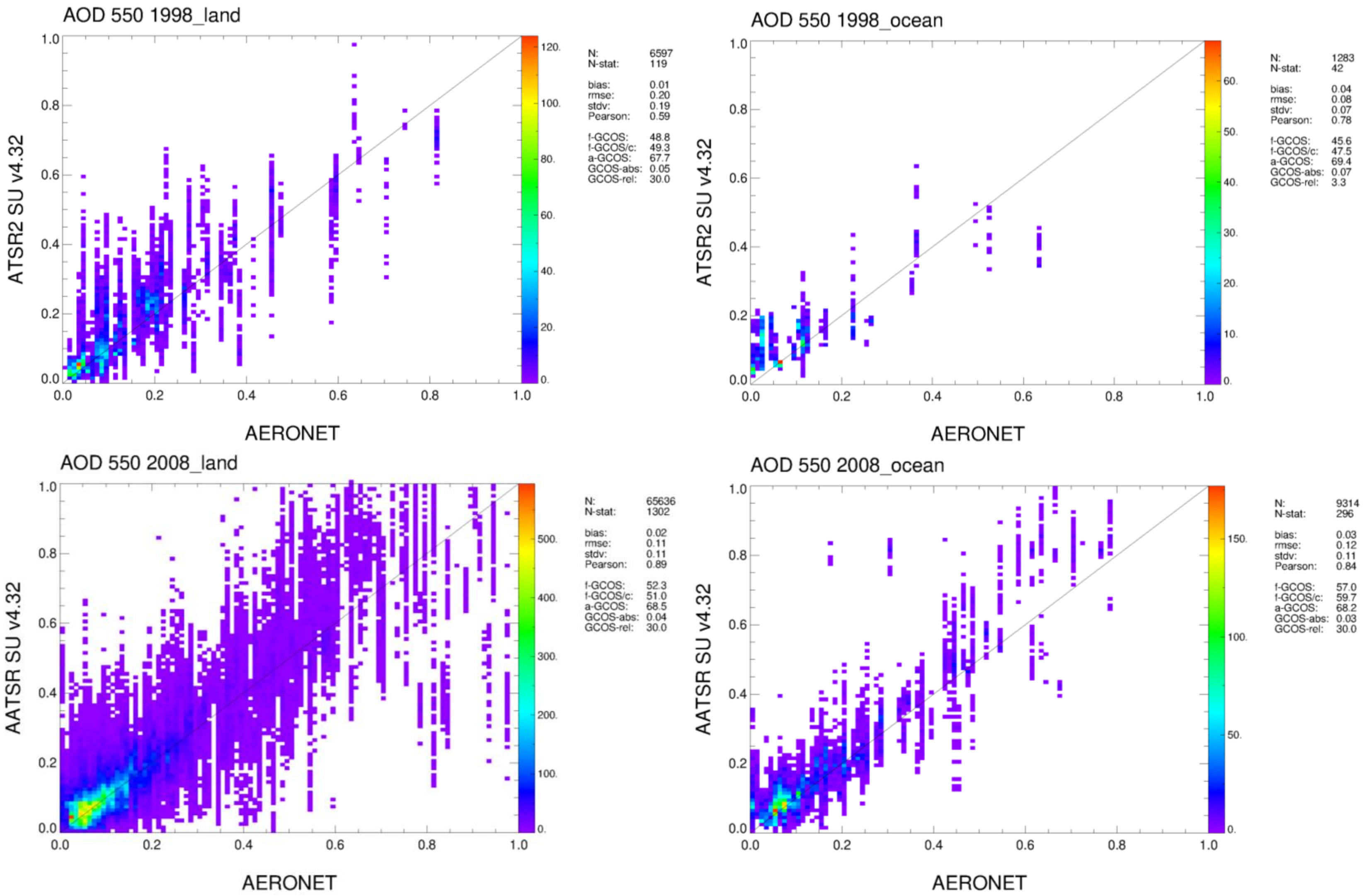

Figure 4.3 *Density scatter plots for ATSR-2 (top) and AATSR (bottom) over land (left) and ocean (right).*

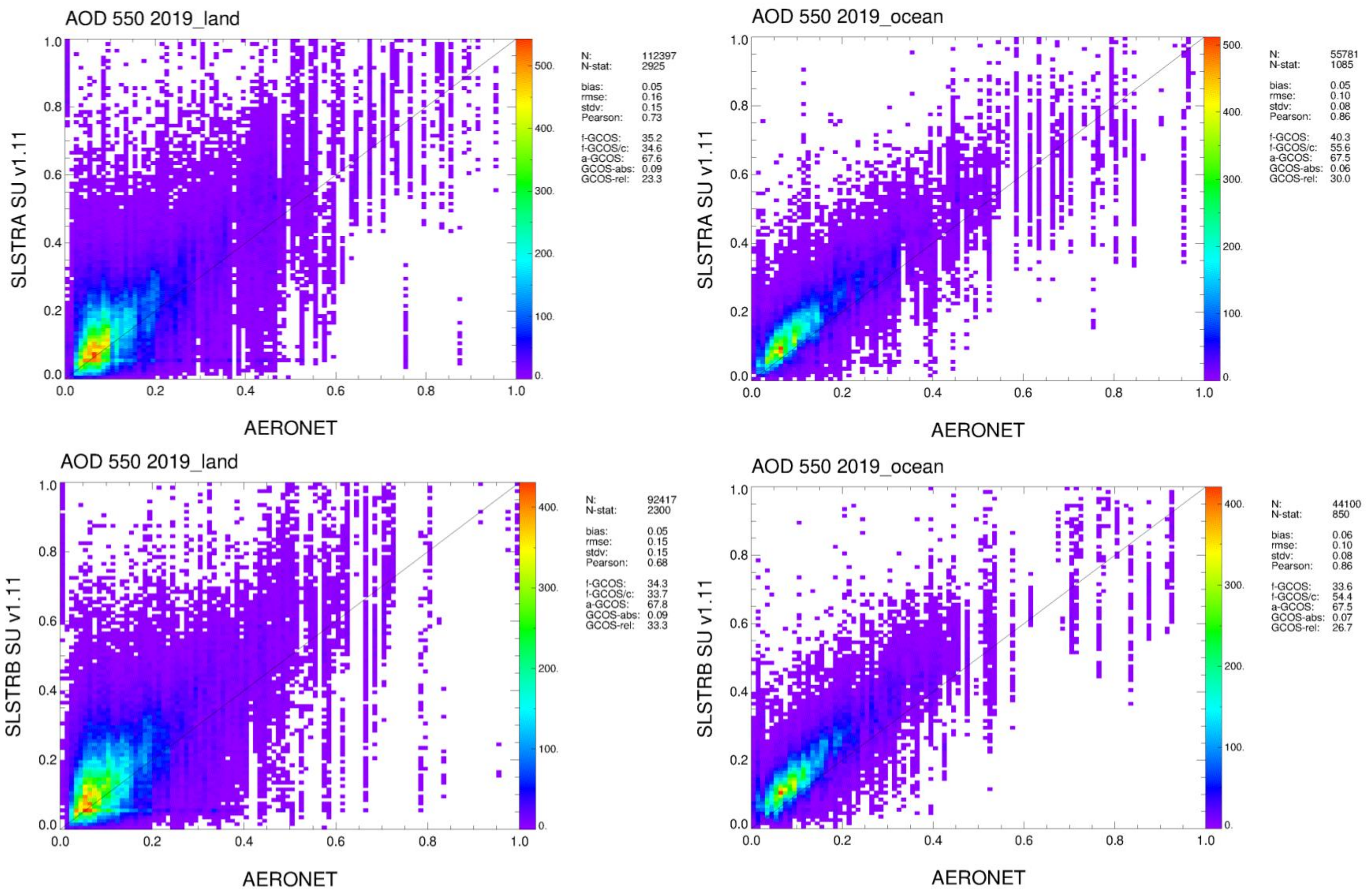

***Figure 4.4** Density scatter plots for SLSTR/3A (top) and SLSTR/3B (bottom) over land (left) and ocean (right).*

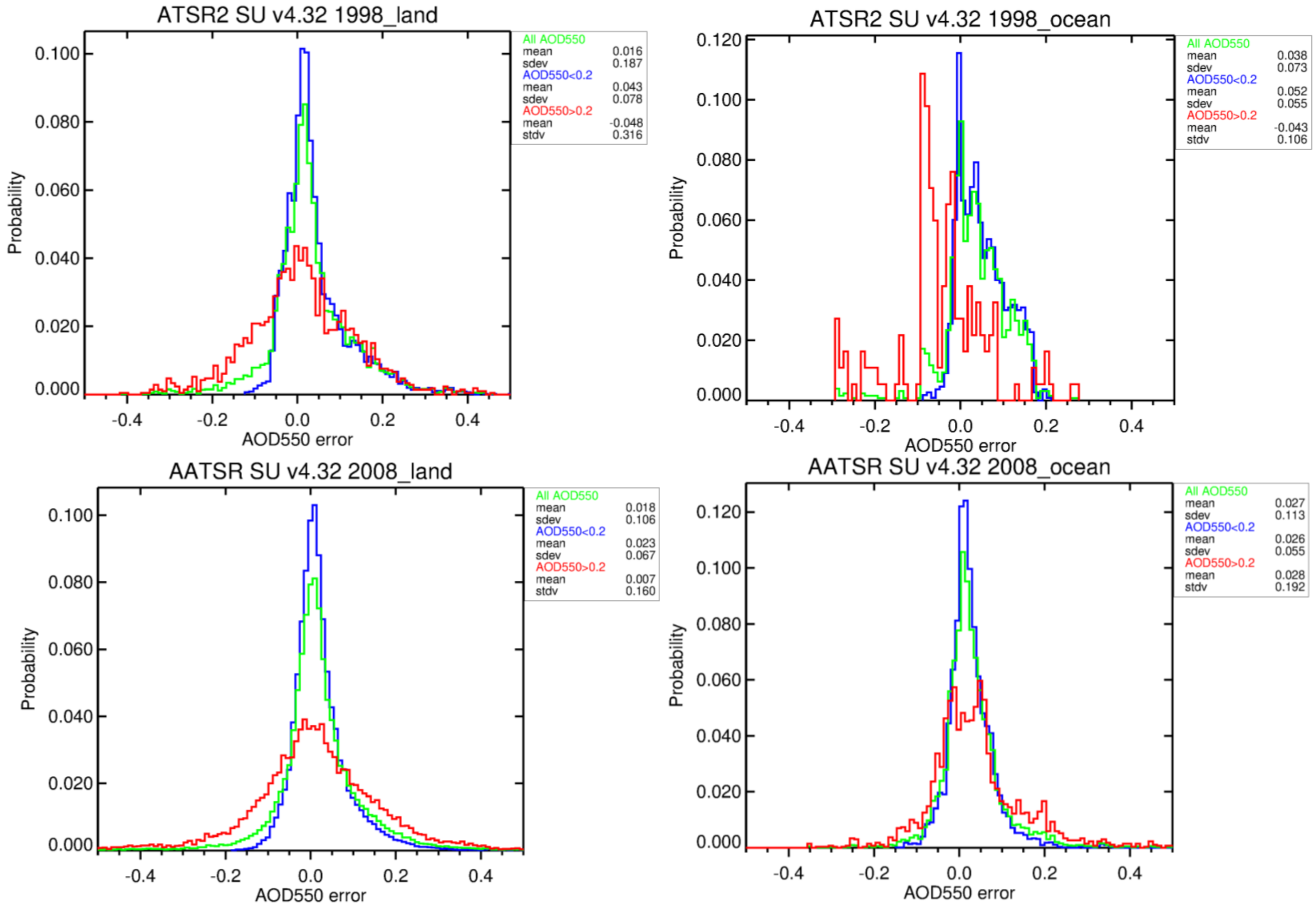

Figure 4.5 *Difference histograms for ATSR-2 (top) and AATSR (bottom) over land (left) and ocean (right).*

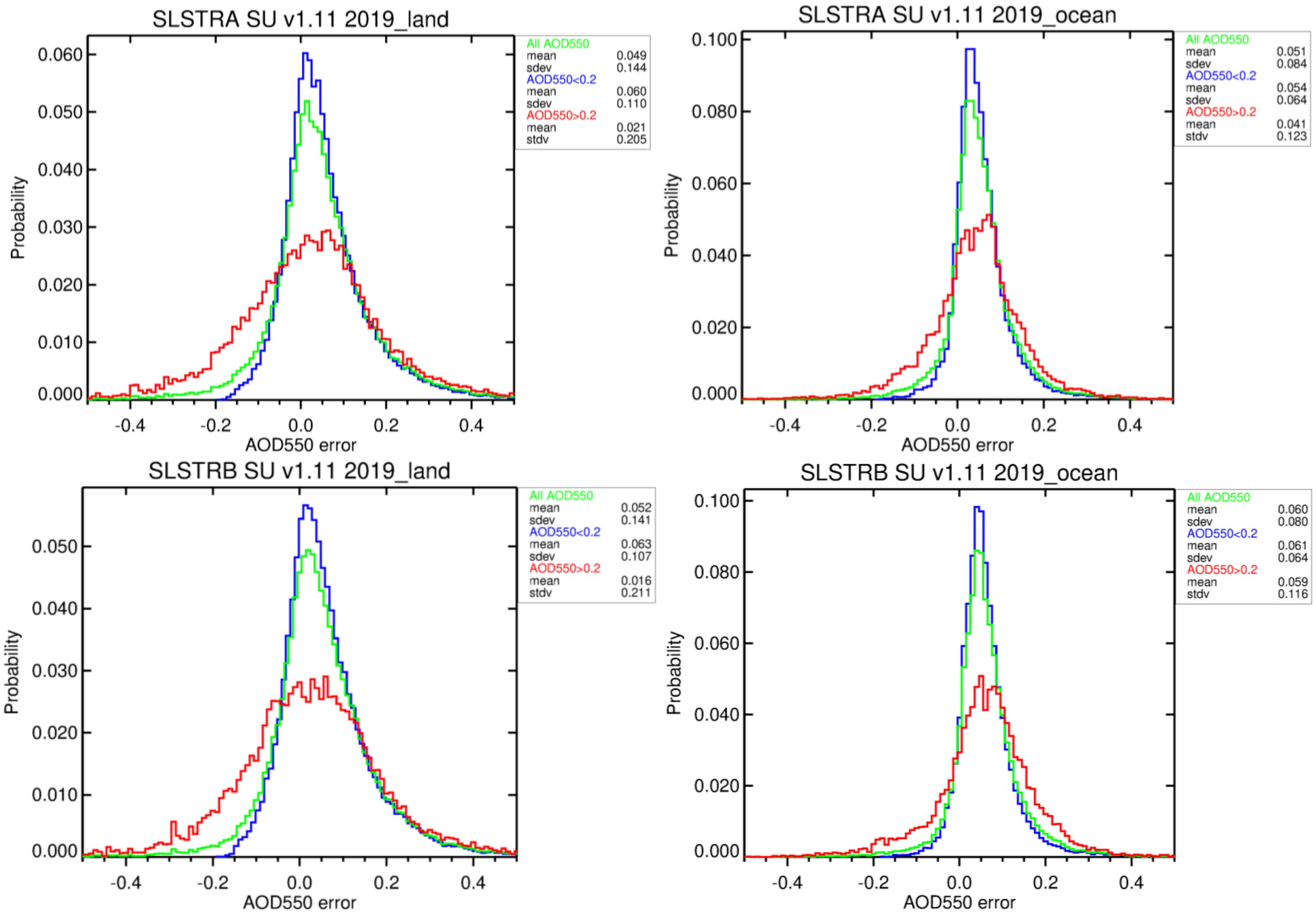

***Figure 4.6** Difference histograms for SLSTR/3A (top) and SLSTR/3B (bottom) over land (left) and ocean (right).*

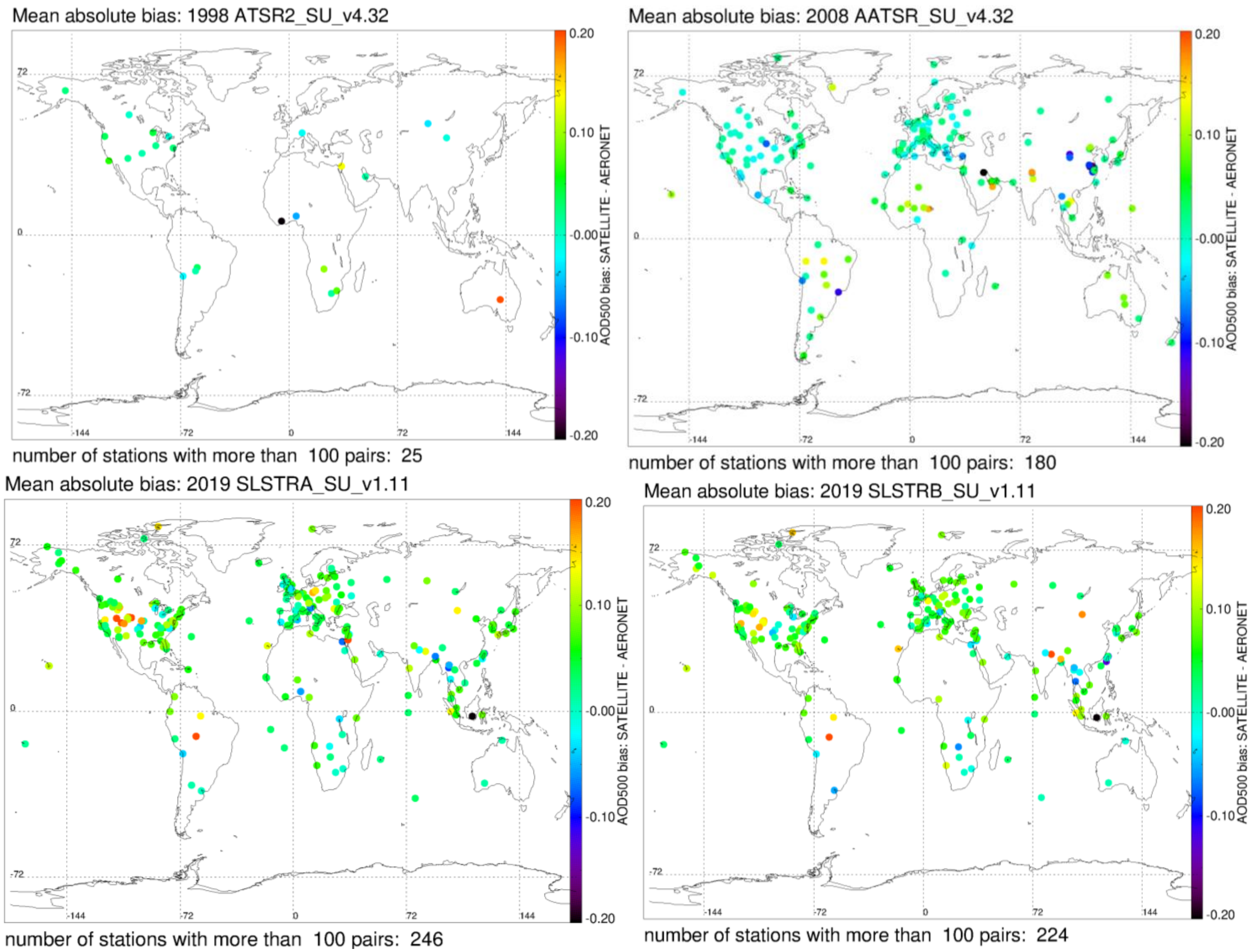

***Figure 4.7** Maps of significant station mean AOD bias (Satellite – AERONET) for all 4 sensors.*

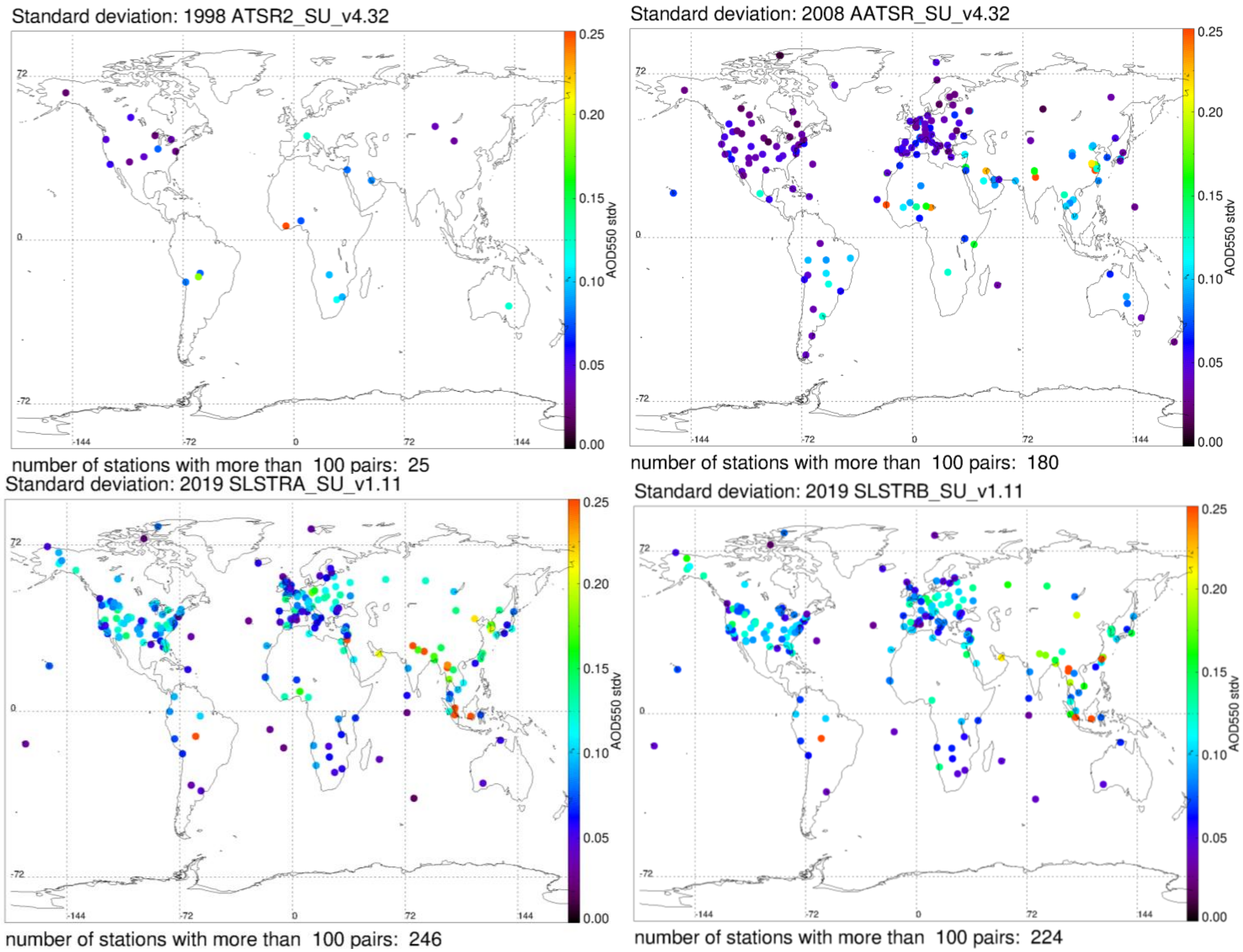

***Figure 4.8** Maps of significant station AOD stdv of Satellite and AERONET for all 4 sensors.*

4.2 Validation of FM-AOD550

The valdiation of FM_AOD at 550 nm is conducted similarly to the valdiation of total AOD. As one exception no GCOS fractions are calculated since there is no such envelope defined by GCOS for FM-AOD. Also no pixel-level uncertainties are provided. It is noteworthy that the uncertainty of FM-AOD from AERONET calculated with the SDA algorithm must also be considered larger than the one for AOD, especially for low AOD values. The analysis shown for FM-AOD contains again an overview Table (Tab 4.3), box-whisker plots (fig. 4.9 and fig. 4.10, but without uncertainties), density scatterplots (fig. 4.11 and fig. 4.12) and maps of mean bias and stdv per station (fig. 4.13 and fig. 4.14).

Table 4.3** Validation statistics for FM-AOD **at 550nm

year	sensor	alg_version	area	Number of sat pixel	number1 of stat obs	bias	rmse	stdv	Pearson corr
1998	ATSR2	SU_v4.32	land	5514	94	0.06	0.11	0.09	0.77
1998	ATSR2	SU_v4.32	ocean	1044	33	0.04	0.06	0.04	0.82
2008	AATSR	SU_v4.32	land	49679	993	0.03	0.09	0.08	0.88
2008	AATSR	SU_v4.32	ocean	7117	232	0.05	0.11	0.10	0.58
2019	SLSTRA	SU_v1.11	land	102805	2670	0.07	0.15	0.13	0.77
2019	SLSTRA	SU_v1.11	ocean	46384	932	0.07	0.12	0.09	0.79
2019	SLSTRB	SU_v1.11	land	83991	2080	0.08	0.15	0.13	0.67
2019	SLSTRB	SU_v1.11	ocean	36817	737	0.08	0.12	0.09	0.77

Overall, there is a positive bias of FM-AOD for all sensors over land and ocean (larger for SLSTR with ~0.075 than for the ATSR instruments with ~0.045), while stdv values over land are again larger for SLSTR (0.13) than for the ATSR instruments ~0.085); over ocean stdv values are similar (~0.095) except for the statistically weak ATSR analysis (0.04). Correlations range from 0.7 (SLSTR/3A) to 0.9 (AATSR) over land and are ~0.8 over ocean (except for AATSR with 0.6). Over ocean the FM-AOD bias appears to increase with increasing AOD for SLSTR. The geographical patterns follow largely those of the AOD errors (e.g. large positive bias for AATSR over the Atlantic off Africa in June and in South America, large negative bias over East and South Asia in March, September and December; for SLSTR over-estimations in Central North America in March and September, and under-estimations in March over South Asia, and in September over Eastern Asia and East Europe).

Summary for the validation of FM-AOD

- Overall positive bias for all sensors over land and ocean
- Bias and stdv over land larger for SLSTR than for the ATSR instruments with ~0.045)
- Over ocean bias appears to increase with increasing AOD for SLSTR
- Geographical patterns follow largely those of the AOD errors

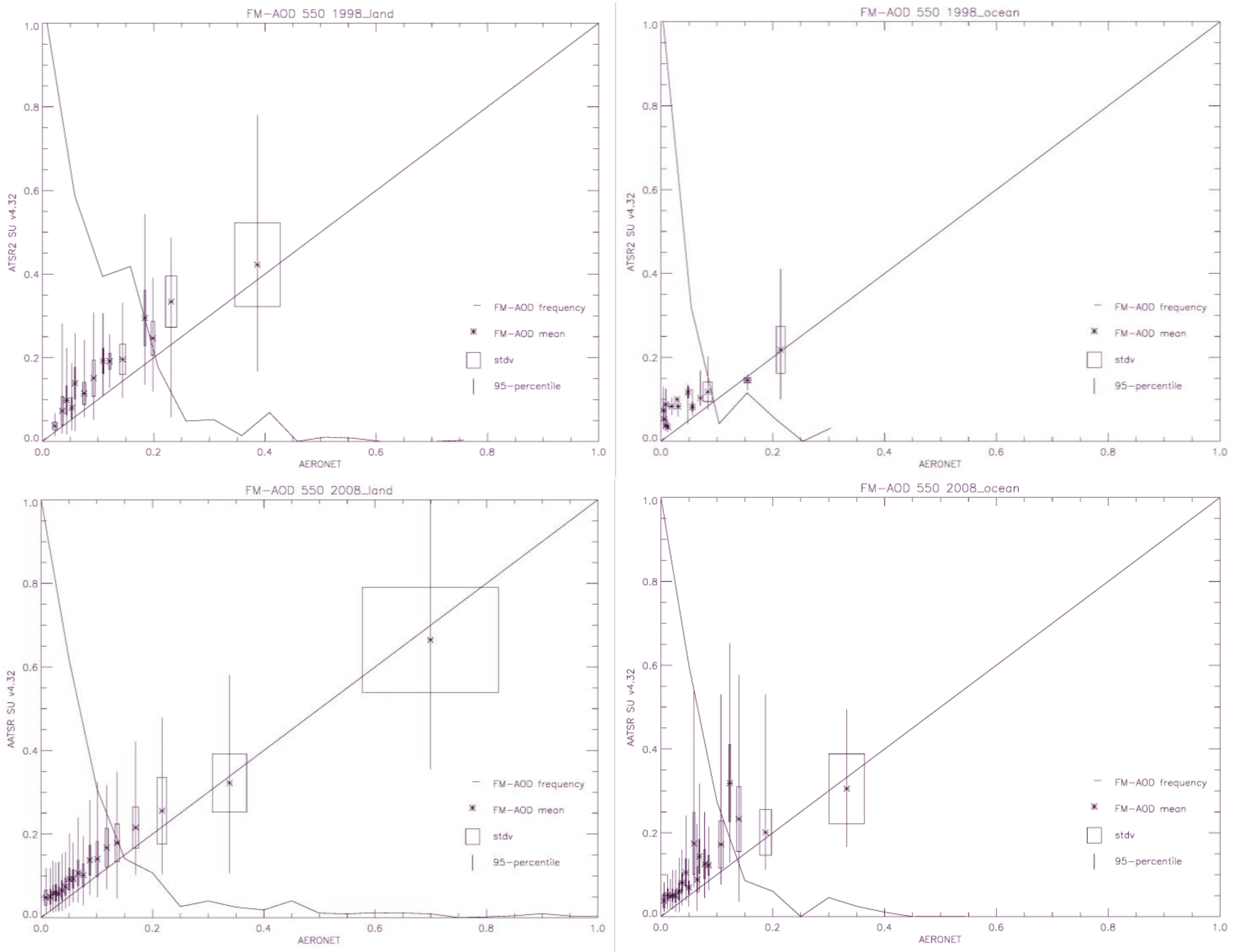

Figure 4.9 *Validation summary plots for FM-AOD of ATSR-2 (top) and AATSR (bottom) over land (left) and ocean (right).*

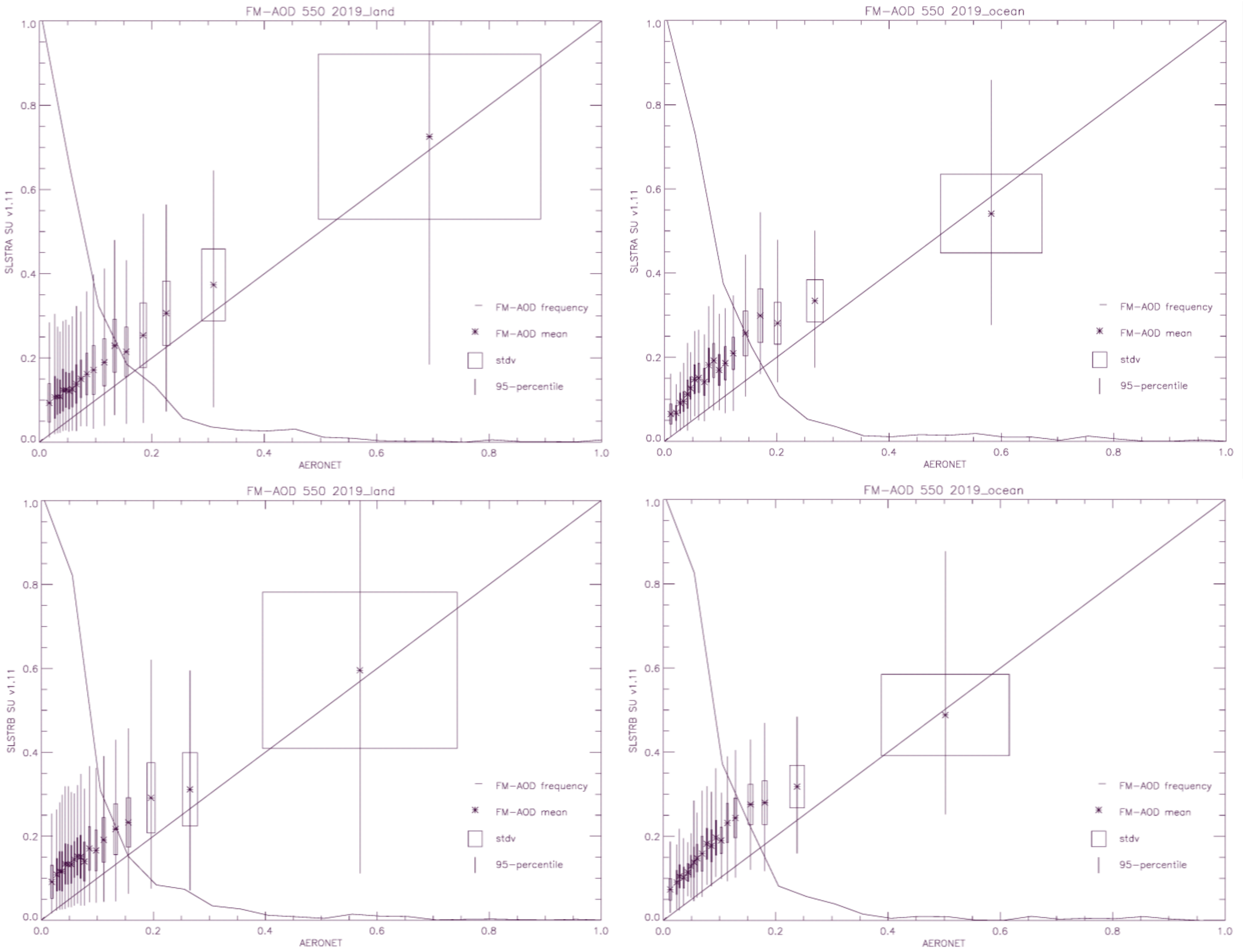

***Figure 4.10** Validation summary plots for FM-AOD of SLSTR/3A (top) and SLSTR/3B (bottom) over land (left) and ocean (right).*

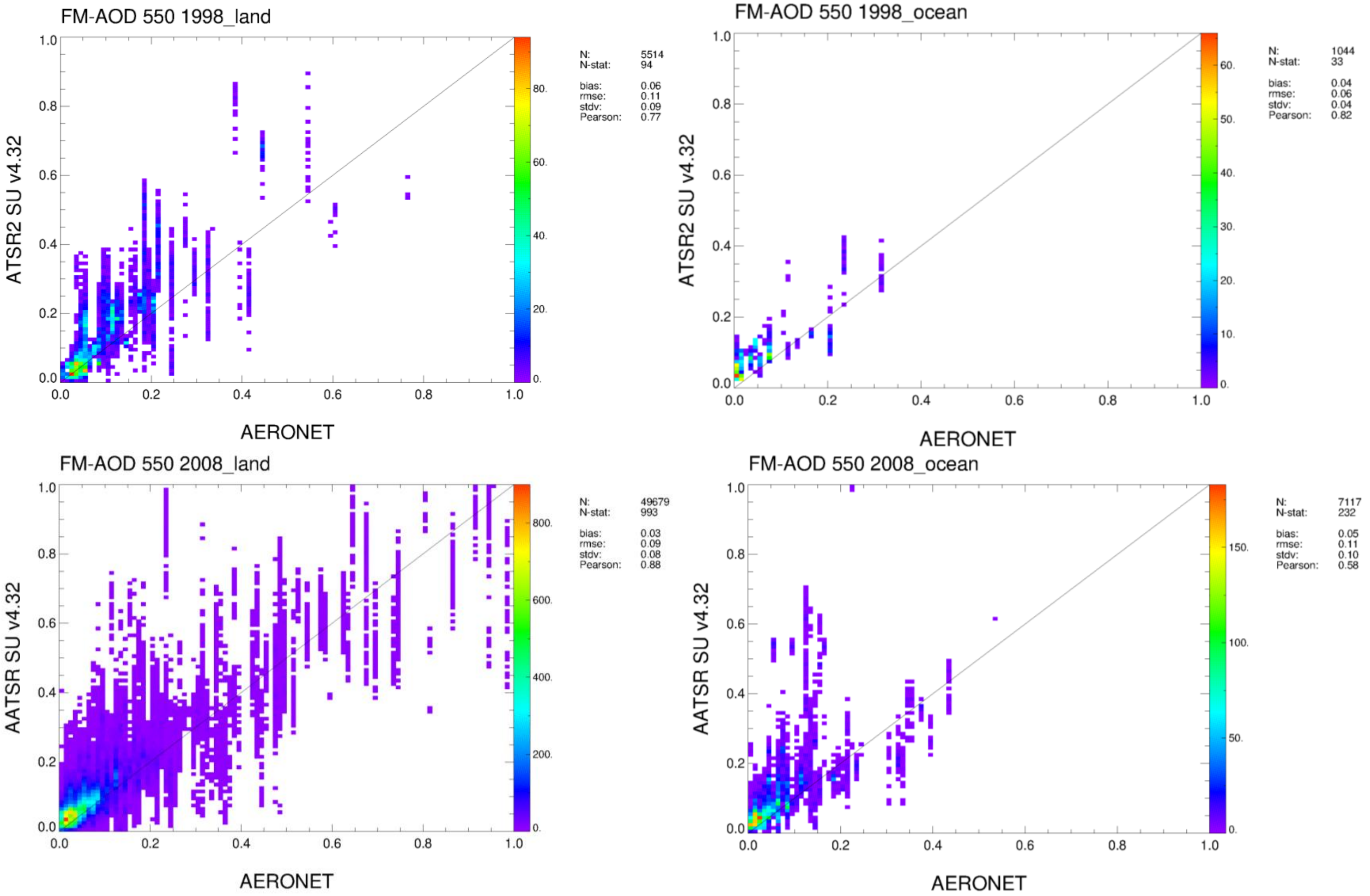

Figure 4.11 *Density scatter plots for FM-AOD of ATSR-2 (top) and AATSR (bottom) over land (left) and ocean (right).*

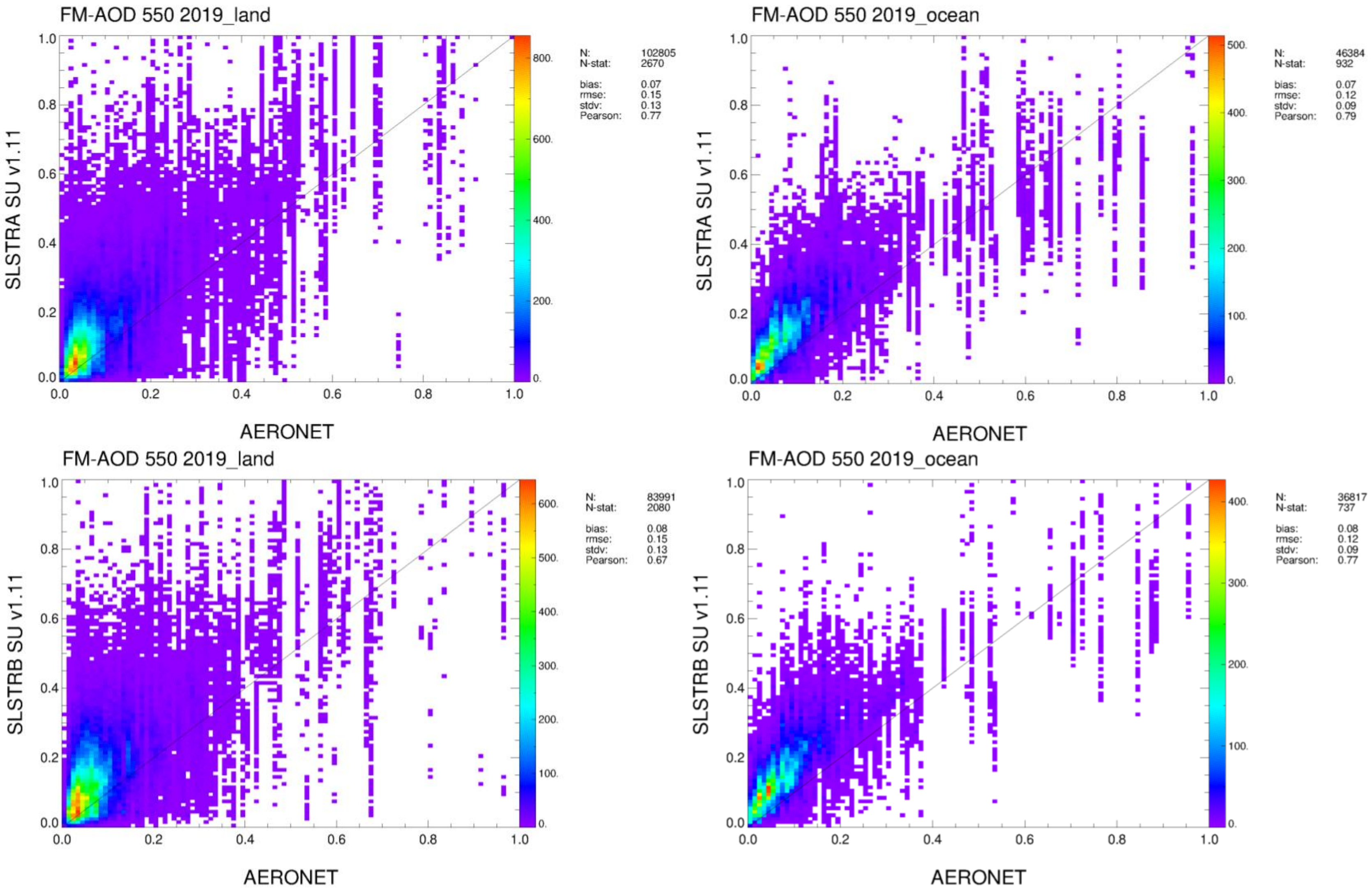

***Figure 4.12** Density scatter plots for FM-AOD of SLSTR/3A (top) and SLSTR/3B (bottom) over land (left) and ocean (right).*

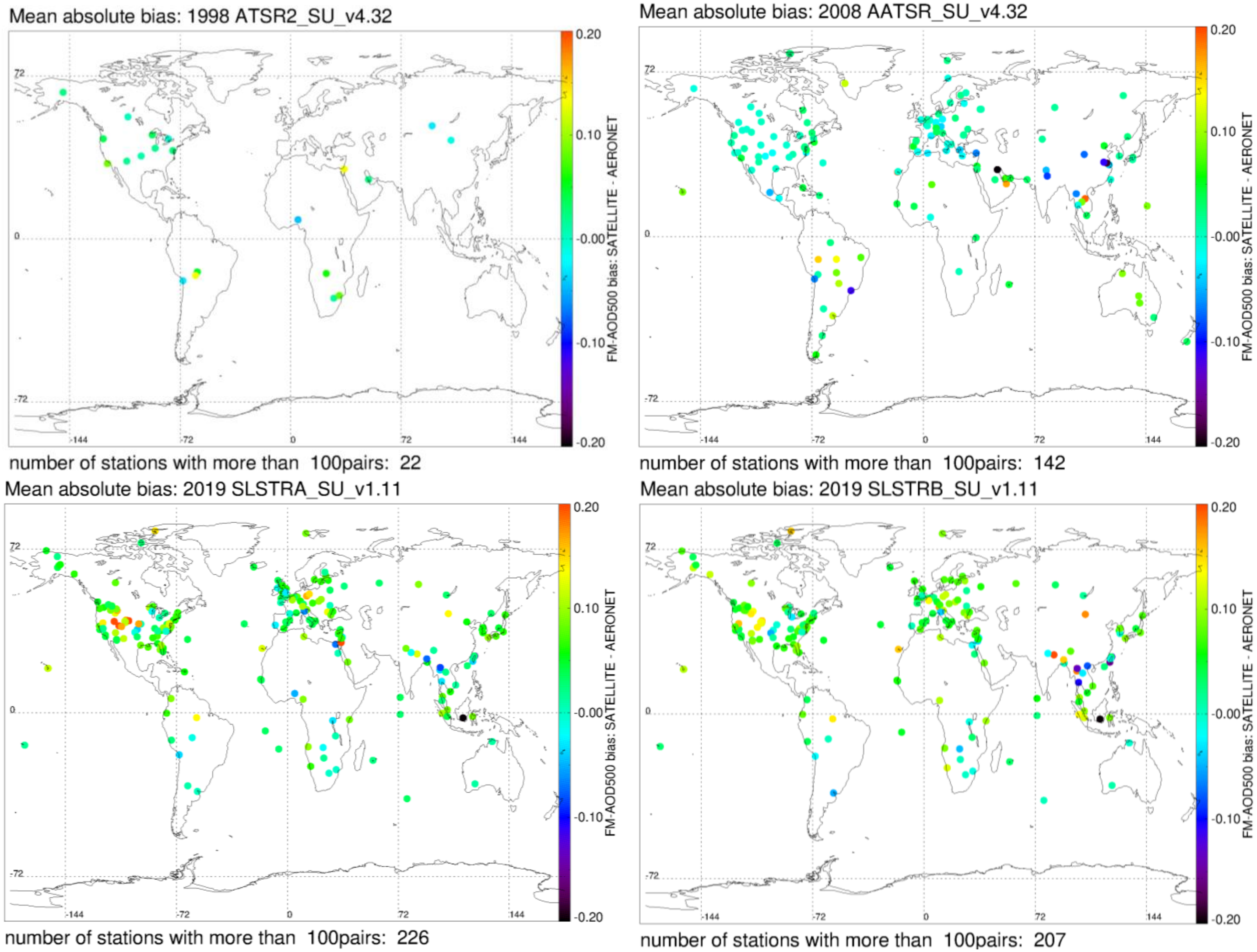

Figure 4.13 *Maps of significant station mean FM-AOD bias (Satellite – AERONET) for all 4 sensors.*

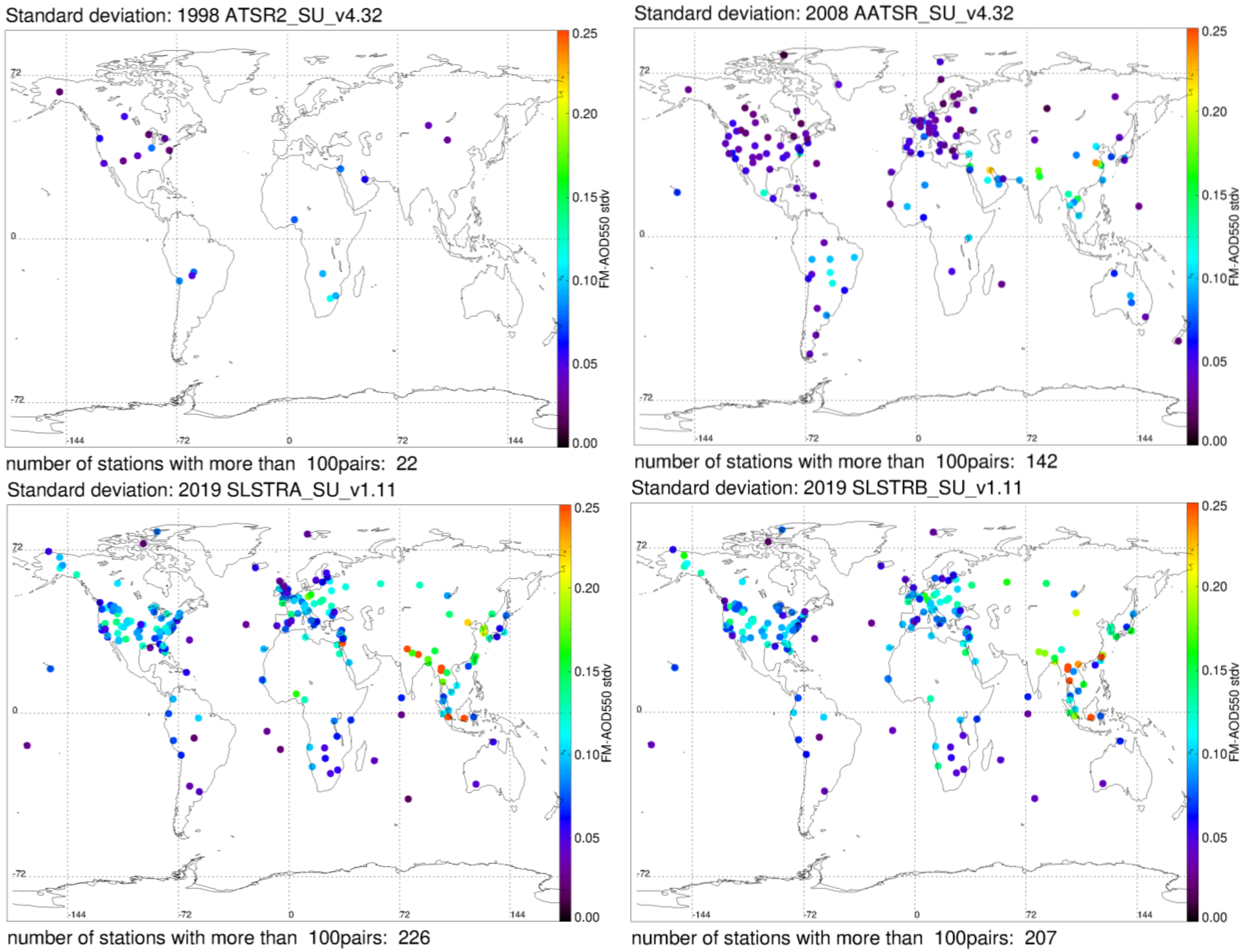

Figure 4.14 *Maps of significant station FM-AOD stdv of Satellite and AERONET for all 4 sensors.*

5 EVALUATION OF LEVEL2 UNCERTAINTIES

5.1 Global validation of pixel-level uncertainties

Aerosol_cci products strive to contain prognostic pixel-level uncertainties calculated by error propagation (Popp, et al., 2016) according to the best practices developed during the first two phases of the CCI program (Merchant, et al., 2017). Therefore, the prognostic pixel-level uncertainties contained in the data files have been compared to estimated true errors (represented by the difference between satellite and AERONET AOD) to assess the quality of the uncertainties. Again this analysis is stratified per sensor / year and over land and ocean as well as for stations.

Pixel-level uncertainties must not be mixed up with errors, since the predicted uncertainties contained in the data files are “standard uncertainties” which means that they define the width of a Gaussian error distribution around the retrieval value, whereas an error is one random sample from such a distribution. Therefore, pixel-level uncertainties can only be compared to individual pixel errors by statistical means.

We use here the quantity “expected discrepancy” as defined by Sayer et al. 2020:

$$\varepsilon_T = \sqrt{[\varepsilon_{Sat}^2 + \varepsilon_{Aeronet}^2]}$$

ε_T allows to also consider other sources of errors in the validation, namely a small term due to the AERONET reference uncertainties (set to $\varepsilon_{Aeronet} = 0.01$) while we cannot quantify easily a third term due to sampling biases between the station point measurement and satellite pixel covered area; $\varepsilon_{Aeronet}$ matters only for small ε_{Sat}.

Furthermore, we also use the quantity “normalized error”:

$$\Delta = (AOD_{Sat} - AOD_{Aeronet}) / \varepsilon_T.$$

If the uncertainty is a good representation of the expected discrepancy, Δ will be normally distributed so that a fraction $F_\Delta = 68.3\%$ of values should fall within the range [-1, +1], with zero mean $M_\Delta = 0.$ and unit standard deviation $S_\Delta = 1$. A non-zero mean ($M_\Delta \neq 0$) indicates the presence of residual systematic errors (an issue for algorithm development). A standard deviation less than one ($S_\Delta < 1.$) indicates uncertainties are overestimated ($f_\Delta > 68.3\%$), which could result from overestimation of individual sources of error, while a standard deviation greater than one ($S_\Delta > 1.$) indicates an underestimate ($f_\Delta < 68.3\%$), e.g. due to neglecting an important source of error .

Finally, we conduct a mean-bias correction for the error distributions in some of the subsequent analysis, since the concept of standard uncertainties requires bias-free error distributions (which can be interpreted as absence of remaining systematic and quantifiable biases).

In the following figures we show first (fig. 5.1 and fig. 5.2) the comparison of histograms of the estimated errors (red) and prognostic uncertainties (blue filled bars) to qualitatively illustrate per sensor / year and over land / ocean the distributions of prognostic uncertainties. It is obvious that while the error distributions are Gauss-like with partly some asymmetry and positive shift for SLSTR while all uncertainty distributions show a double peak, which is hardly visible over ocean, but very strong over land, in particular for both SLSTR instruments. The mean of uncertainties is larger over land than over ocean for all sensors and is significantly larger over land for SLSTR (0.15) than for the ATSR instruments (~0.09), while it is similar for all sensors over ocean (0.05 – 0.06); similarly the stdv of uncertainties is larger over land and for both SLSTR.

For a quantitative validation, we developed a new approach shown in fig. 5.3 and fig. 5.4, where we calculate a synthetic cumulative distribution of errors from prognostic uncertainties by adding up one Gaussian error distribution (normalized to a total integral of 1.) for each individual pixel-level uncertainty according to the definition of standard uncertainties. We compare then this synthetic error frequency distribution with the measured error distribution. Furthermore, we subtract the mean bias from the error distribution to make it more symmetric for direct comparison to the synthetic distribution (which by its definition is always symmetric). Finally, we calculate an average correction factor for the synthetic distribution (and thus the prognostic uncertainties) in relation to the mean-bias corrected error distributions as ratio of the standard deviations of both distributions. Those histograms and their width compared to the bias-corrected measured error histograms show that uncertainties are generally performing not too bad and in most cases are slightly too small with typical overall correction factors of ~1.15 for the ATSR instruments (1.28 for AATSR over ocean). For the SLSTR instruments over ocean a larger correction factor is needed (~1.4), while over land uncertainties need a slight decrease (correction factor of ~0.9). It should be noted that with a simple correction factor the bias-corrected measured error distribution and the synthetic error distribution calculated from the corrected uncertainties match reasonably well as shown in Fig. 5.3 and fig. 5.4, but do not match perfectly – this points to remaining unresolved issues for some of the pixels / retrieval conditions. It is also important to understand that this assessment of all uncertainties per senor in a bulk provides an average understanding and is dominated by the most numerous uncertainties as shown in fig. 5.1 and 5.2 (the smaller ones in general and to some extent the larger ones from the second peaks for SLSTR over land).

Following Sayer, et al., 2020 we analyse the potential of the prognostic uncertainties to discriminate between (“good” / “bad”) pixels with likely small / large errors in Fig. 5.5 and Fig. 5.6. We do this by plotting as function of binned uncertainties the absolute error below which are 38%, 68% and 95% of all pixels with this uncertainty. These percentages relate to 0.5 σ, 1 σ, and 2 σ (σ = standard width) for normal error distributions in each bin (along the vertical axis) – those theoretically expected values are shown as dashed lines in black, red and blue. In contrast to the average view of Fig. 5.3 and 5.4 the percentile plots allow a view as function of the amount of uncertainties.

The percentile plots show a reasonable agreement (within statistical noise) with the theoretical lines for the lower range of uncertainties (up to ~0.1 for all sensors or even 0.17 for ATSR-2 over land) while for higher uncertainties the error values are clearly below the expected lines, which means that errors are too small / uncertainties are too large. In summary, the uncertainties allow a reasonable split between “good” and “bad” pixels for the lower range with dominating numbers, but not any longer for the higher values. To indicate the statistical significance and to make the link to the average analysis of Fig. 5.3 and Fig. 5.4, the percentile plots also show the frequency distribution of uncertainties (dashed lines). It is obvious that (in particular for the ATSR instruments) the range of larger uncertainties has only few values and is therefore statistically weaker and contributes little to the average analysis, while for the SLSTR instruments there is a smaller but relevant contribution of larger uncertainties. Finally, it can be observed that the smallest uncertainties in the lowest bin have typically too large errors /are too small (in particular for SLSTR instruments).

Finally, we analyse the statistical distributions of Δ per sensor (fraction F_Δ of values within the range [-1, +1], mean M_Δ, standard deviation S_Δ) in Fig. 5.7 (station map of S_Δ values), Tab. 5.1 (summary statistics per sensor) and Fig. 5.8 (M_Δ and S_Δ per sensor). Maps per sensor of the stdv of distributions of normalized errors Δ in Fig. 5.7 show that at most stations average Δ values are larger than 1. but there is a wide spread of average Δ values. Tab. 5.1 lists and Fig. 5.8 shows the average values per sensor of mean M_Δ, standard deviation S_Δ (and fraction F_Δ). While mean M_Δ is close to 0. for all sensors, mean S_Δ is significantly larger than 1. for all sensors (in particular for SLSTR where $S_\Delta > 2.$) and all F_Δ are slightly below the Gaussian 68% (and even down to 50% for SLSTR over ocean). This means that on average uncertainties (dominating the statistics) are too small and need correction factors larger than 1. (as calculated from the histograms in Fig. 5.3 and 5.4); the need for correction is more significant for SLSTR (also consistent with Fig. 5.4 over ocean, but not over land).

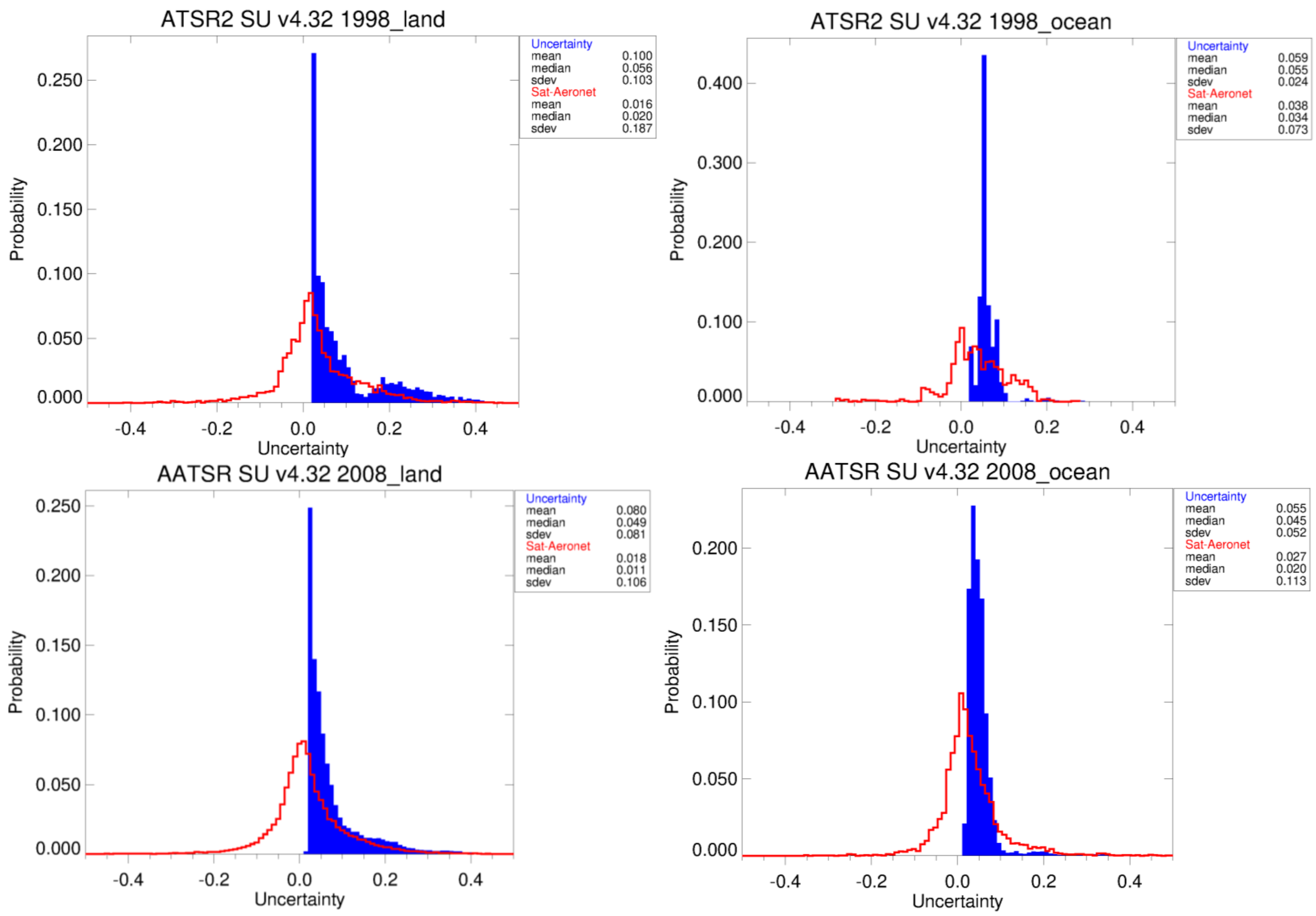

Figure 5.1 *Histograms of errors and uncertainties for ATSR-2 (top) and AATSR (bottom) over land (left) and ocean (right).*

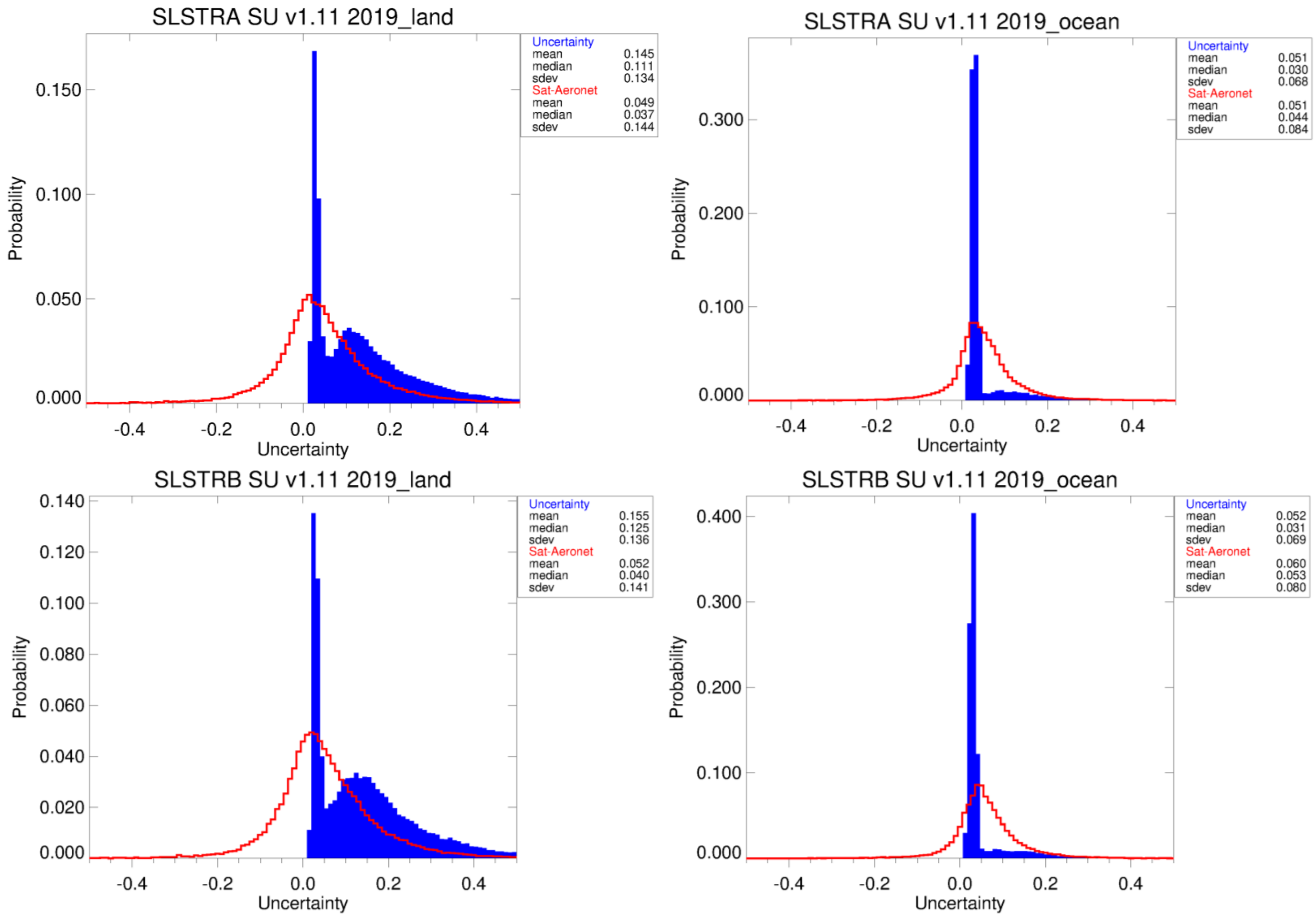

Figure 5.2 *Histograms of errors and uncertainties for SLSTR/3A (top) and SLSTR/3B (bottom) over land (left) and ocean (right).*

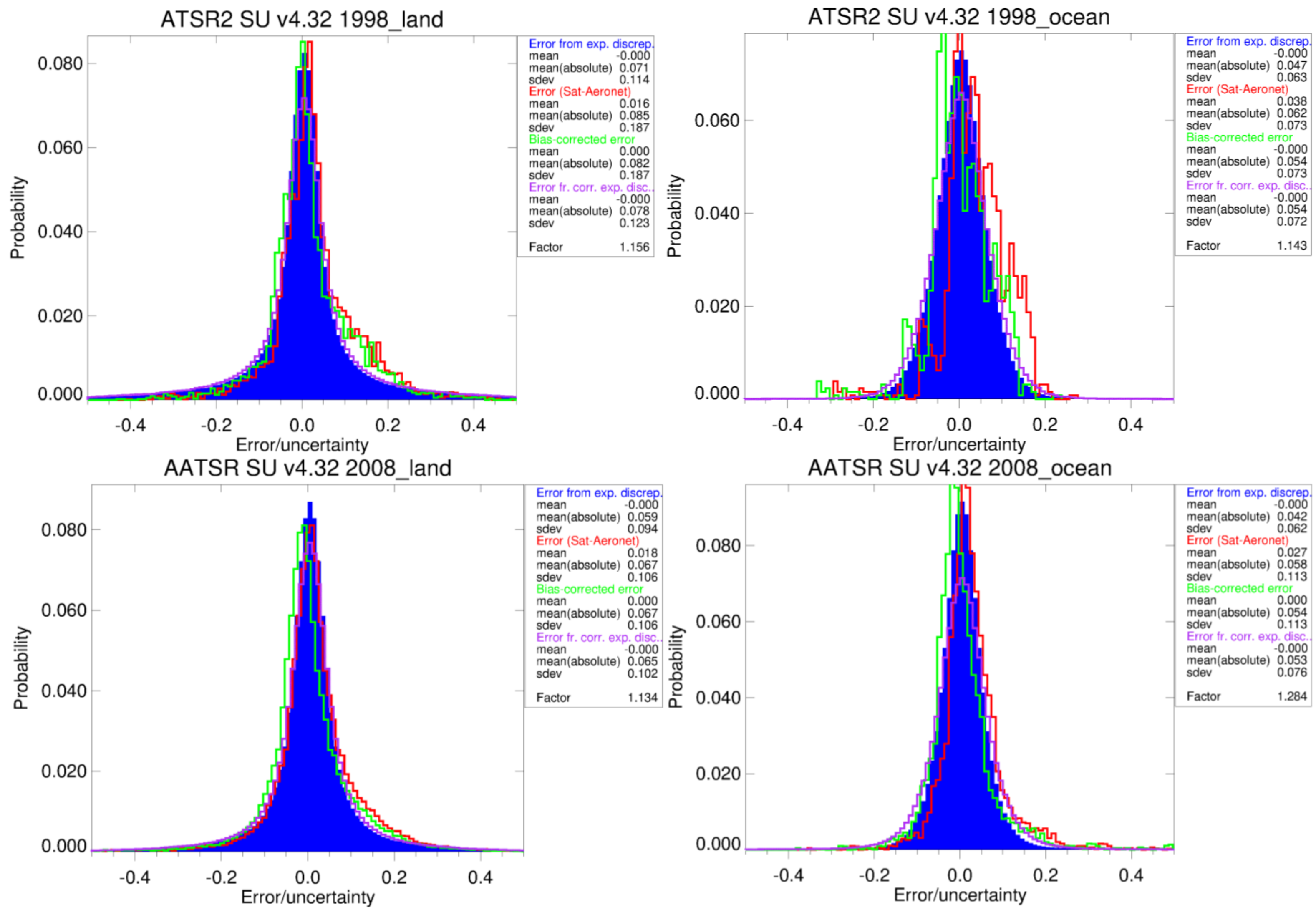

Figure 5.3 *Histograms of estimated errors (red; with bias correction: green) and errors calculated from uncertainties (blue; scaled to best fit the mean-bias corrected error distribution) for ATSR-2 (top) and AATSR (bottom) over land (left) and ocean (right).*

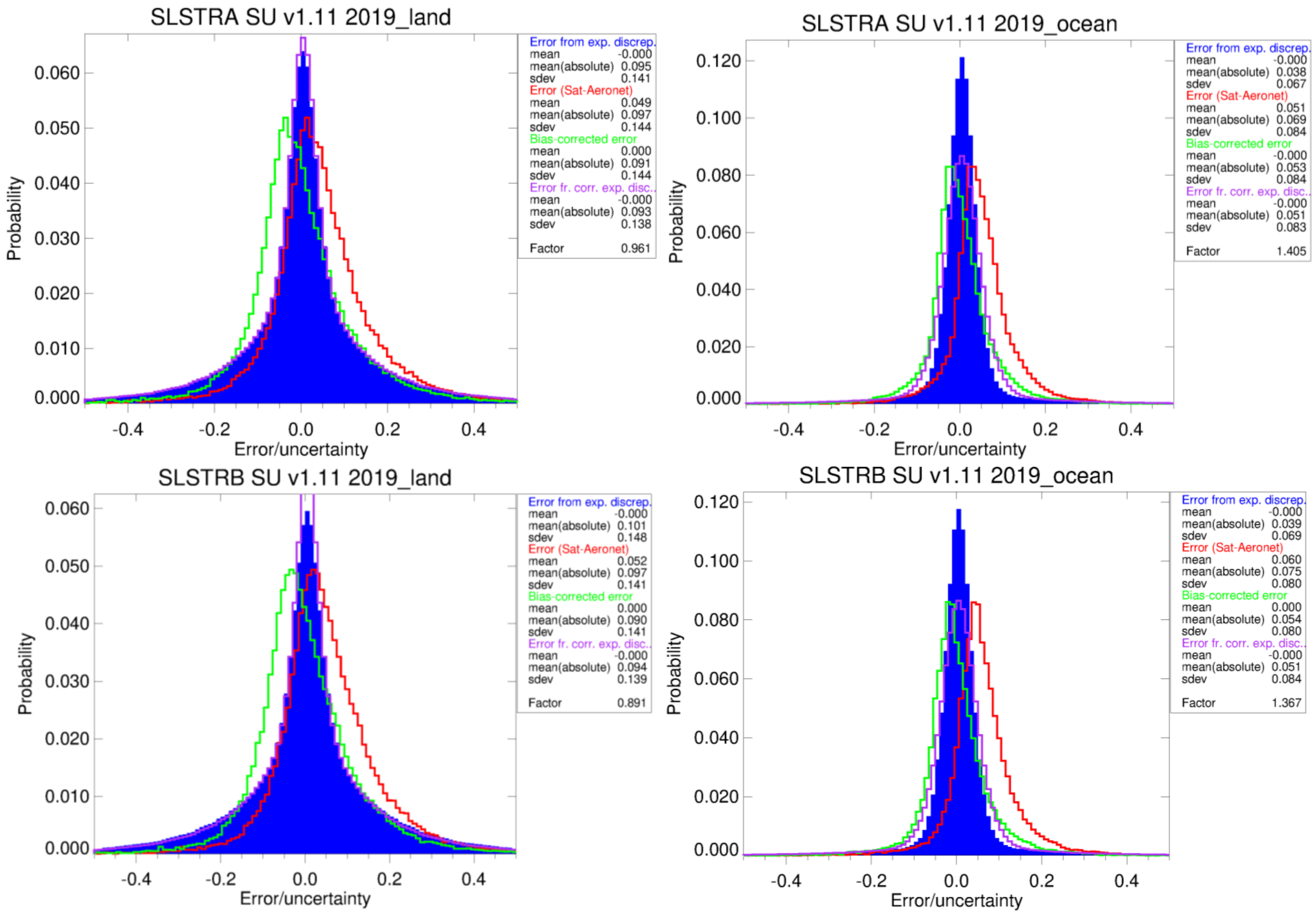

***Figure 5.4** Histograms of estimated errors (red; with bias correction: green) and errors calculated from uncertainties (blue; scaled to best fit the mean-bias corrected error distribution) for SLSTR/3A (top) and SLSTR/3B (bottom) over land (left) and ocean (right).*

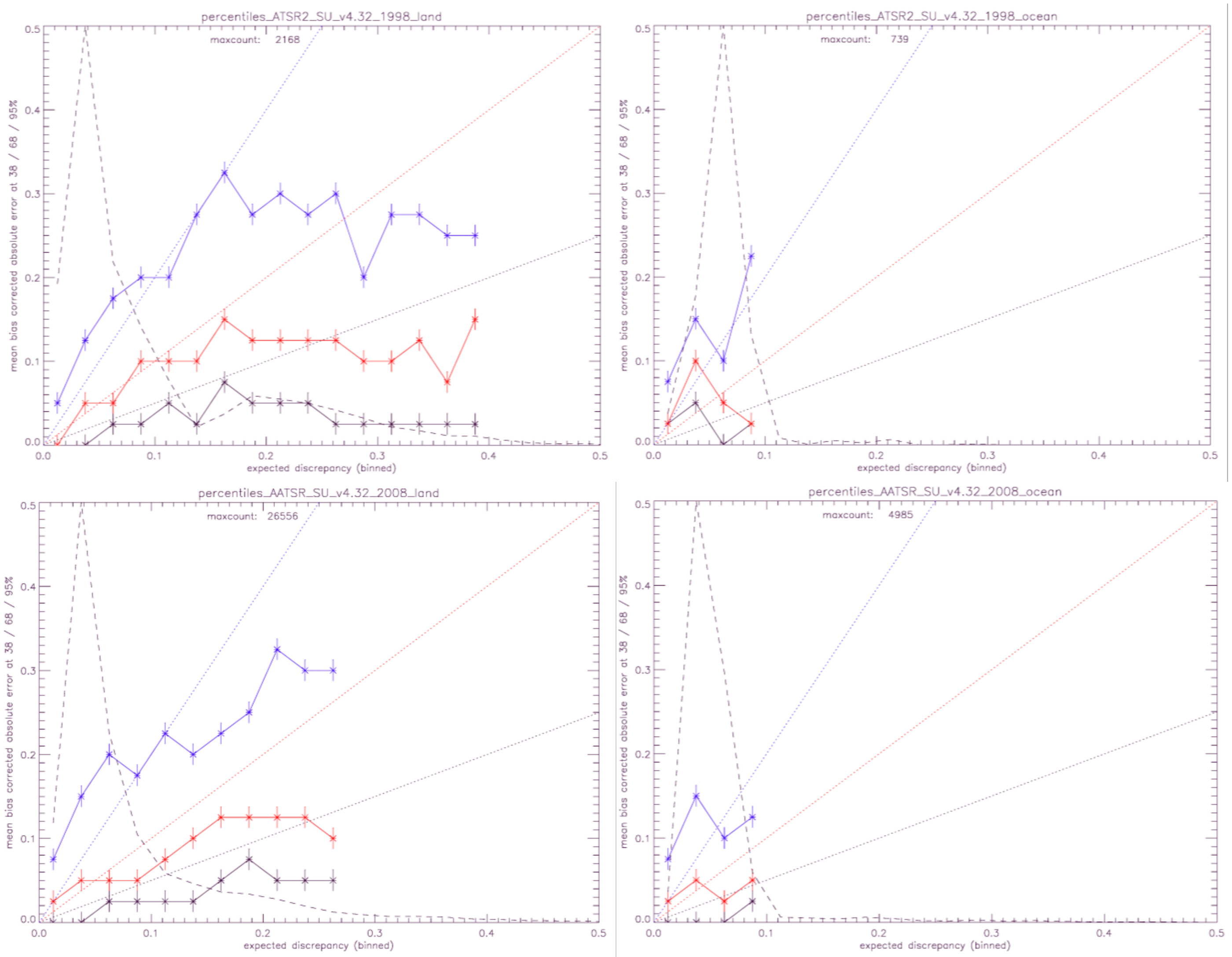

Figure 5.5 *Percentile plots of absolute errors at 38% (black), 68% (red) and 95% (blue) as function of binned expected discrepancy for ATSR-2 (top) and AATSR (bottom) over land (left) and ocean (right); dashed lines show the expected theoretical dependence.*

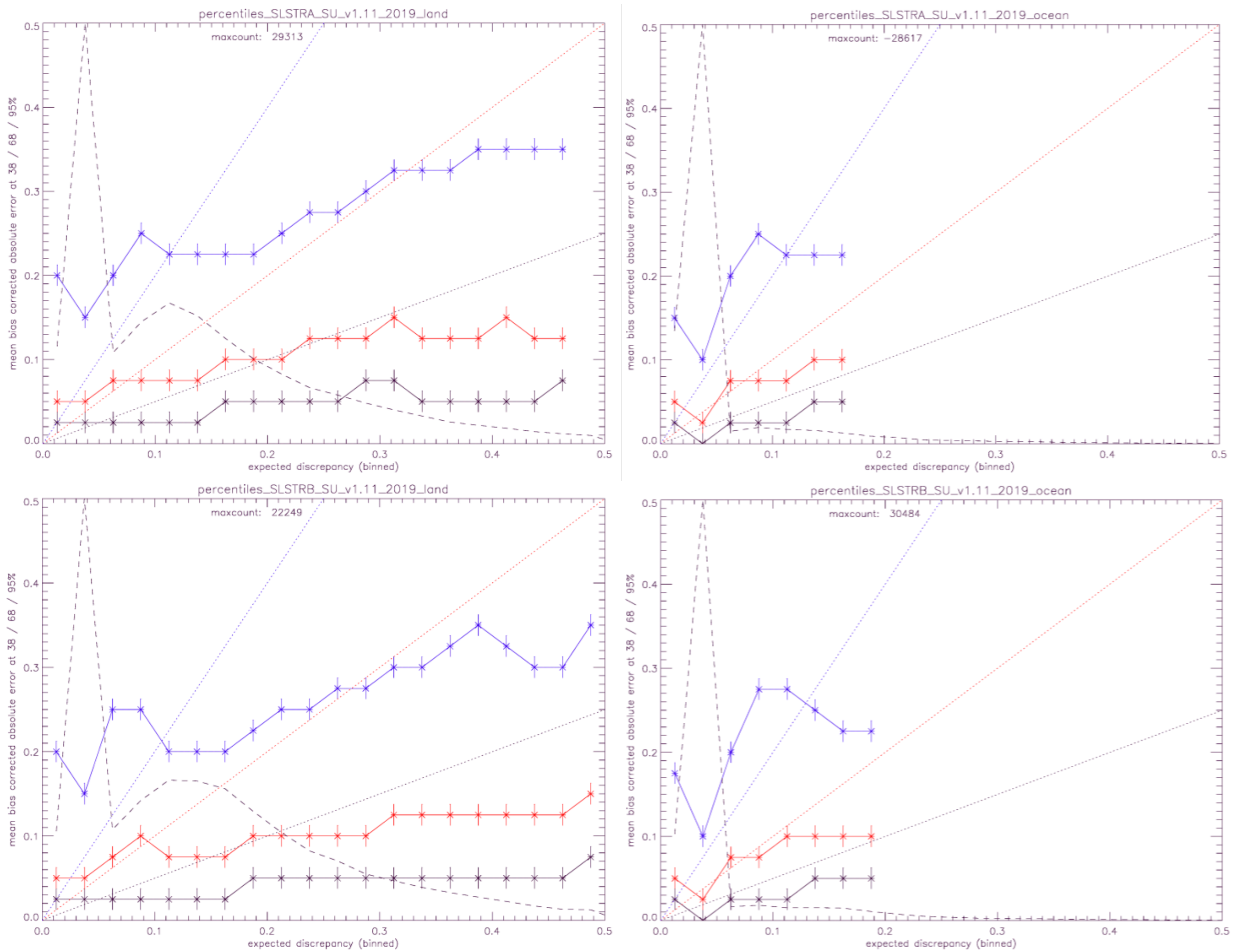

***Figure 5.6** Percentile plots of absolute errors at 38% (black), 68% (red) and 95% (blue) as function of binned expected discrepancy for SLSTR/3A (top) and SLSTR/3B (bottom) over land (left) and ocean (right); dashed lines show the expected theoretical dependence.*

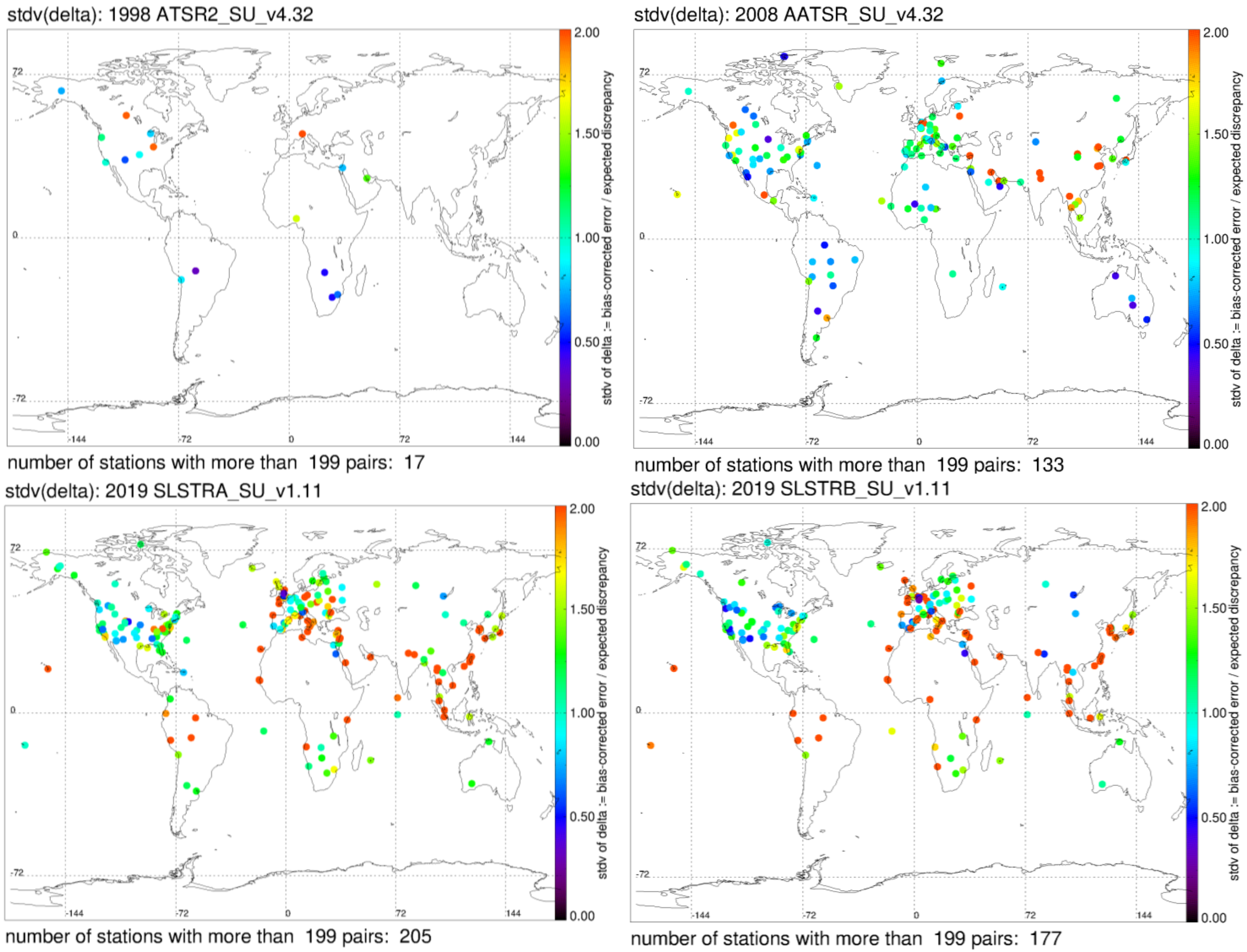

Figure 5.7 *Station maps of significant stdv of normalized errors Δ for the 4 sensors.*

Table 5.1 *Statistical summary of validating distributions of the normalized errors Δ for the 4 sensors*

year	**sensor**	**alg_version**	**area**	**mean-delta**	**stdv-delta**	**fraction-delta [%]**
Theoretical expectation				0.	1.	68.3
1998	ATSR2	SU_v4.32	land	0.02	2.57	64.8
1998	ATSR2	SU_v4.32	ocean	-0.03	1.49	62.9
2008	AATSR	SU_v4.32	land	-0.24	1.84	62.4
2008	AATSR	SU_v4.32	ocean	0.02	1.81	63.8
2019	SLSTRA	SU_v1.11	land	-0.04	2.45	65.6
2019	SLSTRA	SU_v1.11	ocean	0.06	2.41	49.8
2019	SLSTRB	SU_v1.11	land	0.03	2.48	68.4
2019	SLSTRB	SU_v1.11	ocean	0.12	2.44	51.0

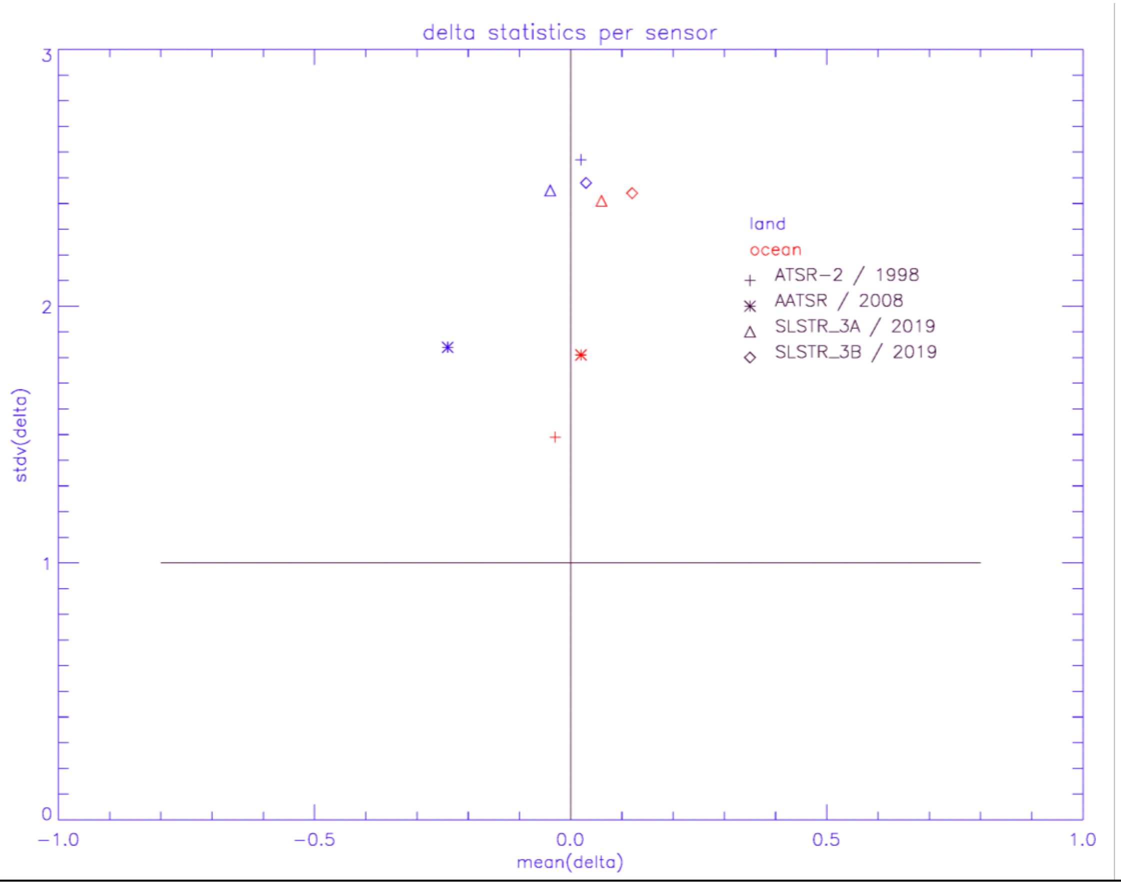

Figure 5.8 *Statistics of Δ (mean, stdv) per sensor over land and ocean.*

5.2 Separate validation of pixel-level uncertainties for both hemispheres

The double peaks in histograms of the uncertainteis in Fig. 5.1 and Fig. 5.2 and theoretical understanding motivated the following additional analysis where we split the assessment for stations in the Northern and Southern hemisphere. Prognositc uncertainteis are expected to increase with increasing AOD and increasing surface brightness, but also to strongly depend on the observation geometry where backscatter conditions also lead to increasing uncertainties. It is understood that dual view instrument observation geometry (mostly in the off-nadir view) differs significantly between the two hemispheres. In addition, the distribution of AERONET stations is largely uneven between the two hemispheres. Finally, the design of the two ATSR instruments has one major differnece from the design of the two SLSTR instruments: Whereas ATSR has a forward view, SLSTR has a rearward view. As a consequnce of this opposite viewing directions, ATSR has more favourable retrieval conditions in the North where most Aeronet stations lie, while SLSTR has better conditions in the South with less Aeronet stations. Therefore, we expect that, on global average, SLSTR (with less stations in the best conditions of the South) will have larger errors and larger uncertainties than ATSR (with msot stations innthe more favourable North of the globe). To verify this hypothesis, the analysis conducted in section 5.1 was split into the two hemispheres for AATSR and SLSTR / S3A (ATSR-2 has too few stations to split the statitics and SLSTR / S3B is not shown but had similar results as for SLSTR / S3A; also analysis over ocena was made with equivalent results and is not shown here).

Fig 5.9 and Fig. 5.10 show that for both AATSR and SLSTR the favourable hemisphere (which is opposite to each other) has smaller uncertainties and the double peak is gone; those need some increase, while in the unfavourable hemisphere uncertainties are larger and need to be (significantly) decreased. Fig. 5.11 shows the percentile plots for AATSR and SLSTR/3A split into hemispheres, which proves a larger range of meaningful uncertainteis over the favourable hemisphere which are appropriate to discriminate “good” and “bad” pixels.

Table 5.2 shows also a tendency (but not in all metrics and cases) that for the ATSR instruments the pixel level uncertainties in the South are on average larger (more over land) and need to be decreased by a correction factor ~0.6 – 0.8 (over both land and ocean) to match the measured bias while in the North they need to be increased by ~1.1 – 1.3 (note lower number for the statistics of ATSR-2). For the SLSTR instruments both measured biases and pixel level uncertainties are smaller in the South, but they are too small and thus need to be increased by correction factors > 2. over land and ~1.2 over ocean.

Table 5.2 *Statistical summary of validating pixel level uncertainty distributions over the Southern / Northern hemisphere for the 4 sensors*

				Error from discrepancy		Mean-bias corrected error		Correction factor
year	**sensor**	**Algorithm / version**	**area**	**Mean(abs)**	**Stdv**	**Mean(abs)**	**Stdv**	
1998	ATSR2	SU_v4.32	land	0.07 0.05 0.15	0.11 0.07 0.19	0.08 0.08 0.09	0.19 0.20 0.12	1.16 1.71 0.62
1998	ATSR2	SU_v4.32	ocean	0.05 0.05 0.05	0.06 0.06 0.06	0.05 0.05 -	0.07 0.07 -	1.14 1.14 -
2008	AATSR	SU_v4.32	land	0.06 0.05 0.11	0.09 0.08 0.16	0.07 0.06 0.07	0.11 0.11 0.10	1.12 1.26 0.64
2008	AATSR	SU_v4.32	ocean	0.04 0.04 0.03	0.06 0.06 0.04	0.05 0.06 0.03	0.11 0.12 0.03	1.28 1.31 0.82
2019	SLSTRA	SU_v1.11	land	0.10 0.11 0.04	0.14 0.15 0.05	0.09 0.09 0.07	0.14 0.14 0.18	0.96 0.88 2.00
2019	SLSTRA	SU_v1.11	ocean	0.04 0.04 0.02	0.07 0.07 0.03	0.05 0.06 0.03	0.08 0.09 0.04	1.41 1.40 1.11
2019	SLSTRB	SU_v1.11	land	0.10 0.11 0.03	0.15 0.16 0.05	0.09 0.09 0.08	0.14 0.13 0.18	0.89 0.80 2.37
2019	SLSTRB	SU_v1.11	ocean	0.04 0.04 0.02	0.07 0.07 0.03	0.05 0.05 0.03	0.08 0.08 0.04	1.37 1.36 1.25

All North South "South validation is worse" "South validation is better"

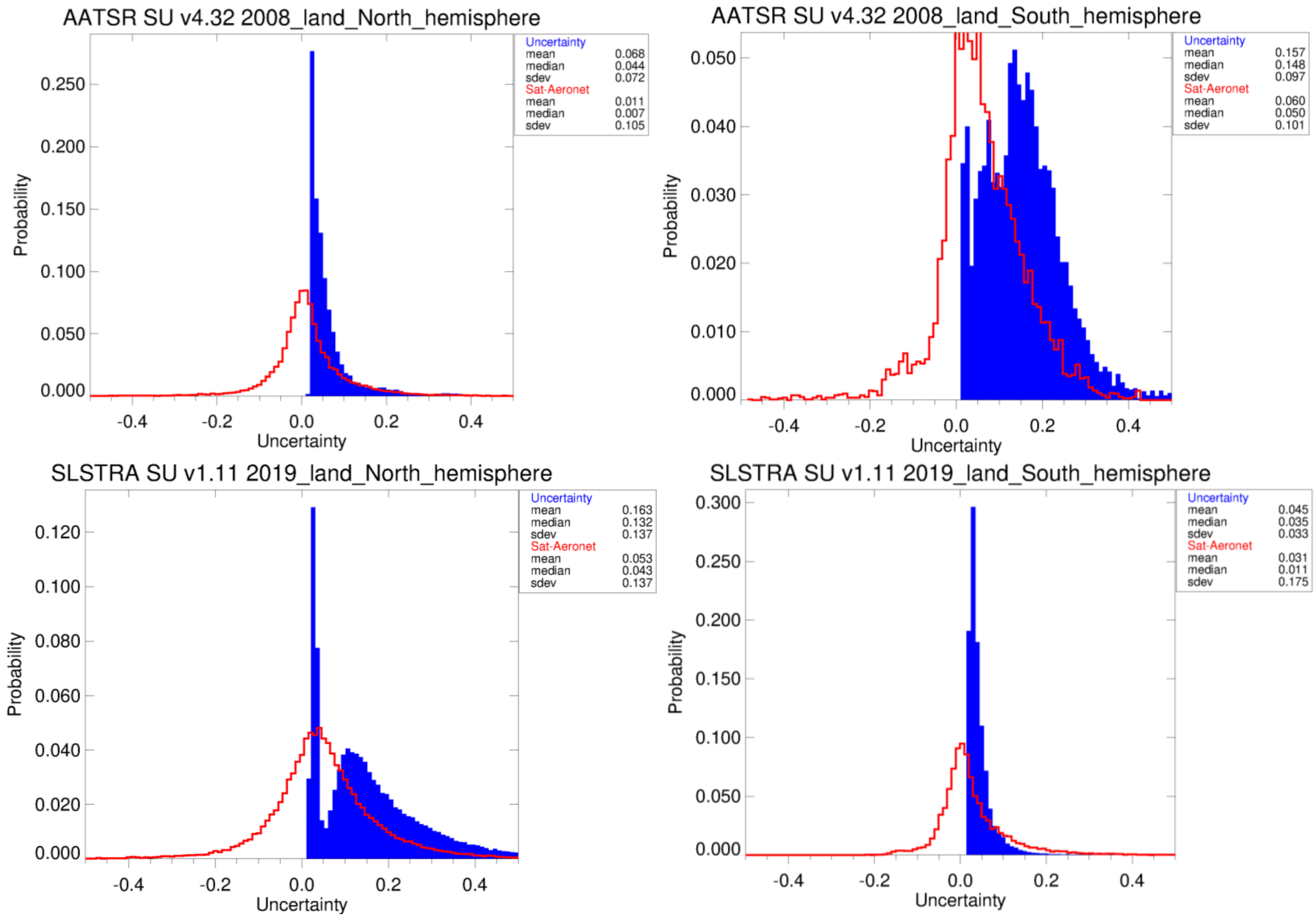

***Figure 5.9** Histograms of errors and uncertainties for AATSR (top) and SLSTR/3A (bottom) over the North (left) and South hemisphere (right).*

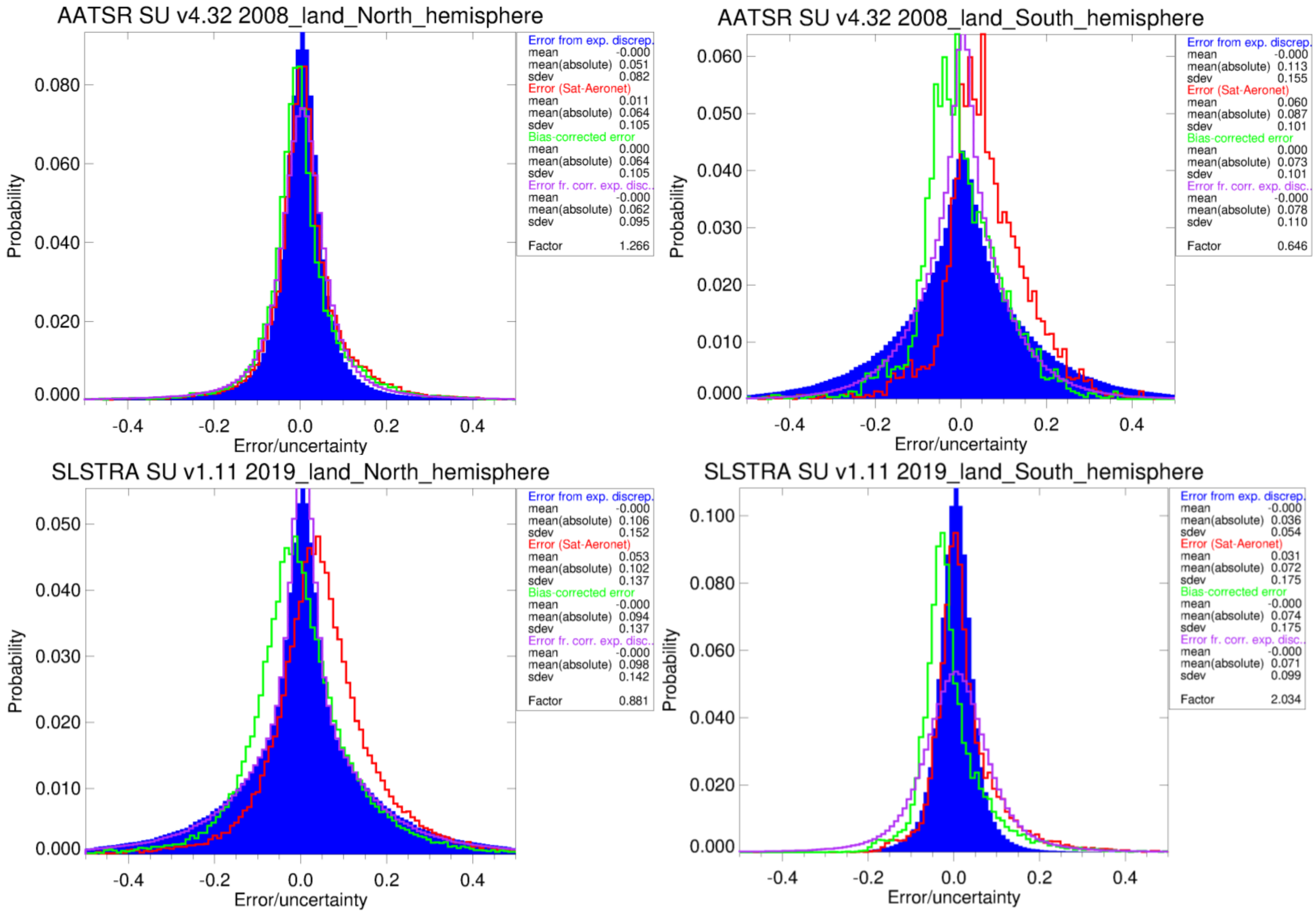

Figure 5.10 *Histograms of estimated errors (red; with bias correction: green) and errors calculated from uncertainties (blue; scaled to best fit the mean-bias corrected error distribution) for AATSR (top) and SLSTR/3A (bottom) over the North (left) and South (right) hemisphere.*

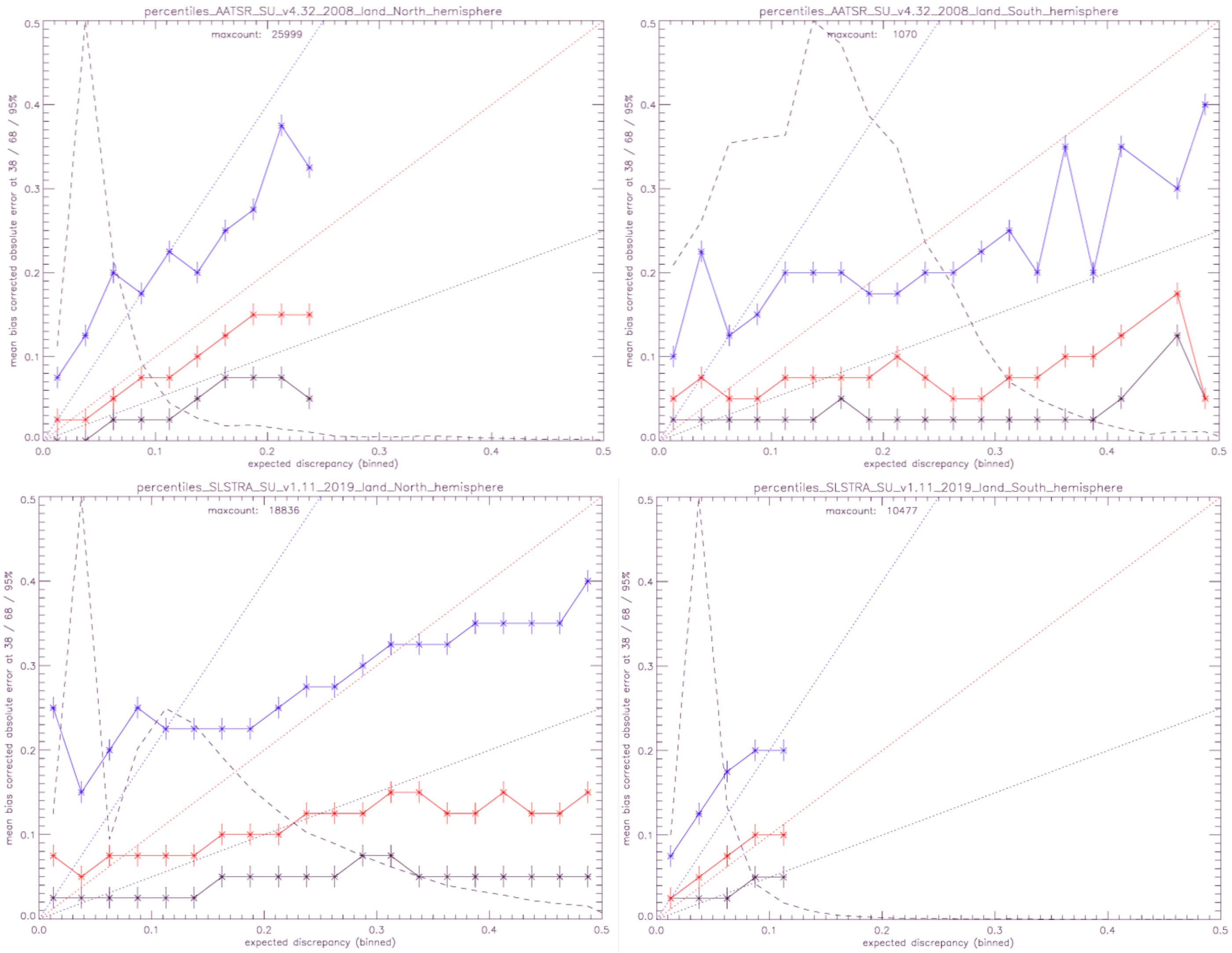

Figure 5.11 *Percentile plots of absolute errors at 38% (black), 68% (red) and 95% (blue) as function of binned expected discrepancy for AATSR (top) and SLSTR/3A (bottom) over the North (left) and South (right) hemisphere; dashed lines show the expected theoretical dependence.*

Summary for the validation of AOD prognostic uncertainties

- all uncertainty distributions show a double peak (strong over land, in particular for both SLSTR instruments)
- mean of uncertainties is larger over land than over ocean for all sensors
- mean and stdv of uncertainties are significantly larger over land for SLSTR than for the ATSR instruments but similar for all sensors over ocean
- uncertainties are generally slightly too small; for the SLSTR instruments over ocean a larger correction factor is needed, while over land uncertainties need a slight decrease
- uncertainties allow a reasonable split between “good” and “bad” pixels for the lower range of prognostic uncertainties with dominating numbers, but not any longer for the higher values
- the smallest uncertainties in the lowest bin have typically too large errors /are too small (in particular for SLSTR instruments)
- statistical distributions of normalized errors per sensor show that on average uncertainties (dominating the statistics) are too small and need correction factors larger than 1. (in particular for SLSTR)
- separate analysis of the two hemispheres proves the favourable scattering angle conditions (avoiding backscatter) which have smaller uncertainties with less need for correction and more meaningful information to split “good” and “bad” pixels; those favourable conditions are in the Northern hemisphere for ATSR (with most AERONET stations dominating the validation statistics) , while they lie in the Southern hemisphere for SLSTR (with less AERONET stations). This is one reason for the weaker performance of AOD from SLSTR than ATSR, but also of the prognostic uncertainties.

6 INTER-COMPARISON TO OTHER SATELLITE DATASETS

6.1 Level3 evaluation: inter-comparison of monthly products

6.1.1 Monthly global AOD

Evaluation of the L3 (1deg resolution) monthly (March, June, September and December) AOD products from the AATSR and Sentinel-3A, -3B (S3A, S3B) has been performed for years 2008 and 2019, respectively. AATSR monthly AOD product has been compared with MODIS, MISR and POLDER/GRASP AOD. S3A and S3B AOD products were inter-compared; both S3A and S3B AOD products were compared with MODIS and MISR AOD.

Total AOD monthly maps for AATSR, MODIS, MISR and POLDER for year 2008 are shown in Fig. 6.1. In March and December, AOD is not retrieved North of ~50-60°N (Northern Europe, Canada, central Russia and Siberia). The retrieval is limited over those areas by low solar zenith angle, which limits the radiative transfer calculations, and snow cover. Better coverage of MODIS instrument is clearly seen in more smoothed AOD maps.

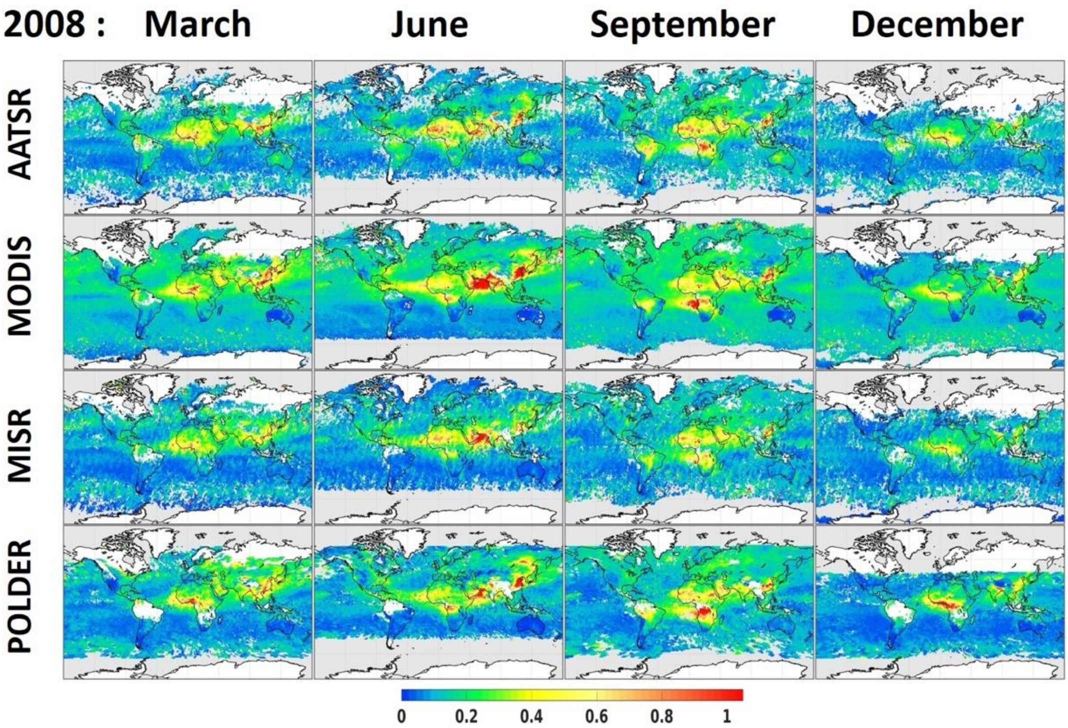

Figure 6.1 *AATSR, MODIS, MISR and POLDER total AOD for March, June, September and December 2008.*

Besides difference in coverage, difference in AOD is clear over the areas of potential high AOD loading (dust areas, biomass burning areas, areas of strong anthropogenic pollution). One of the main reasons for the difference in AOD is cloud screening. With more strict cloud screening, high AOD episodes cannot be retrieved, if high aerosol loading is recognised as cloud in the cloud screening module. Difference in AOD over ocean, where AOD loading is in general low (0.1-0.15) is also observed between products. Visual analysis of the maps gives an impression that AATSR, MISR and POLDER monthly AOD are close to each other, while MODIS provides higher AOD. Detailed analysis is provided in sections 6.1.2 and 6.1.3.

Total AOD monthly maps for S3A, S3B, MODIS and MISR for year 2019 are shown in Fig. 6.2. Sentinel-3 instruments have wider swath, as compared to AATSR, which results in better coverage. In 2019, S3A and S3B AOD monthly maps look as smooth as MODIS AOD maps.

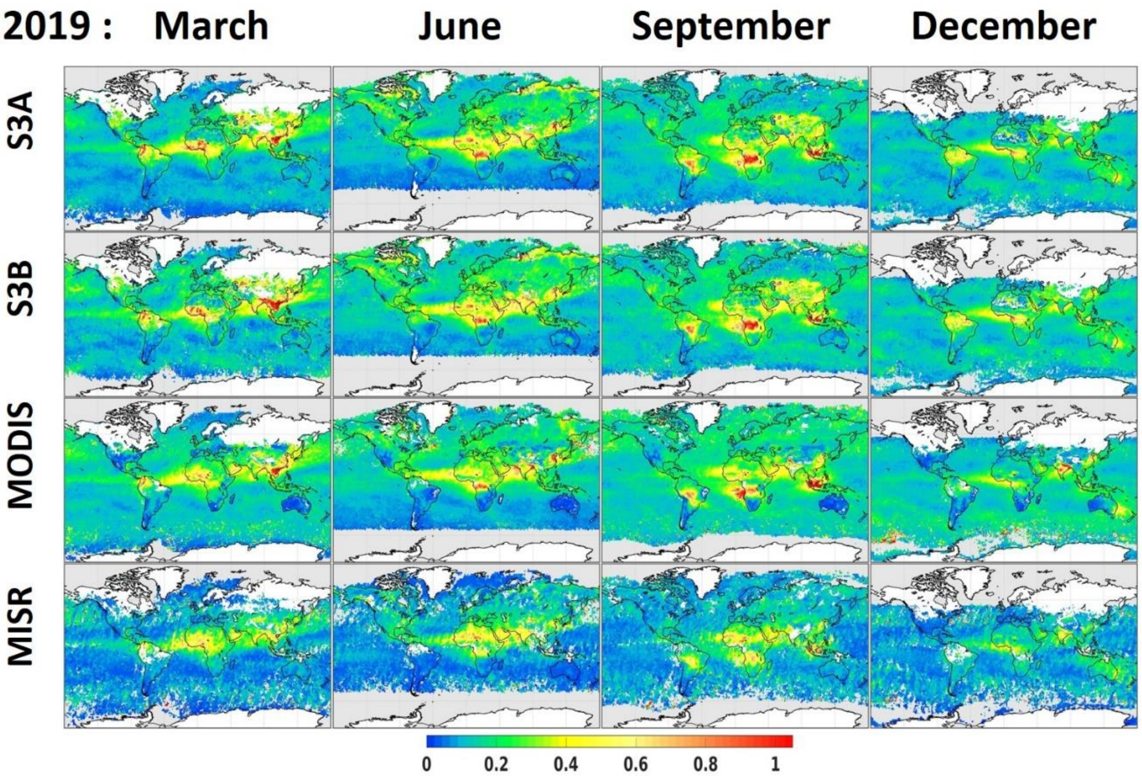

Figure 6.2 *Sentinel-3A (S3A), Sentinel-3B (S3B), MODIS and MISR total AOD for March, June, September and December 2019.*

6.1.2 Monthly regional AOD

In this study, we focus on different regions across the globe, as regional differences in AOD loading, types, seasonality and surface reflectance exist, which can affect the retrieval regional quality considerably. As such, applications drawn from the products will be analysed on a regional level.

To study regional differences over the globe, we chose 15 regions that seem likely to represent different aerosol / surface conditions (Fig. 1). There are 11 land regions: Europe (Eur), Boreal (Bor), Northern, Eastern and Western Asia (AsN, AsE and AsW, respectively), Australia (Aus), Northern and Southern Africa (AfN and AfS), Southern America (AmS), East and West of Northern America (NAE and NAW); Indian Ocean (InO), Pacific ocean (PO), two regions over Atlantic ocean: Saharan dust outbreak over the central Atlantic (AOd) and possible biomass burning outbreak over southern Atlantic (AOb), and one region, Indonesia (Ind), that includes both land and ocean. Furthermore, we studied AOD over all land, all ocean and globally, when observed. South-Eastern China (ChinaSE), which is part of the AsE region, was also considered separately as an area with considerable AOD changes during the last 25 years. Altogether, we consider the AOD in 17 regions, AOD over land, ocean and Global AOD.

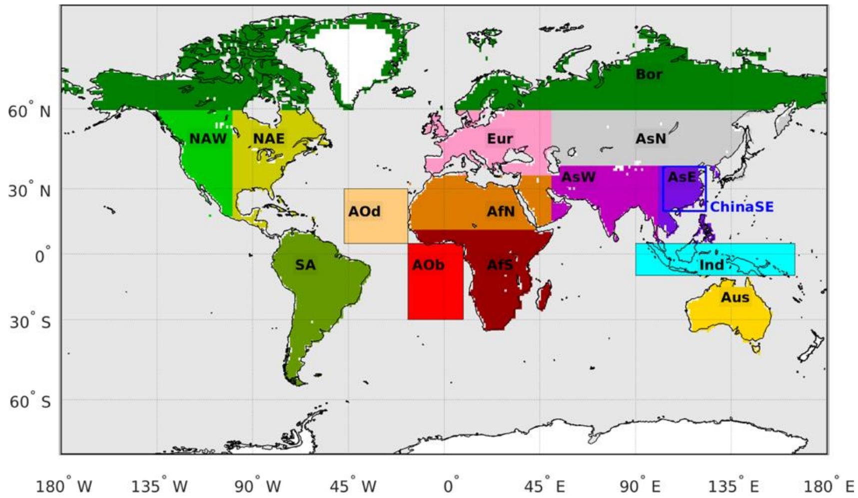

Figure 6.3 *17 Land and ocean regions defined in this study: Europe (Eur), Boreal (Bor), northern Asia (AsN), eastern Asia (AsE), western Asia (AsW), Australia (Aus), northern Africa (AfN), southern Africa (AfS), South America (SA), eastern North America (NAE), western North America (NAW), Indonesia (Ind), Atlantic Ocean dust outbreak (AOd), Atlantic Ocean biomass burning outbreak (AOb). In addition, Southeast China (ChinaSE), which is part of the AsE region, marked with a blue frame, is considered separately. Indian Ocean (InO) and Pacific Ocean (PO) regions are not shown. Land, ocean and global AOD were also considered.*

Monthly regional AOD for AATSR, MODIS, MISR and POLDER (2008) and for S3A, S3B, MODIS and MISR (2019) are shown in Fig. 6.4.

In both years, all products have similar tendency of high AOD over Asia (AsW, AsE and ChinaSE), Africa (AfN, AfS), the area of the Saharan dust transport (AOd) and over the Atlantic Ocean, influenced by the transport of biomass burning aerosols (AOb).

In 2008 in Asia, MODIS and POLDER AOD are higher than those from the AATSR and MISR products in March and June, while in September and December the difference between AATSR and MODIS and POLDER is smaller. Global AOD is similar for AATSR, MISR and POLDER, while MODIS global AOD is higher. For details, see Table 6.1, Table 6.4 and discussion below.

In the year 2019, the difference between S3A and S3B AOD is small in all regions, except for AsE and ChinaSE, where S3B is slightly higher (for details, see Table 6.2, Table 6.5 and discussion below). S3A and S3B total AOD is close to the MODIS product for Europe, Asia, Indonesia, dust and biomass burning areas, while in South Africa, South and North America S3A and S3B AOD is higher than MODIS and the MODIS AOD product is close to MISR.

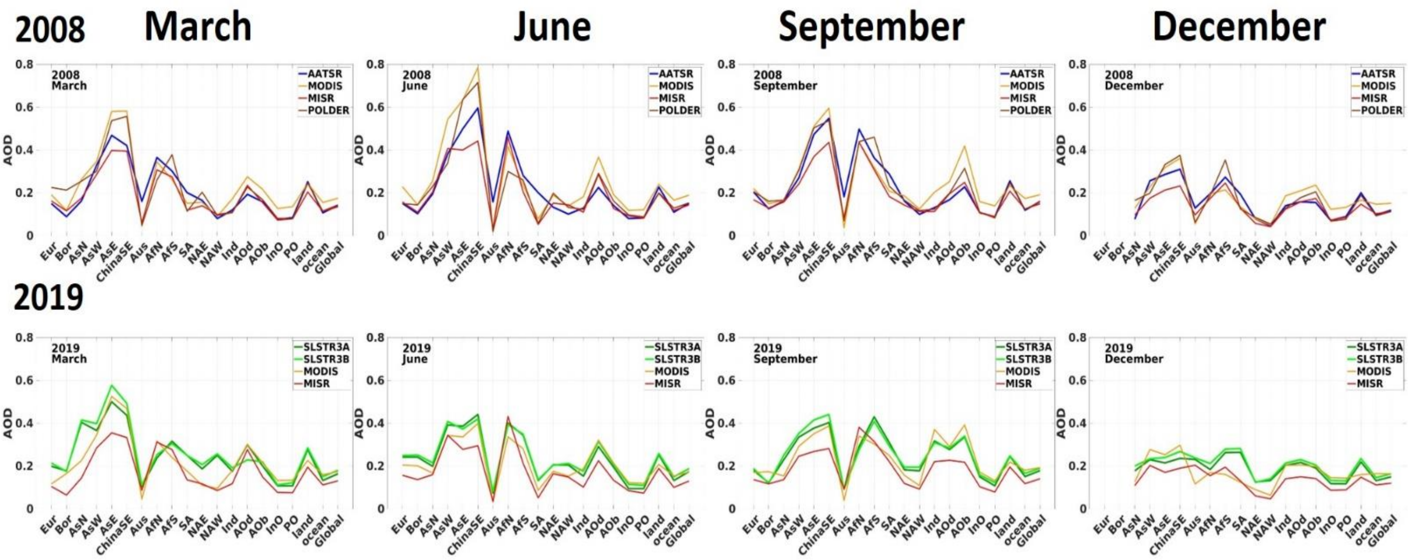

Figure 6.4 Monthly AOD for AATSR, MODIS, MISR and POLDER (2008, upper panel) and for S3A, S3B, MODIS and MISR (2019, lower panel) for different regions, as in Fig. 6.3

6.1.3 Regional and global difference in monthly AOD

Maps of the difference in monthly AOD between AATSR and MODIS, AATSR and MISR (middle panel), AATSR and POLDER (lower panel) total AOD monthly products are shown in Fig. 6.5. Maps of the difference in monthly AOD between S3A and S3B, S3A and MODIS, S3B and MODIS, S3A and MISR, S3B and MISR total AOD monthly products are shown in Fig.6.6.

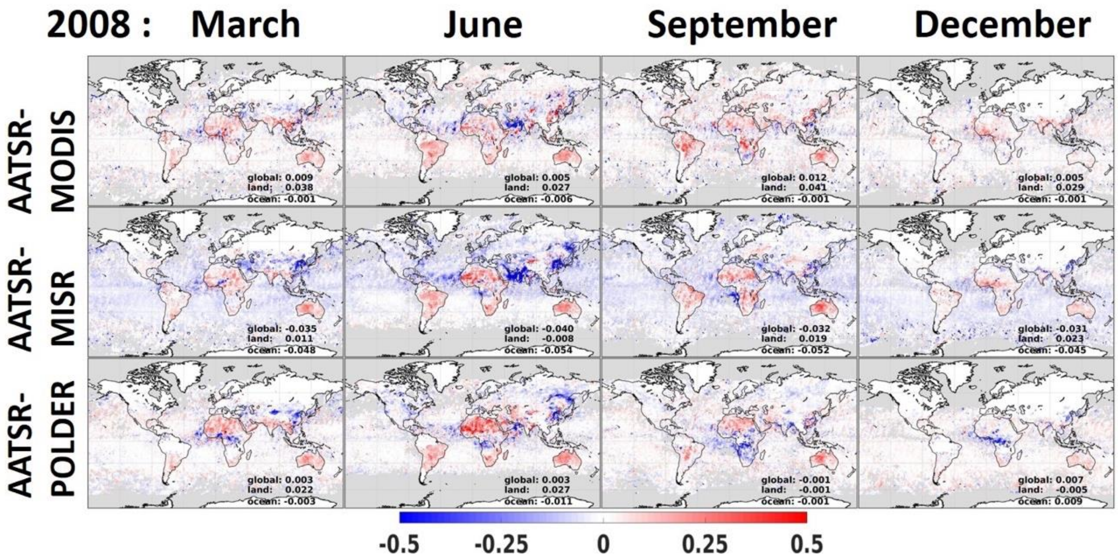

Figure 6.5 *Difference between AATSR and MODIS (upper panel), AATSR and MISR (middle panel), AATSR and POLDER (lower panel) total AOD monthly products, for year 2008.*

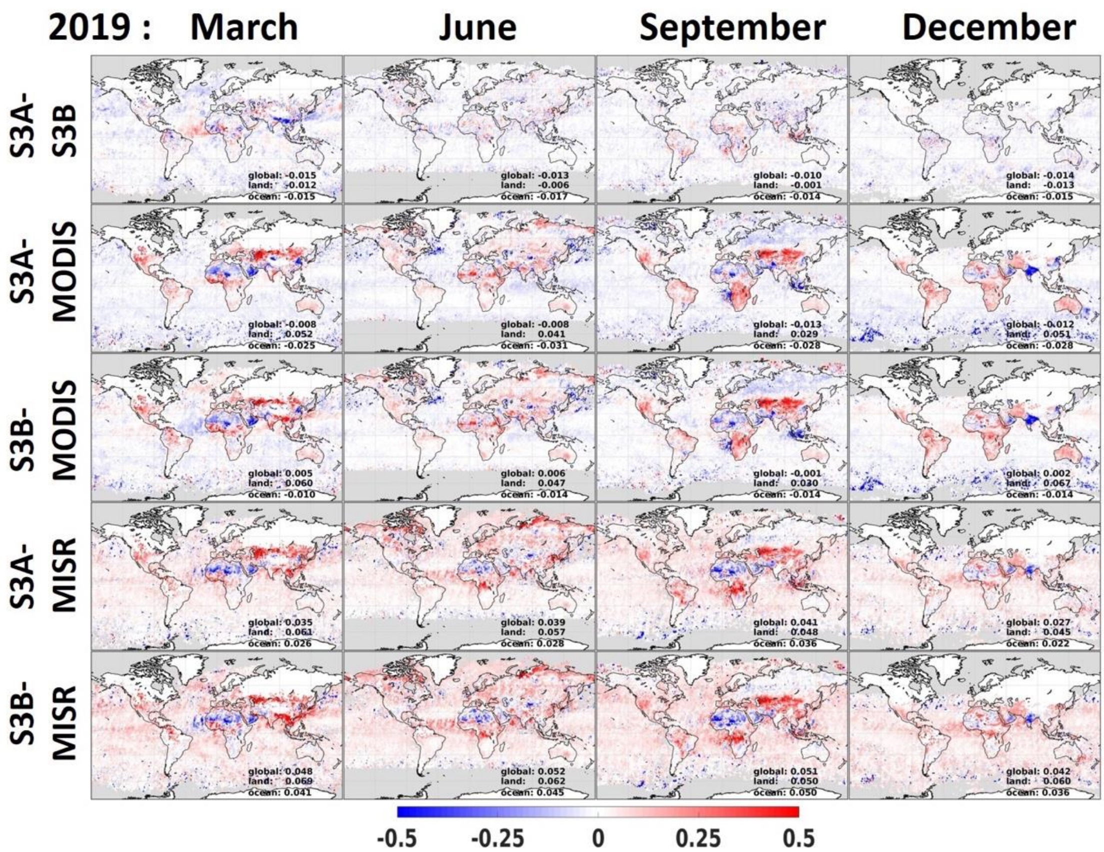

Figure 6.6 *Difference between S3A and S3B (upper panel), S3A and MODIS, S3B and MODIS, S3A and MISR, S3B and MISR total AOD monthly products, for year 2019.*

Absolute differences in AOD monthly means between satellite products over selected regions are summarised in Table 6.1 (for year 2008) and Table 6.2 (for year 2019).

Table 6.1 *Offset between AATSR and MODIS, MISR and POLDER monthly AOD for regions defined as in Figure 6.3*

regions	Eur	Bor	AsN	AsW	AsE	ChinaSE	Aus	AfN	AfS	SA
March										
AATSR-MODIS	-0.041	-0.029	-0.101	-0.018	-0.112	-0.161	0.115	0.020	0.040	0.050
AATSR-MISR	-0.012	-0.027	-0.013	0.043	0.070	0.026	0.099	0.058	0.027	0.082
AATSR-POLDER	-0.075	-0.124	-0.092	0.028	-0.069	-0.136	0.112	0.105	-0.076	0.087
June										
AATSR-MODIS	-0.077	-0.042	-0.060	-0.161	-0.134	-0.189	0.133	0.072	0.043	0.122
AATSR-MISR	-0.006	-0.007	-0.009	-0.025	0.099	0.154	0.123	0.028	0.076	0.148
AATSR-POLDER	0.001	-0.041	-0.035	0.043	-0.136	-0.119	0.138	0.188	0.021	0.143
September										
AATSR-MODIS	-0.016	-0.023	-0.003	-0.042	-0.037	-0.048	0.145	0.061	0.045	0.080
AATSR-MISR	0.036	-0.003	0.004	0.028	0.104	0.112	0.098	0.061	0.055	0.105
AATSR-POLDER	-0.002	-0.035	-0.005	-0.035	-0.030	0.011	0.113	0.058	-0.097	0.057
December										
AATSR-MODIS	-0.043	NaN	-0.051	0.028	-0.032	-0.051	0.074	0.000	0.059	0.058
AATSR-MISR	-0.013	NaN	-0.020	0.081	0.073	0.078	0.032	0.022	0.027	0.065
AATSR-POLDER	-0.031	NaN	-0.088	0.058	-0.046	-0.065	0.067	0.008	-0.080	0.069

***Table 6.1** continued*

regions	NAE	NAW	Ind	AOd	AOb	InO	PO	Land	Ocean	Globe
March										
AATSR-MODIS	0.009	-0.010	-0.052	-0.082	-0.058	-0.051	-0.052	0.007	-0.048	-0.034
AATSR-MISR	0.025	-0.019	0.010	-0.042	0.004	0.003	0.005	0.048	-0.007	0.006
AATSR-POLDER	-0.038	-0.015	0.012	-0.034	-0.010	-0.005	0.005	0.007	-0.008	-0.003
June										
AATSR-MODIS	-0.056	-0.038	-0.053	-0.142	-0.051	-0.038	-0.038	-0.013	-0.056	-0.037
AATSR-MISR	-0.019	-0.043	0.019	-0.061	0.014	-0.013	0.001	0.029	-0.008	0.008
AATSR-POLDER	-0.065	-0.031	0.006	-0.066	-0.021	-0.017	-0.005	0.027	-0.019	-0.001
September										
AATSR-MODIS	-0.024	-0.025	-0.072	-0.085	-0.191	-0.051	-0.051	0.022	-0.055	-0.031
AATSR-MISR	0.019	-0.013	0.018	-0.028	-0.021	0.002	-0.002	0.048	-0.006	0.011
AATSR-POLDER	-0.004	-0.017	0.007	-0.031	-0.087	-0.002	0.005	0.008	-0.004	0.001
December										
AATSR-MODIS	0.000	-0.004	-0.046	-0.052	-0.081	-0.052	-0.044	0.034	-0.050	-0.032
AATSR-MISR	0.021	0.004	0.016	0.000	-0.019	-0.002	0.004	0.053	-0.006	0.006
AATSR-POLDER	-0.006	-0.009	0.012	-0.020	-0.050	0.003	0.012	0.011	0.004	0.006

***Table 6.2** Offset between S3A and S3B, S3A and MODIS, S3B and MODIS, S3A and MISR, S3B and MISR monthly AOD for regions defined as in Figure 6.3*

(table cont. ->)

regions	Eur	Bor	AsN	AsW	AsE	ChinaSE	Aus	AfN	AfS	SA
March										
S3A-S3B	-0.015	0.003	-0.011	-0.032	-0.077	-0.056	-0.006	-0.015	0.011	0.000
S3A-MODIS	0.082	0.013	0.178	0.021	-0.025	-0.032	0.059	-0.079	0.076	0.073
S3A-MISR	0.094	0.113	0.259	0.081	0.145	0.104	0.018	-0.074	0.039	0.114
S3B-MODIS	0.097	0.010	0.189	0.053	0.052	0.024	0.065	-0.064	0.065	0.073
S3B-MISR	0.109	0.110	0.270	0.113	0.222	0.160	0.024	-0.059	0.028	0.114
June										
S3A-S3B	-0.007	-0.010	-0.016	-0.016	0.013	0.021	-0.008	0.008	-0.005	-0.004
S3A-MODIS	0.037	0.041	0.031	0.049	0.050	0.042	0.042	0.064	0.063	0.046
S3A-MISR	0.085	0.105	0.039	0.048	0.108	0.146	0.038	-0.031	0.131	0.081
S3B-MODIS	0.044	0.051	0.047	0.065	0.037	0.021	0.050	0.056	0.068	0.050
S3B-MISR	0.092	0.115	0.055	0.064	0.095	0.125	0.046	-0.039	0.136	0.085
September										
S3A-S3B	-0.009	0.003	-0.021	-0.017	-0.038	-0.038	0.003	0.016	0.021	0.016
S3A-MODIS	0.010	-0.052	0.075	0.043	0.026	0.016	0.055	-0.048	0.127	0.060
S3A-MISR	0.043	0.005	0.092	0.089	0.109	0.121	0.003	-0.089	0.115	0.089
S3B-MODIS	0.019	-0.055	0.096	0.060	0.064	0.054	0.052	-0.064	0.106	0.044
S3B-MISR	0.052	0.002	0.113	0.106	0.147	0.159	0.000	-0.105	0.094	0.073
December										
S3A-S3B	-0.003	NaN	-0.022	-0.004	-0.025	-0.032	-0.007	-0.028	-0.016	-0.018
S3A-MODIS	-0.013	NaN	0.052	-0.047	-0.038	-0.061	0.115	0.014	0.102	0.139
S3A-MISR	0.031	NaN	0.069	0.027	0.044	0.046	0.027	0.029	0.068	0.133
S3B-MODIS	-0.010	NaN	0.074	-0.043	-0.013	-0.029	0.122	0.042	0.118	0.157
S3B-MISR	0.034	NaN	0.091	0.031	0.069	0.078	0.034	0.057	0.084	0.151

***Table 6.2** continued*

regions	NAE	NAW	Ind	AOd	AOb	InO	PO	Land	Ocean	Globe
March										
S3A-S3B	-0.020	-0.007	-0.016	0.071	-0.019	-0.004	-0.014	-0.008	-0.018	-0.016
S3A-MODIS	0.077	0.154	-0.004	-0.001	-0.015	-0.025	-0.026	0.051	-0.027	-0.010
S3A-MISR	0.070	0.164	0.058	0.023	0.051	0.031	0.032	0.082	0.021	0.033
S3B-MODIS	0.097	0.161	0.012	-0.072	0.004	-0.021	-0.012	0.059	-0.009	0.006
S3B-MISR	0.090	0.171	0.074	-0.048	0.070	0.035	0.046	0.090	0.039	0.049
June										
S3A-S3B	0.002	-0.007	-0.023	-0.024	-0.013	-0.020	-0.015	-0.006	-0.017	-0.014
S3A-MODIS	0.030	0.052	-0.035	-0.030	-0.019	-0.028	-0.024	0.045	-0.021	0.002
S3A-MISR	0.042	0.056	0.051	0.066	0.061	0.010	0.021	0.064	0.032	0.044
S3B-MODIS	0.028	0.059	-0.012	-0.006	-0.006	-0.008	-0.009	0.051	-0.004	0.016
S3B-MISR	0.040	0.063	0.074	0.090	0.074	0.030	0.036	0.070	0.049	0.058
September										
S3A-S3B	-0.012	-0.017	0.008	-0.008	-0.004	-0.009	-0.015	-0.002	-0.015	-0.011
S3A-MODIS	0.026	0.069	-0.054	-0.014	-0.057	-0.022	-0.024	0.027	-0.030	-0.014
S3A-MISR	0.064	0.085	0.096	0.050	0.118	0.046	0.029	0.050	0.033	0.038
S3B-MODIS	0.038	0.086	-0.062	-0.006	-0.053	-0.013	-0.009	0.029	-0.015	-0.003
S3B-MISR	0.076	0.102	0.088	0.058	0.122	0.055	0.044	0.052	0.048	0.049
December										
S3A-S3B	0.002	-0.008	-0.011	-0.013	-0.014	-0.015	-0.014	-0.016	-0.014	-0.014
S3A-MODIS	0.036	0.069	0.000	0.012	-0.007	-0.028	-0.027	0.059	-0.033	-0.014
S3A-MISR	0.065	0.086	0.062	0.067	0.049	0.031	0.028	0.071	0.020	0.030
S3B-MODIS	0.034	0.077	0.011	0.025	0.007	-0.013	-0.013	0.075	-0.019	0.000
S3B-MISR	0.063	0.094	0.073	0.080	0.063	0.046	0.042	0.087	0.034	0.044

To estimate the maximum value (limit) for the difference in AOD between two products, which allows to conclude if products are close to each other (difference between products is below that limit) or significant difference between products exists (difference between products is above that limit), we introduce the concept of an accepted difference (AD).The root sum squared method, which assumes that the normal distribution describes the variation of dimensions, has been applied to calculate an accepted difference (AD) as in:

$$AD = \sqrt{ae_1^2 + ae_2^2},$$

where ae_1 and ae_2 are accepted errors for the inter-compared AOD products 1 (AOD_1, product for evaluation) and 2 (AOD_2, reference product), respectively.

Accepted errors were defined based on the GCOS requirements for AOD (003; 10%) applied to the monthly AOD averaged over each region of interest. For AOD<=0.3, *ae*=0.03; for AOD>0.3, *ae*=AOD*0.1 (10% of AOD).

Relative difference (RD) has been calculated as in

$$RD = \frac{AOD_1 - AOD_2}{AD},$$

|RD|<1 shows that the difference between two products is within the AD.

RD results showing the difference between products above the accepted difference (|RD|>1) were classified according to the *sign of difference* (negative difference, **N**, when AOD from the evaluated product is lower than that from the reference product (AOD_1<AOD_2)), or positive difference, **P**, opposite case when AOD_1>AOD_2) and *value of difference* (RD increases from group 1 (**g1**) to group 3 (**g3**)), as summarized in Table 6.3.

Table 6.3 *Classification of the groups considered in the analysis of the relative difference between the products, based on the RD sign and range.*

RD	<-2.0	<-1.5	<-1.0		>1.0	>1.5	>2.0
Group	Ng3	Ng2	Ng1		Pg1	Pg2	Pg3

Relative differences between evaluating (AATSR, S3A, S3B) and reference (MODIS, MISR, PARASOL) products, and between S3A and S3B, are presented in Table 6.4. Cases where RD accedes the AD are coloured (blue for negative, red for positive); intensity of the colour increases with the RD increase, according to the group classification.

Over land, ocean and globe, the difference between AATSR and GRASP is within the accepted difference. AATSR AOD is higher than MISR AOD (Pg1) over land and lower than MODIS AOD (Ng1) over ocean. Differences between AATSR and MISR over ocean and AATSR and MODIS over lands are within AD.

Regional analysis shows a considerable difference between the products. In March, June and September, AATSR AOD over Australia is much higher (Pg3) than AOD from MODIS, MISR and POLDER. Similar differences (Pg2, Pg3) are often observed over South America. Over China SE, AATSR AOD is lower than MODIS but often higher than MISR. AATSR AOD is often lower over the Atlantic, both over dust transport (Ng3 with MODIS in March, June and September) and biomass burning transport (Ng3 with MODIS and POLDER in September) areas. Over Eur, AATSR retrieves lower AOD than POLDER in March and June (both are in Ng2), while difference with MODIS and MISR AOD is within accepted value. AATSR product shows negligible of negative AOD difference with MODIS and MISR over Bor, AsN, NAW, NAE, Ind, AOd, AOb, InO and PO.

Table 6.4 *Relative AOD difference between AATSR and MODIS, MISR and POLDER monthly AOD for regions defined as in Figure 6.3, for year 2008. Cases with RD>1 (AOD difference is outside the accepted difference) are coloured; legend below the table.*

regions	Eur	Bor	AsN	AsW	AsE	ChinaSE	Aus	AfN	AfS	SA	NAW	NAE	Ind	AOd	AOb	InO	PO	Land	Ocean	Globe
March																				
AATSR-MODIS	-0.97	-0.68	-2.38	-0.38	-1.50	-2.24	2.71	0.40	0.94	1.18	0.21	-0.24	-1.23	-1.93	-1.37	-1.20	-1.23	0.16	-1.13	-0.80
AATSR-MISR	-0.28	-0.64	-0.31	0.97	1.14	0.45	2.33	1.22	0.63	1.93	0.59	-0.45	0.24	-0.99	0.09	0.07	0.12	1.13	-0.16	0.14
AATSR-POLDER	-1.77	-2.92	-2.17	0.63	-0.97	-1.95	2.64	2.22	-1.57	2.05	-0.90	-0.35	0.28	-0.80	-0.24	-0.12	0.12	0.16	-0.19	-0.07
June																				
AATSR-MODIS	-1.81	-0.99	-1.41	-2.43	-1.66	-1.92	3.13	1.12	1.01	2.88	-1.32	-0.90	-1.25	-3.00	-1.20	-0.90	-0.90	-0.31	-1.32	-0.87
AATSR-MISR	-0.14	-0.16	-0.21	-0.45	1.55	2.08	2.90	0.42	1.79	3.49	-0.45	-1.01	0.45	-1.44	0.33	-0.31	0.02	0.68	-0.19	0.19
AATSR-POLDER	0.02	-0.97	-0.82	0.84	-1.68	-1.28	3.25	3.28	0.49	3.37	-1.53	-0.73	0.14	-1.56	-0.49	-0.40	-0.12	0.64	-0.45	-0.02
September																				
AATSR-MODIS	-0.38	-0.54	-0.07	-0.97	-0.53	-0.59	3.42	0.92	0.93	1.89	-0.57	-0.59	-1.70	-2.00	-3.71	-1.20	-1.20	0.52	-1.30	-0.73
AATSR-MISR	0.85	-0.07	0.09	0.66	1.73	1.60	2.31	0.92	1.16	2.47	0.45	-0.31	0.42	-0.66	-0.49	0.05	-0.05	1.13	-0.14	0.26
AATSR-POLDER	-0.05	-0.82	-0.12	-0.82	-0.43	0.14	2.66	0.87	-1.66	1.34	-0.09	-0.40	0.16	-0.73	-2.00	-0.05	0.12	0.19	-0.09	0.02
December																				
AATSR-MODIS	-1.01	NaN	-1.20	0.66	-0.73	-1.07	1.74	0.00	1.39	1.37	0.00	-0.09	-1.08	-1.23	-1.91	-1.23	-1.04	0.80	-1.18	-0.75
AATSR-MISR	-0.31	NaN	-0.47	1.91	1.72	1.81	0.75	0.52	0.64	1.53	0.49	0.09	0.38	0.00	-0.45	-0.05	0.09	1.25	-0.14	0.14
AATSR-POLDER	-0.73	NaN	-2.07	1.37	-1.03	-1.34	1.58	0.19	-1.73	1.63	-0.14	-0.21	0.28	-0.47	-1.18	0.07	0.28	0.26	0.09	0.14

RD	<-2.0	<-1.5	<-1.0		>1.0	>1.5	>2.0
Group	Ng3	Ng2	Ng1		Pg1	Pg2	Pg3

Similar analysis has been performed to evaluate a difference between S3A, S3B, MODIS and MISR satellite monthly AOD products. The results of the analysis are shown in Table 6.5.

Differences between S3A and S3B AOD are, with few exceptions (AOd region, March), within the accepted value. Being close to each other in AOD retrieved, S3A and S3B products show similar global and regional differences with MODIS and MISR, respectively. Because of that, difference between S3 products and MODIS and MISR AOD products will be discussed below.

Positive offsets between S3 and MODIS and MISR are observed over land. In both NH and SH, difference between S3 AOD and MISR AOD is high (Pg2, Pg3). AOD difference with MODIS is, in general, within AD in the NH, while in the SH difference with MODIS often as high as for Pg2-Pg3.

AfN is the only region, where S3 AOD is lower than MODIS and MISR AOD in March and September. In June and December difference with MISR is within the AD, difference with MODIS is slightly above the AD (Pg1) in June and within the AD in December.

Over ocean, difference between S3 and MODIS and MISR is, with only few exceptions, within the AD. However, S3 AOD is higher (Pg1-Pg3) than MISR AOD in dust and biomass burning transport areas (AOd, AOb). AOd region in March is the only region, where the difference between S3A and S3B AOD fits to the group Pg2. Over Indian and Pacific oceans difference between S3 and MODIS (all cases) and MISR (except for few cases from Pg1) is within AD.

Globally, differences between S3A and MODIS and MISR are within AD. Difference between S3B and MODIS is within AD, while difference with MISR is a bit higher (Pg1).

Table 6.5 *Relative AOD difference between S3A, S3B, MODIS and MISR monthly AOD for regions defined as in Figure 6.3, for year 2019. Cases with RD>1(AOD difference is outside the accepted difference) and regions from the Northern and Southern hemispheres (NH and SH, respectively) are coloured; legend below the Table.*

regions	Eur	Bor	AsN	AsW	AsE	ChinaSE	Aus	AfN	AfS	SA	NAW	NAE	Ind	AOd	AOb	InO	PO	Land	Ocean	Globe
March																				
S3A-S3B	-0.35	0.07	-0.19	-0.59	-1.01	-0.85	-0.14	-0.35	0.25	0.00	-0.47	-0.16	-0.38	1.67	-0.45	-0.09	-0.33	-0.19	-0.42	-0.38
S3A-MODIS	1.93	0.31	3.54	0.42	-0.34	-0.50	1.39	-1.81	1.74	1.72	1.81	3.63	-0.09	-0.02	-0.35	-0.59	-0.61	1.20	-0.64	-0.24
S3A-MISR	2.22	2.66	5.15	1.71	2.36	1.89	0.42	-1.71	0.90	2.69	1.65	3.87	1.37	0.54	1.20	0.73	0.75	1.93	0.49	0.78
S3B-MODIS	2.29	0.24	3.69	1.01	0.67	0.35	1.53	-1.47	1.52	1.72	2.29	3.79	0.28	-1.69	0.09	-0.49	-0.28	1.39	-0.21	0.14
S3B-MISR	2.57	2.59	5.27	2.27	3.28	2.69	0.57	-1.36	0.65	2.69	2.12	4.03	1.74	-1.13	1.65	0.82	1.08	2.12	0.92	1.15
June																				
S3A-S3B	-0.16	-0.24	-0.38	-0.28	0.24	0.34	-0.19	0.14	-0.10	-0.09	0.05	-0.16	-0.54	-0.55	-0.31	-0.47	-0.35	-0.14	-0.40	-0.33
S3A-MODIS	0.87	0.97	0.73	0.94	0.98	0.71	0.99	1.22	1.38	1.08	0.71	1.23	-0.82	-0.68	-0.45	-0.66	-0.57	1.06	-0.49	0.05
S3A-MISR	2.00	2.47	0.92	0.92	2.21	2.74	0.90	-0.53	2.87	1.91	0.99	1.32	1.20	1.56	1.44	0.24	0.49	1.51	0.75	1.04
S3B-MODIS	1.04	1.20	1.11	1.22	0.74	0.36	1.18	1.08	1.48	1.18	0.66	1.39	-0.28	-0.13	-0.14	-0.19	-0.21	1.20	-0.09	0.38
S3B-MISR	2.17	2.71	1.30	1.20	1.98	2.42	1.08	-0.67	2.96	2.00	0.94	1.48	1.74	2.07	1.74	0.71	0.85	1.65	1.15	1.37
September																				
S3A-S3B	-0.21	0.07	-0.49	-0.35	-0.68	-0.64	0.07	0.38	0.35	0.37	-0.28	-0.40	0.18	-0.19	-0.08	-0.21	-0.35	-0.05	-0.35	-0.26
S3A-MODIS	0.24	-1.23	1.77	0.96	0.50	0.29	1.30	-1.06	2.41	1.39	0.61	1.63	-1.11	-0.33	-1.10	-0.52	-0.57	0.64	-0.71	-0.33
S3A-MISR	1.01	0.12	2.17	1.98	2.26	2.41	0.07	-1.84	2.16	2.06	1.51	2.00	2.20	1.18	2.62	1.08	0.68	1.18	0.78	0.90
S3B-MODIS	0.45	-1.30	2.26	1.30	1.18	0.92	1.23	-1.41	2.08	1.04	0.90	2.03	-1.28	-0.14	-1.02	-0.31	-0.21	0.68	-0.35	-0.07
S3B-MISR	1.23	0.05	2.66	2.29	2.87	2.98	0.00	-2.17	1.82	1.72	1.79	2.40	2.04	1.37	2.69	1.30	1.04	1.23	1.13	1.15
December																				
S3A-S3B	-0.07	NaN	-0.52	-0.09	-0.59	-0.75	-0.16	-0.66	-0.38	-0.42	0.05	-0.19	-0.26	-0.31	-0.33	-0.35	-0.33	-0.38	-0.33	-0.33
S3A-MODIS	-0.31	NaN	1.23	-1.11	-0.90	-1.44	2.71	0.33	2.40	3.28	0.85	1.63	0.00	0.28	-0.16	-0.66	-0.64	1.39	-0.78	-0.33
S3A-MISR	0.73	NaN	1.63	0.64	1.04	1.08	0.64	0.68	1.60	3.13	1.53	2.03	1.46	1.58	1.15	0.73	0.66	1.67	0.47	0.71
S3B-MODIS	-0.24	NaN	1.74	-1.01	-0.31	-0.68	2.88	0.99	2.78	3.70	0.80	1.81	0.26	0.59	0.16	-0.31	-0.31	1.77	-0.45	0.00
S3B-MISR	0.80	NaN	2.14	0.73	1.63	1.84	0.80	1.34	1.98	3.56	1.48	2.22	1.72	1.89	1.48	1.08	0.99	2.05	0.80	1.04

NH	SH		RD	<-2.0	<-1.5	<-1.0		>1.0	>1.5	>2.0
			Group	Ng3	Ng2	Ng1		Pg1	Pg2	Pg3

Summary for the inter-comparison to other satellite AOD products

-
- Over land, ocean and globally, the difference between AATSR and GRASP is within the accepted difference estimated with the root sum squared method considering the GCOS requirements for AOD. AATSR AOD is higher than MISR AOD over land and lower than MODIS AOD over ocean; both differenced are slightly above the accepted difference. Differences between AATSR and MISR over ocean and AATSR and MODIS over lands are within AD. Regional analysis shows a considerable difference between the products.
- Differences between S3A and S3B AOD are, with one exception for AOd region in March, within the accepted value.
- Positive offsets between S3 (S3A and S3B) and MODIS/MISR AOD products are observed over land. Over ocean, difference between S3 and MODIS and MISR is, with only few exceptions, within the AD. Globally, differences between S3A and MODIS and MISR are within AD. Difference between S3B and MODIS is within AD, while difference with MISR is slightly higher. Regional analysis shows a considerable difference between the products.

7 SUMMARY

Summary for the validation of total AOD

- High positive bias and larger scatter for SLSTR
- decreasing for bias for SLSTR with increasing AOD over land
- constant bias for SLSTR over the whole AOD range over ocean
- SLSTR uncertainties over land significantly larger
- Indication of hemispheric differences in data quality (with less stations in the South), swapped for ATSR and SLSTR

Summary for the validation of FM-AOD

- Overall positive bias for all sensors over land and ocean
- Bias and stdv over land larger for SLSTR than for the ATSR instruments with ~0.045)
- Over ocean bias appears to increase with increasing AOD for SLSTR
- Geographical patterns follow largely those of the AOD errors

Summary for the validation of AOD prognostic uncertainties

- all uncertainty distributions show a double peak (strong over land, in particular for both SLSTR instruments)
- mean of uncertainties is larger over land than over ocean for all sensors
- mean and stdv of uncertainties are significantly larger over land for SLSTR than for the ATSR instruments but similar for all sensors over ocean
- uncertainties are generally slightly too small; for the SLSTR instruments over ocean a larger correction factor is needed, while over land uncertainties need a slight decrease
- uncertainties allow a reasonable split between “good” and “bad” pixels for the lower range with dominating numbers, but not any longer for the higher values
- the smallest uncertainties in the lowest bin have typically too large errors /are too small (in particular for SLSTR instruments)
- statistical distributions of normalized errors per sensor show that on average uncertainties (dominating the statistics) are too small and need correction factors larger than 1. (in particular for SLSTR)
- separate analysis of the two hemispheres proves the favourable scattering angle conditions (avoiding backscatter) which have smaller uncertainties with less need for correction and more meaningful information to split “good” and “bad” pixels; those favourable conditions are in the Northern hemisphere for ATSR (with most AERONET stations dominating the validation statistics) , while they lie in the Southern hemisphere for SLSTR (with less AERONET stations). This is one reason for the weaker performance of AOD from SLSTR than ATSR, but also of the prognostic uncertainties.

Summary for the inter-comparison to other satellite AOD products

-
- Over land, ocean and globally, the difference between AATSR and GRASP is within the accepted difference estimated with the root sum squared method considering the GCOS requirements for AOD. AATSR AOD is higher than MISR AOD over land and lower than MODIS AOD over ocean; both differenced are slightly above the accepted difference. Differences between AATSR and MISR over ocean and AATSR and MODIS over lands are within AD. Regional analysis shows a considerable difference between the products.
- Differences between S3A and S3B AOD are, with one exception for AOd region in March, within the accepted value.
- Positive offsets between S3 (S3A and S3B) and MODIS/MISR AOD products are observed over land. Over ocean, difference between S3 and MODIS and MISR is, with only few exceptions, within the AD. Globally, differences between S3A and MODIS and MISR are within AD. Difference between S3B and MODIS is within AD, while difference with MISR is slightly higher. Regional analysis shows a considerable difference between the products.

8 REFERENCES

Eck, T. F., Holben, B. N., Reid, J. S., Smirnov, A., O'Neill, N. T., Slutsker, I., and Kinne, S.: Wavelength dependence of the optical depth of 5 biomass burning, urban, and desert dust aerosols, J. Geophysical Research, 104, 31 333–31 349, 1999.

Thomas Popp, Gerrit de Leeuw, Christine Bingen, Christoph Brühl, Virginie Capelle, Alain Chedin, Lieven Clarisse, Oleg Dubovik, Roy Grainger, Jan Griesfeller, Andreas Heckel, Stefan Kinne, Lars Klüser, Miriam Kosmale, Pekka Kolmonen, Luca Lelli, Pavel Litvinov, Linlu Mei, Peter North, Simon Pinnock, Adam Povey, Charles Robert, Michael Schulz, Larisa Sogacheva, Kerstin Stebel, Deborah Stein Zweers, Gareth Thomas, Lieuwe Gijsbert Tilstra, Sophie Vandenbussche, Pepijn Veefkind, Marco Vountas and Yong Xue, Development, Production and Evaluation of Aerosol Climate Data Records from European Satellite Observations (Aerosol_cci), Remote Sensing, 8, 421; doi:10.3390/rs8050421, 2016

Christopher J. Merchant, Frank Paul, Thomas Popp, Michael Ablain, Sophie Bontemps, Pierre Defourny, Rainer Hollmann, Thomas Lavergne, Alexandra Laeng, Gerrit de Leeuw, Jonathan Mittaz, Caroline Poulsen, Adam C. Povey, Max Reuter, Shubha Sathyendranath, Stein Sandven, Viktoria F. Sofieva and Wolfgang Wagner, Uncertainty information in climate data records from Earth observation, Earth System Science Data, 9, 511–527, https://doi.org/10.5194/essd-9-511-2017, 2017

Sayer, A. M., Govaerts, Y., Kolmonen, P., Lipponen, A., Luffarelli, M., Mielonen, T., Patadia, F., Popp, T., Povey, A. C., Stebel, K., and Witek, M. L.: A review and framework for the evaluation of pixel-level uncertainty estimates in satellite aerosol remote sensing, Atmospheric Measurements and Techniques, 13, 373–404, https://doi.org/10.5194/amt-13-373-2020, 2020.

O'Neill, N. T.,T. F., Eck, A. Smirnov, B. N.Holben, S. Thulasiraman, Spectral discrimination of coarse and fine mode optical depth, J. Geophys. Res., Vol.. 108, No. D17, 4559-4573, 10.1029/2002JD002975, 2003.

9 ANNEX: STATION VALDIATION STATISTICS (AOD550)

***Table 9.1** Station statistics for ATSR-2 / 1998*

ATSR-2 1998 (3, 6, 9, 12)														
station					AOD550									
station_name	**longitude**	**latitude**	**elevation**	**watermask**	**number**	**meanAeronet**	**meanSatellite**	**mean_bias**	**mean_bias(low)**	**mean_bias(high)**	**rmse**	**stdv**	**Pearson**	**GCOS-fraction**
SANTA_CRUZ	-63.18	-17.80	442	0	19	0.06	0.11	0.05	0.05	0.00	0.06	0.04	-	31.6
Sevilleta	-106.89	34.35	1477	0	444	0.03	0.05	0.02	0.02	0.00	0.03	0.03	0.56	84.5
Kaashidhoo	73.47	4.97	10	1	27	0.24	0.17	-0.06	0.04	-0.08	0.07	0.04	0.91	7.4
SEDE_BOKER	34.78	30.85	480	0	680	0.18	0.31	0.13	0.15	0.09	0.15	0.08	0.80	12.1
LAMTO-STATION	-5.03	6.22	105	0	125	1.40	0.46	-0.94	0.00	-0.94	1.22	0.78	-0.33	1.6
Bermuda	-64.70	32.37	10	1	58	0.13	0.11	-0.02	-0.02	0.00	0.02	0.02	0.68	89.7
Ispra	8.63	45.80	235	0	454	0.27	0.25	-0.02	0.01	-0.04	0.12	0.12	0.77	48.9
Saturn_Island	-123.13	48.78	193	0	22	0.06	0.08	0.02	0.02	0.00	0.02	0.02	-0.00	86.4
Surinam	-55.20	5.80	12	0	37	0.21	0.40	0.19	0.17	0.20	0.20	0.07	0.90	0.0
BONDVILLE	-88.37	40.05	212	0	626	0.18	0.20	0.02	0.04	-0.01	0.08	0.08	0.63	40.1
GSFC	-76.84	38.99	87	0	141	0.10	0.14	0.04	0.04	-0.14	0.05	0.04	0.93	61.7
Tinga_Tingana	139.99	-28.98	38	0	164	0.04	0.23	0.19	0.19	0.00	0.23	0.12	0.49	9.1
LOS_FIEROS_98	-60.93	-14.56	208	0	298	0.11	0.14	0.03	0.03	0.00	0.08	0.08	-0.17	62.8
Arica	-70.31	-18.47	25	0	237	0.28	0.25	-0.02	-0.00	-0.03	0.08	0.08	0.70	35.4
Waskesiu	-106.07	53.91	569	0	291	0.12	0.12	-0.00	-0.01	0.02	0.05	0.05	0.81	65.6
HJAndrews	-122.22	44.24	830	0	316	0.03	0.06	0.03	0.03	0.00	0.06	0.05	0.44	78.8
San_Nicolas	-119.49	33.26	133	1	597	0.04	0.11	0.06	0.06	0.00	0.08	0.06	0.22	42.7
Ulaangom	92.08	49.97	944	0	127	0.10	0.07	-0.03	-0.03	0.00	0.05	0.04	0.35	46.5
CART_SITE	-97.49	36.61	318	0	462	0.13	0.14	0.01	0.01	-0.00	0.04	0.04	0.89	74.5
Barbados	-59.62	13.15	112	1	4	0.26	0.14	-0.12	0.00	-0.12	0.13	0.03	-	0.0
Dalanzadgad	104.42	43.58	1470	0	125	0.07	0.06	-0.01	-0.01	0.00	0.03	0.03	0.56	69.6
Concepcion	-62.03	-16.14	500	0	158	0.28	0.29	0.01	0.00	0.01	0.18	0.18	-0.81	0.0
Rame_Head	-4.22	50.32	105	1	63	0.05	0.07	0.02	0.02	0.00	0.03	0.03	0.77	85.7
Egbert	-79.78	44.23	264	0	151	0.11	0.10	-0.01	-0.01	0.00	0.04	0.04	0.29	75.5
Thompson	-97.85	55.80	218	0	49	0.20	0.20	-0.00	0.03	-0.00	0.05	0.05	0.27	71.4
Bo-za_Creek	-148.32	64.74	353	0	228	0.09	0.11	0.02	0.02	0.00	0.03	0.02	0.45	82.0
Mauna_Loa	-155.58	19.54	3402	1	90	0.01	0.11	0.10	0.10	0.00	0.11	0.04	0.11	3.3
Mongu	23.15	-15.25	1047	0	249	0.34	0.43	0.09	0.12	0.08	0.13	0.10	0.84	30.1
Joberg	28.03	-26.19	1736	0	284	0.17	0.18	0.01	0.05	-0.03	0.11	0.11	0.33	34.2
Bahrain	50.61	26.21	25	1	365	0.19	0.21	0.01	0.04	-0.03	0.08	0.08	0.79	51.0

Chequamegon	-90.25	45.93	485	0	248	0.17	0.21	0.04	0.04	0.00	0.05	0.02	0.92	44.8
Oyster	-75.93	37.30	8	1	32	0.39	0.34	-0.06	-0.00	-0.07	0.07	0.05	0.93	40.6
USDA	-76.88	39.03	50	0	172	0.10	0.13	0.03	0.03	-0.03	0.04	0.03	0.91	69.2
NCU_Taiwan	121.19	24.97	171	1	45	0.11	0.14	0.03	0.03	0.00	0.08	0.08	-0.00	42.2
Skukuza	31.59	-24.99	265	0	232	0.21	0.28	0.08	0.01	0.16	0.12	0.09	0.92	35.8
Ilorin	4.67	8.48	400	0	258	0.64	0.58	-0.05	0.00	-0.05	0.09	0.07	0.95	52.7

Table 9.2 *Station statistics for AATSR / 2008*

AATSR 2008 (3, 6, 9, 12)														
station					AOD550									
station_name	**longitude**	**latitude**	**elevation**	**watermask**	**number**	**meanAeronet**	**meanSatellite**	**mean_bias**	**mean_bias(low)**	**mean_bias(high)**	**rmse**	**stdv**	**Pearson**	**GCOS-fraction**
Hefei	117.16	31.90	36	0	313	0.72	0.54	-0.18	0.00	-0.18	0.29	0.23	-0.29	38.0
REUNION_ST_DENIS	55.48	-20.90	93	1	338	0.06	0.09	0.03	0.03	0.00	0.05	0.03	0.44	58.6
DMN_Maine_Soroa	12.02	13.22	350	0	772	0.48	0.64	0.16	0.13	0.17	0.28	0.23	0.71	14.4
ETNA	15.02	37.61	736	1	242	0.08	0.06	-0.02	-0.02	0.00	0.05	0.05	0.34	61.6
Lecce_University	18.11	40.34	30	1	400	0.12	0.12	0.00	0.00	0.00	0.03	0.03	0.75	82.0
Cabo_Raso	-9.49	38.71	20	1	153	0.09	0.09	0.00	0.00	0.00	0.05	0.05	0.16	63.4
Caceres	-6.34	39.48	397	0	892	0.06	0.11	0.05	0.05	0.00	0.07	0.05	0.61	54.0
El_Arenosillo	-6.73	37.10	59	0	697	0.09	0.10	0.01	0.01	0.00	0.04	0.04	0.52	77.6
Saada	-8.16	31.63	420	0	999	0.17	0.18	0.01	-0.01	0.03	0.07	0.07	0.91	52.6
Walker_Branch	-84.29	35.96	365	0	522	0.13	0.14	0.01	0.01	-0.05	0.05	0.05	0.72	66.5
Hermosillo	-110.96	29.07	237	0	558	0.10	0.09	-0.02	-0.02	-0.01	0.05	0.04	0.77	64.5
Yaqui	-109.91	27.28	40	0	260	0.07	0.04	-0.03	-0.03	0.00	0.04	0.03	0.46	58.5
Guam	144.80	13.43	62	1	119	0.00	0.09	0.09	0.09	0.00	0.09	0.03	-	0.0
Jingtai	104.10	37.33	1583	0	255	0.35	0.23	-0.12	0.02	-0.12	0.15	0.09	0.48	30.2
Kuwait_University	47.97	29.33	42	0	550	0.57	0.34	-0.23	-0.01	-0.25	0.32	0.23	0.63	18.2
Solar_Village	46.40	24.91	764	0	999	0.42	0.44	0.02	0.07	0.01	0.12	0.11	0.94	31.4
Avignon	4.88	43.93	32	0	714	0.17	0.14	-0.03	-0.02	-0.10	0.07	0.07	0.93	73.8
Barcelona	2.11	41.39	125	0	539	0.11	0.09	-0.02	0.01	-0.12	0.07	0.06	0.59	65.5
Blida	2.88	36.51	230	0	738	0.15	0.13	-0.03	-0.01	-0.08	0.07	0.06	0.88	63.0
Burjassot	-0.42	39.51	104	0	551	0.09	0.10	0.01	0.01	-0.08	0.05	0.05	0.50	67.2
Carpentras	5.06	44.08	107	0	667	0.15	0.13	-0.02	-0.01	-0.12	0.08	0.08	0.87	68.8
IER_Cinzana	-5.93	13.28	285	0	999	0.41	0.48	0.07	0.03	0.07	0.13	0.11	0.88	34.9
OHP_OBSERVATOIRE	5.71	43.94	680	0	484	0.09	0.10	0.02	0.02	0.00	0.03	0.03	0.83	80.0
Manaus	-60.04	-2.60	93	0	207	0.20	0.22	0.02	0.03	0.01	0.04	0.03	0.83	76.3
COVE_SEAPRISM	-75.71	36.90	24	1	218	0.17	0.18	0.01	0.02	-0.00	0.04	0.04	0.90	77.1
Wallops	-75.47	37.93	37	1	261	0.12	0.16	0.04	0.05	-0.04	0.07	0.06	0.58	53.3
Mauna_Loa	-155.58	19.54	3402	1	246	0.01	0.11	0.10	0.10	0.00	0.12	0.07	0.09	20.3
Tinga_Tingana	139.99	-28.98	38	0	999	0.03	0.11	0.08	0.08	0.00	0.11	0.08	0.07	22.2
Mukdahan	104.68	16.61	166	0	379	0.66	0.79	0.13	0.00	0.13	0.17	0.10	0.89	17.7
Pimai	102.56	15.18	220	0	467	0.57	0.65	0.08	0.00	0.08	0.12	0.09	0.88	34.3
Silpakorn_Univ	100.04	13.82	72	0	606	0.53	0.53	-0.00	0.04	-0.01	0.10	0.10	0.95	47.7

Kanpur	80.23	26.51	123	0	249	0.44	0.56	0.12	0.46	-0.05	0.29	0.27	0.53	15.7
Abu_Al_Bukhoosh	53.15	25.50	24	1	633	0.39	0.45	0.06	0.07	0.06	0.10	0.08	0.95	31.9
Mezaira	53.75	23.10	201	0	468	0.26	0.42	0.17	0.16	0.17	0.19	0.09	0.92	3.4
IMS-METU-ERDEMLI	34.26	36.56	3	0	749	0.22	0.16	-0.06	0.01	-0.14	0.13	0.11	0.67	53.0
Sevastopol	33.52	44.62	80	1	154	0.17	0.20	0.04	0.03	0.05	0.07	0.06	0.65	55.2
Modena	10.95	44.63	56	0	691	0.17	0.13	-0.04	-0.03	-0.06	0.07	0.06	0.81	48.5
Tamanrasset_INM	5.53	22.79	1377	0	999	0.25	0.32	0.07	0.07	0.08	0.11	0.09	0.92	24.7
Toulon	6.01	43.14	50	1	298	0.12	0.13	0.00	0.02	-0.25	0.07	0.07	0.95	79.5
Venise	12.51	45.31	10	0	588	0.19	0.20	0.00	0.03	-0.03	0.06	0.06	0.81	55.3
Capo_Verde	-22.94	16.73	60	1	410	0.38	0.43	0.04	0.01	0.05	0.07	0.05	0.98	54.6
Campo_Grande_SONDA	-54.54	-20.44	677	0	283	0.10	0.20	0.10	0.10	0.00	0.16	0.12	-0.11	26.5
Trelew	-65.31	-43.25	15	0	273	0.04	0.06	0.02	0.02	0.00	0.05	0.04	0.40	78.0
Halifax	-63.59	44.64	65	0	21	0.06	0.17	0.12	0.12	0.00	0.12	0.03	-0.84	0.0
Fresno	-119.77	36.78	97	0	547	0.17	0.18	0.02	0.01	0.07	0.07	0.07	0.89	68.9
Canberra	149.11	-35.27	600	0	638	0.04	0.06	0.02	0.02	0.00	0.04	0.04	-0.15	66.8
Lake_Argyle	128.75	-16.11	150	0	708	0.08	0.16	0.09	0.09	0.00	0.11	0.07	0.45	25.3
Hong_Kong_PolyU	114.18	22.30	30	1	15	0.32	0.37	0.05	0.00	0.05	0.10	0.08	0.93	53.3
ICIPE-Mbita	34.21	-0.43	1152	0	168	0.22	0.25	0.03	-0.01	0.05	0.07	0.07	0.84	53.0
Dakar	-16.96	14.39	21	1	568	0.48	0.52	0.04	0.04	0.04	0.36	0.36	0.62	28.7
La_Parguera	-67.05	17.97	12	1	602	0.10	0.12	0.02	0.02	0.04	0.05	0.04	0.88	70.9
EPA-NCU	121.19	24.97	144	1	105	0.48	0.44	-0.04	0.00	-0.04	0.11	0.11	0.70	28.6
Qiandaohu	119.05	29.56	133	0	157	0.86	0.77	-0.09	0.00	-0.09	0.29	0.27	0.81	30.6
Taihu	120.22	31.42	20	0	165	0.48	0.45	-0.03	0.02	-0.03	0.13	0.13	0.88	33.3
Taipei_CWB	121.54	25.01	26	1	59	0.48	0.46	-0.02	0.00	-0.02	0.12	0.12	0.93	33.9
Issyk-Kul	76.98	42.62	1650	0	294	0.13	0.14	0.01	0.01	0.03	0.04	0.03	0.89	88.1
CRPSM_Malindi	40.19	-3.00	12	0	101	0.25	0.23	-0.02	-0.03	-0.02	0.16	0.15	0.21	30.7
Granada	-3.61	37.16	680	0	593	0.10	0.08	-0.02	-0.02	0.00	0.05	0.04	0.53	59.2
GSFC	-76.84	38.99	87	0	471	0.13	0.16	0.04	0.04	0.03	0.06	0.05	0.80	61.6
MD_Science_Center	-76.61	39.28	15	0	226	0.13	0.15	0.02	0.02	-0.02	0.05	0.05	0.81	62.8
Birdsville	139.35	-25.90	46	0	999	0.03	0.11	0.08	0.10	-0.26	0.13	0.09	0.13	17.5
Agoufou	-1.48	15.35	305	0	999	0.34	0.46	0.12	0.10	0.13	0.15	0.09	0.93	11.8
Frenchman_Flat	-115.93	36.81	940	0	67	0.06	0.04	-0.02	-0.02	0.00	0.03	0.02	0.24	85.1
Railroad_Valley	-115.69	38.50	1437	0	950	0.06	0.07	0.01	0.01	0.00	0.04	0.04	0.33	68.7
Nes_Ziona	34.79	31.92	40	0	63	0.48	0.40	-0.08	0.00	-0.08	0.11	0.07	0.95	41.3
SEDE_BOKER	34.78	30.85	480	0	999	0.24	0.29	0.05	0.10	-0.01	0.16	0.15	0.69	12.0
Izana	-16.50	28.31	2401	1	198	0.08	0.29	0.21	0.13	0.51	0.27	0.17	0.97	4.0

Tudor_Hill	-64.88	32.26	51	1	335	0.12	0.13	0.01	0.01	0.00	0.04	0.03	0.85	74.3
Karachi	67.14	24.95	49	0	725	0.40	0.43	0.03	0.02	0.03	0.10	0.09	0.88	40.1
Bucharest_Inoe	26.03	44.35	89	0	281	0.20	0.18	-0.02	-0.02	-0.02	0.06	0.06	0.80	56.2
Le_Fauga	1.28	43.38	193	0	17	0.12	0.09	-0.03	-0.03	0.00	0.03	0.01	0.00	82.4
Petrolina_SONDA	-40.32	-9.07	381	0	476	0.11	0.19	0.08	0.08	0.06	0.12	0.10	0.60	36.1
BSRN_BAO_Boulder	-105.01	40.05	1604	0	604	0.11	0.09	-0.02	-0.02	-0.00	0.05	0.05	0.76	57.3
Chiang_Mai_Met_Sta	98.97	18.77	312	0	681	0.47	0.41	-0.06	-0.00	-0.07	0.14	0.13	0.92	33.6
MCO-Hanimaadhoo	73.18	6.78	13	1	64	0.16	0.14	-0.03	-0.00	-0.11	0.06	0.05	0.91	84.4
CART_SITE	-97.49	36.61	318	0	721	0.12	0.10	-0.02	-0.02	0.00	0.05	0.05	0.61	60.3
Univ_of_Houston	-95.34	29.72	65	0	254	0.14	0.14	-0.00	-0.00	0.00	0.04	0.04	0.76	78.0
Monterey	-121.85	36.59	50	0	646	0.07	0.07	-0.01	-0.00	-0.08	0.04	0.04	0.44	84.5
Bac_Lieu	105.73	9.28	10	1	226	0.19	0.23	0.04	0.04	0.04	0.11	0.10	0.32	24.8
XiangHe	116.96	39.75	36	0	565	0.47	0.50	0.04	0.03	0.05	0.13	0.12	0.97	58.2
Gandhi_College	84.13	25.87	60	0	99	0.70	0.54	-0.16	0.00	-0.16	0.18	0.08	-0.00	12.1
Tuxtla_Gutierrez	-93.15	16.75	590	0	282	0.11	0.10	-0.02	-0.02	0.00	0.06	0.05	0.26	53.9
NUIST	118.72	32.21	62	0	293	0.92	0.75	-0.18	0.00	-0.18	0.25	0.18	0.64	20.8
Xanthi	24.92	41.15	54	0	74	0.36	0.27	-0.08	0.03	-0.10	0.10	0.06	0.75	16.2
Ragged_Point	-59.43	13.17	40	1	99	0.05	0.07	0.02	0.02	0.00	0.03	0.01	0.46	90.9
White_Sands_HELSTF	-106.34	32.63	1207	0	999	0.05	0.06	0.01	0.01	0.00	0.04	0.03	0.38	83.0
Mexico_City	-99.18	19.33	2268	0	329	0.22	0.17	-0.05	-0.05	-0.05	0.13	0.12	0.15	20.7
Banizoumbou	2.67	13.55	274	0	956	0.43	0.51	0.08	0.05	0.09	0.16	0.13	0.83	33.8
IMAA_Potenza	15.72	40.60	770	0	390	0.18	0.17	-0.01	0.00	-0.03	0.05	0.05	0.96	70.0
Rome_Tor_Vergata	12.65	41.84	130	0	542	0.16	0.13	-0.03	-0.01	-0.10	0.06	0.05	0.71	62.4
Tremiti	15.49	42.12	40	1	6	0.07	0.02	-0.05	-0.05	0.00	0.05	0.00	-	0.0
CEILAP-BA	-58.51	-34.56	26	0	470	0.09	0.18	0.09	0.11	-0.04	0.15	0.12	0.01	23.8
Gwangju_GIST	126.84	35.23	52	0	315	0.22	0.24	0.02	0.02	0.01	0.08	0.07	0.95	66.7
FORTH_CRETE	25.28	35.33	20	1	362	0.15	0.13	-0.02	-0.01	-0.05	0.05	0.05	0.82	66.9
Midway_Island	-177.38	28.21	20	1	62	0.06	0.06	0.00	-0.00	0.07	0.02	0.02	0.98	93.5
Osaka	135.59	34.65	50	0	204	0.22	0.25	0.03	0.02	0.03	0.10	0.10	0.19	43.6
Shirahama	135.36	33.69	10	1	277	0.18	0.19	0.02	0.04	-0.03	0.04	0.04	0.96	62.5
La_Laguna	-16.32	28.48	568	1	93	0.22	0.27	0.05	-0.01	0.19	0.11	0.10	1.00	66.7
Santa_Cruz_Tenerife	-16.25	28.47	52	1	187	0.22	0.22	-0.00	-0.02	0.04	0.04	0.04	0.99	64.2
Guadeloup	-61.53	16.22	39	1	47	0.14	0.13	-0.01	0.02	-0.03	0.03	0.03	0.98	78.7
EVK2-CNR	86.81	27.96	5079	0	42	0.03	0.08	0.05	0.05	0.00	0.07	0.04	-0.12	35.7

Palencia	-4.52	41.99	750	0	531	0.12	0.14	0.02	0.02	0.00	0.05	0.05	0.74	58.8
Skukuza	31.59	-24.99	265	0	12	0.13	0.20	0.07	0.07	0.00	0.09	0.05	-	33.3
Villefranche	7.33	43.68	130	0	289	0.08	0.11	0.02	0.02	0.00	0.05	0.05	0.57	67.1
Dunedin	170.51	-45.86	43	1	143	0.02	0.06	0.03	0.03	0.00	0.04	0.03	-0.15	65.0
Xinglong	117.58	40.40	899	0	420	0.21	0.31	0.10	0.08	0.14	0.14	0.10	0.95	37.4
Lahore	74.26	31.48	209	0	56	0.35	0.25	-0.10	0.00	-0.10	0.10	0.02	-0.00	0.0
CCNY	-73.95	40.82	100	0	153	0.09	0.08	-0.01	-0.01	0.00	0.03	0.03	0.48	71.2
SACOL	104.14	35.95	1965	0	526	0.23	0.16	-0.08	-0.05	-0.13	0.11	0.08	0.59	19.0
Billerica	-71.27	42.53	82	0	276	0.11	0.13	0.02	0.02	0.00	0.04	0.03	0.88	80.8
Beijing	116.38	39.98	92	0	64	0.12	0.15	0.03	0.03	0.00	0.03	0.02	-0.00	79.7
Zinder_DMN	8.98	13.78	460	0	451	0.40	0.50	0.10	0.13	0.10	0.19	0.16	0.89	10.0
NCU_Taiwan	121.19	24.97	171	1	134	0.12	0.13	0.00	0.03	-0.17	0.09	0.09	0.71	53.0
Hamburg	9.97	53.57	120	0	244	0.14	0.16	0.01	0.02	-0.03	0.05	0.04	0.81	70.5
Karlsruhe	8.43	49.09	140	0	113	0.10	0.12	0.02	0.02	0.00	0.04	0.03	0.95	73.5
Munich_University	11.57	48.15	533	0	295	0.18	0.17	-0.01	-0.00	-0.07	0.06	0.06	0.74	49.8
Singapore	103.78	1.30	30	1	7	0.18	0.81	0.63	0.63	0.00	0.63	0.03	0.00	0.0
Mongu	23.15	-15.25	1047	0	926	0.30	0.30	0.01	0.01	0.00	0.12	0.12	0.86	36.6
Minsk	27.60	53.92	235	0	230	0.24	0.22	-0.02	-0.05	0.01	0.07	0.07	0.89	31.3
Brussels	4.35	50.78	120	0	208	0.20	0.20	-0.00	0.04	-0.07	0.08	0.08	0.76	54.8
Noto	137.14	37.33	200	1	144	0.14	0.19	0.05	0.05	0.00	0.06	0.03	0.76	40.3
Yakutsk	129.37	61.66	118	0	585	0.16	0.18	0.02	0.02	0.01	0.04	0.03	0.93	77.3
Kandahar	65.85	31.51	1007	0	50	0.43	0.43	0.01	0.00	0.01	0.08	0.08	-0.68	28.0
Kuujjuarapik	-77.76	55.28	20	0	101	0.09	0.12	0.03	0.03	0.00	0.04	0.03	0.17	75.2
Bratts_Lake	-104.71	50.20	586	0	658	0.09	0.08	-0.00	-0.00	0.01	0.03	0.03	0.79	83.6
Bo-za_Creek	-148.32	64.74	353	0	226	0.08	0.07	-0.01	-0.01	0.00	0.03	0.03	0.82	86.7
Hangzhou_City	120.16	30.29	30	0	134	0.32	0.36	0.04	0.00	0.04	0.13	0.12	0.86	53.7
Irkutsk	103.09	51.80	670	0	99	0.20	0.13	-0.07	-0.01	-0.14	0.10	0.08	-0.51	13.1
La_Paz	-68.07	-16.54	3439	0	205	0.08	0.08	0.01	0.01	0.00	0.04	0.04	0.01	87.3
Key_Biscayne	-80.16	25.73	10	1	41	0.25	0.20	-0.05	-0.02	-0.08	0.06	0.04	0.98	51.2
SERC	12.51	45.31	10	0	368	0.13	0.15	0.02	0.02	0.03	0.05	0.05	0.84	67.4
Gustav_Dalen_Tower	17.47	58.59	25	1	167	0.13	0.14	0.01	0.01	0.00	0.02	0.02	0.93	98.2
Helgoland	7.89	54.18	33	1	89	0.14	0.16	0.02	0.03	-0.05	0.04	0.03	0.90	61.8
Leipzig	12.44	51.35	125	0	159	0.15	0.12	-0.03	-0.02	-0.11	0.04	0.03	0.90	64.2
Hornsund	15.54	77.00	12	1	264	0.09	0.11	0.02	0.02	0.00	0.05	0.05	0.05	52.3
Alta_Floresta	-56.10	-9.87	277	0	575	0.20	0.34	0.14	0.14	0.12	0.16	0.09	0.96	8.3
Appledore_Island	-70.62	42.99	35	0	128	0.09	0.14	0.05	0.05	0.00	0.06	0.04	0.72	50.0
Kangerlussuaq	-50.62	67.00	320	0	207	0.06	0.17	0.11	0.11	0.00	0.12	0.05	0.64	7.7
Pickle_Lake	-90.22	51.45	393	0	91	0.07	0.10	0.03	0.03	-0.01	0.03	0.02	0.94	74.7
UCSB	-119.85	34.42	33	0	82	0.11	0.08	-0.03	-0.03	0.00	0.05	0.04	0.38	58.5

Belsk	20.79	51.84	190	0	176	0.18	0.21	0.03	0.03	0.01	0.05	0.04	0.93	71.6
Helsinki_Lighthouse	24.93	59.95	20	0	96	0.08	0.10	0.02	0.02	0.00	0.03	0.02	0.44	68.8
Hyytiala	24.30	61.85	191	0	112	0.11	0.13	0.02	0.02	0.00	0.03	0.03	0.93	70.5
Kuopio	27.63	62.89	105	0	138	0.10	0.10	0.00	0.00	0.05	0.02	0.02	0.86	88.4
Toravere	26.47	58.26	85	0	385	0.11	0.09	-0.02	-0.02	0.00	0.03	0.03	0.69	71.7
Evora	-7.91	38.57	293	0	836	0.08	0.10	0.03	0.03	0.04	0.06	0.06	0.52	72.2
UAHuntsville	-86.64	34.73	223	0	383	0.18	0.17	-0.01	0.02	-0.03	0.05	0.05	0.64	64.0
Waskesiu	-106.07	53.91	569	0	208	0.08	0.07	-0.01	-0.01	0.00	0.03	0.03	0.62	84.1
Bushland	-102.09	35.19	1168	0	801	0.10	0.08	-0.02	-0.02	0.00	0.04	0.04	0.57	67.2
Kyiv	30.50	50.36	200	0	166	0.20	0.19	-0.02	-0.04	0.03	0.05	0.05	0.96	41.6
Moscow_MSU_MO	37.52	55.71	192	0	182	0.24	0.24	0.01	-0.00	0.02	0.08	0.08	0.94	57.1
Zvenigorod	36.78	55.69	200	0	134	0.15	0.16	0.01	0.01	0.00	0.03	0.02	0.87	91.8
CUIABA-MIRANDA	-56.07	-15.73	210	0	397	0.34	0.42	0.08	0.05	0.09	0.13	0.10	0.92	41.6
Fort_McMurray	-111.48	56.75	360	0	201	0.10	0.10	-0.00	-0.00	0.00	0.02	0.02	0.96	97.0
Chilbolton	-1.44	51.14	88	0	185	0.23	0.22	-0.01	0.02	-0.01	0.05	0.05	0.65	60.0
Chapais	-74.98	49.82	373	0	118	0.05	0.07	0.02	0.02	0.00	0.02	0.02	0.90	89.0
Egbert	-79.78	44.23	264	0	140	0.11	0.12	0.00	0.00	0.00	0.02	0.02	0.92	94.3
Toronto	-79.47	43.79	186	0	14	0.05	0.06	0.01	0.01	0.00	0.06	0.06	-0.00	64.3
Kirtland_AFB	-106.51	34.95	1711	0	999	0.06	0.06	0.00	0.00	0.00	0.04	0.04	0.28	78.9
Ussuriysk	132.16	43.70	280	0	496	0.26	0.29	0.03	0.01	0.04	0.06	0.05	0.96	75.4
Fontainebleau	2.68	48.41	85	0	223	0.15	0.15	0.00	0.01	-0.11	0.06	0.06	0.64	57.4
Mainz	8.30	50.00	150	0	229	0.15	0.13	-0.02	-0.04	0.00	0.05	0.04	0.86	46.7
Harvard_Forest	-72.19	42.53	339	0	96	0.11	0.15	0.05	0.05	0.00	0.06	0.03	0.00	44.8
MVCO	-70.57	41.33	10	1	161	0.11	0.15	0.04	0.06	-0.01	0.08	0.06	0.55	48.4
Sioux_Falls	-96.63	43.74	505	0	249	0.07	0.07	0.00	0.00	0.00	0.02	0.02	0.75	89.2
Eilat	34.92	29.50	15	0	308	0.22	0.24	0.02	0.03	0.02	0.07	0.07	0.69	43.2
Ersa	9.36	43.00	80	1	248	0.16	0.18	0.02	0.02	0.01	0.04	0.04	0.83	75.0
BONDVILLE	-88.37	40.05	212	0	620	0.20	0.18	-0.02	-0.02	-0.03	0.04	0.04	0.98	85.0
Messina	15.57	38.20	15	1	158	0.27	0.26	-0.00	-0.03	-0.00	0.04	0.04	0.81	55.7
Howland	-68.74	45.20	120	0	37	0.13	0.20	0.07	0.02	0.12	0.09	0.06	0.97	45.9
Thompson_Farm	-70.95	43.11	26	0	229	0.09	0.10	0.01	0.01	0.00	0.03	0.02	0.80	86.0
Kelowna_UAS	-119.40	49.94	456	0	358	0.09	0.08	-0.00	-0.02	0.08	0.06	0.06	0.92	85.5
Trinidad_Head	-124.15	41.05	105	0	466	0.07	0.08	0.01	0.01	0.00	0.04	0.04	0.57	65.0
Rimrock	-116.99	46.49	824	0	493	0.09	0.08	-0.00	0.00	-0.18	0.05	0.05	0.78	81.3
Zhangye	100.28	39.08	1461	0	81	0.10	0.08	-0.01	-0.01	0.00	0.04	0.04	0.00	79.0
Yekaterinburg	59.54	57.04	300	0	61	0.17	0.13	-0.03	-0.03	0.00	0.04	0.02	0.71	63.9
ATHENS-NOA	23.72	37.97	130	1	108	0.18	0.14	-0.04	-0.02	-0.06	0.05	0.03	0.94	43.5
Oostende	2.92	51.22	23	0	249	0.17	0.17	-0.01	-0.02	0.01	0.03	0.03	0.75	73.5
Saturn_Island	-123.13	48.78	193	0	78	0.04	0.08	0.04	0.04	0.00	0.05	0.04	0.85	73.1

Missoula	-114.08	46.92	976	0	587	0.07	0.06	-0.01	-0.01	0.15	0.03	0.02	0.82	93.4
Bozeman	-111.05	45.66	1507	0	184	0.07	0.07	0.00	0.00	0.00	0.02	0.02	0.61	96.2
Palaiseau	2.21	48.71	156	0	264	0.15	0.13	-0.02	-0.01	-0.06	0.05	0.05	0.52	72.3
PEARL	-86.42	80.05	615	0	372	0.03	0.06	0.03	0.03	0.00	0.03	0.01	0.57	80.4
Ilorin	4.67	8.48	400	0	249	0.63	0.61	-0.02	0.00	-0.02	0.07	0.06	0.98	68.7
Iqaluit	-68.54	63.75	15	0	56	0.03	0.09	0.06	0.06	0.00	0.07	0.03	-0.17	16.1
New_Delhi	77.18	28.63	240	0	4	0.87	0.76	-0.10	0.00	-0.10	0.10	0.00	-	0.0
Dhabi	54.38	24.48	15	0	40	0.62	0.87	0.25	0.00	0.25	0.25	0.04	0.73	0.0
Davos	9.84	46.81	1589	0	4	0.10	0.09	-0.02	-0.02	0.00	0.03	0.02	-	100.0
Laegeren	8.36	47.48	763	0	204	0.07	0.11	0.04	0.04	0.00	0.06	0.04	0.47	54.9
OPAL	-85.94	79.99	5	0	558	0.03	0.05	0.02	0.02	0.00	0.03	0.01	0.16	92.3
Valladolid_Sci	-4.71	41.66	701	0	192	0.11	0.15	0.03	0.03	0.00	0.05	0.03	0.93	53.1
Rio_Branco	-67.87	-9.96	212	0	348	0.22	0.35	0.13	0.19	0.06	0.16	0.10	0.90	20.1
Thule	-68.77	76.52	225	1	20	0.04	0.06	0.02	0.02	0.00	0.02	0.01	0.87	85.0
Bac_Giang	106.23	21.29	15	0	9	1.02	0.64	-0.38	0.00	-0.38	0.38	0.04	-0.00	0.0
Shouxian	116.78	32.56	22	0	191	0.74	0.65	-0.09	0.00	-0.09	0.23	0.21	0.96	26.7
Baneasa	26.08	44.51	127	0	108	0.15	0.17	0.02	0.00	0.06	0.05	0.04	0.95	71.3
Arica	-70.31	-18.47	25	0	202	0.16	0.09	-0.07	-0.05	-0.16	0.09	0.06	-0.08	31.7
Tomsk	85.05	56.48	174	0	110	0.16	0.17	0.02	0.02	0.00	0.02	0.01	0.01	94.5
Moldova	28.82	47.00	205	0	193	0.17	0.19	0.02	0.02	0.02	0.02	0.02	0.97	93.3
CARTEL	-71.93	45.38	251	0	326	0.11	0.14	0.03	0.02	0.05	0.05	0.04	0.93	72.1
HJAndrews	-122.22	44.24	830	0	533	0.08	0.10	0.02	0.01	0.12	0.05	0.05	0.92	82.4
Thessaloniki	22.96	40.63	60	0	200	0.30	0.28	-0.01	0.02	-0.04	0.05	0.05	0.98	72.5
Sao_Paulo	-46.73	-23.56	786	0	128	0.27	0.16	-0.11	-0.09	-0.12	0.13	0.06	0.62	9.4
Nauru	166.92	-0.52	7	1	18	0.03	0.07	0.04	0.04	0.00	0.04	0.01	0.98	72.2
Amsterdam_Isla nd	77.57	-37.80	49	1	95	0.07	0.08	0.01	0.01	0.00	0.02	0.01	0.60	98.9
Autilla	-4.60	42.00	873	0	180	0.14	0.16	0.02	0.02	0.00	0.05	0.05	-0.02	74.4
Churchill	-93.82	58.74	10	1	70	0.08	0.11	0.03	0.03	0.00	0.04	0.03	0.57	65.7
Andenes	16.01	69.28	379	1	238	0.08	0.07	-0.01	-0.01	0.00	0.03	0.03	-0.17	78.2
Cabauw	4.93	51.97	0	0	160	0.18	0.21	0.03	0.02	0.03	0.06	0.05	0.71	51.2
Lille	3.14	50.61	60	0	314	0.27	0.24	-0.03	-0.02	-0.04	0.08	0.07	0.74	56.4
Paris	2.36	48.85	50	0	207	0.14	0.14	-0.00	-0.00	0.00	0.03	0.03	0.59	92.3
Ji_Parana_SE	-61.85	-10.93	218	0	22	0.47	0.64	0.17	0.00	0.17	0.17	0.04	0.00	0.0
KONZA_EDC	-96.61	39.10	341	0	81	0.13	0.06	-0.07	-0.07	0.00	0.07	0.01	0.00	0.0
Pantnagar	79.52	29.05	241	0	445	0.44	0.41	-0.03	0.00	-0.03	0.18	0.17	0.47	22.9
TABLE_MOUN TAIN_CA	-117.68	34.38	2200	0	401	0.04	0.08	0.04	0.04	0.00	0.07	0.06	0.55	64.3
Ispra	8.63	45.80	235	0	104	0.07	0.11	0.03	0.03	0.08	0.05	0.03	0.92	61.5
Ames	-93.77	42.02	338	0	124	0.13	0.05	-0.08	-0.08	-0.07	0.08	0.01	0.98	1.6
Dunkerque	2.37	51.04	5	0	115	0.18	0.20	0.02	0.04	0.01	0.04	0.03	0.71	80.0
CEILAP-RG	-69.32	-51.60	19	0	115	0.02	0.07	0.06	0.06	0.00	0.07	0.04	0.17	38.3

Songkhla_Met_Sta	100.60	7.18	15	0	50	0.08	0.13	0.05	0.05	0.00	0.06	0.03	0.00	52.0
Cape_San_Juan	-65.62	18.38	15	1	43	0.03	0.06	0.03	0.03	0.00	0.03	0.01	0.68	90.7
Cordoba-CETT	-64.46	-31.52	730	0	266	0.07	0.07	0.01	0.01	0.00	0.04	0.04	0.51	83.1
Dhadnah	56.32	25.51	81	1	284	0.11	0.16	0.05	0.05	0.04	0.07	0.05	0.88	60.2
Gual_Pahari	77.15	28.43	250	0	60	0.40	0.45	0.05	0.00	0.05	0.21	0.20	0.72	11.7
Nainital	79.46	29.36	1939	0	171	0.07	0.25	0.17	0.17	0.00	0.23	0.16	0.07	21.6
Camaguey	-77.85	21.42	122	0	126	0.04	0.08	0.04	0.04	0.00	0.06	0.04	0.06	68.3
Hong_Kong_Hok_Tsui	114.26	22.21	80	1	6	0.20	0.21	0.01	0.01	0.00	0.02	0.01	-	100.0
Crozet_Island	51.85	-46.43	221	1	39	0.06	0.09	0.03	0.03	0.00	0.04	0.01	-0.00	71.8
Ascension_Island	-14.41	-7.98	30	1	60	0.21	0.17	-0.03	0.02	-0.04	0.04	0.02	0.77	60.0
Malaga	-4.48	36.72	56	0	3	0.04	0.08	0.04	0.04	0.00	0.04	0.00	-0.00	100.0
Arcachon	-1.16	44.66	11	0	32	0.18	0.13	-0.05	-0.05	0.00	0.05	0.01	-0.00	25.0

Table 9.3 *Station statistics for SLSTR/SENTINEL-3A / 2019*

SLSTR / S3A 2019 (3, 6, 9, 12)														
station					AOD550									
station_name	longitude	latitude	elevation	watermask	number	meanAeronet	meanSatellite	mean_bias	mean_bias(low)	mean_bias(high)	rmse	stdv	Pearson	gcos-fraction
Jabiru	132.89	-12.66	30	0	999	0.08	0.09	0.01	0.01	0.00	0.05	0.05	0.53	74.2
Anmyon	126.33	36.54	47	1	999	0.33	0.38	0.05	0.06	0.04	0.15	0.14	0.83	27.6
Kaohsiung	120.29	22.68	15	1	799	0.56	0.53	-0.02	0.06	-0.03	0.15	0.15	0.83	37.0
REUNION_ST_DENIS	55.48	-20.90	93	1	999	0.07	0.09	0.02	0.02	0.00	0.05	0.04	0.52	71.2
IMS-METU-ERDEMLI	34.26	36.56	3	0	453	0.12	0.16	0.04	0.04	0.06	0.08	0.07	0.79	58.3
Migal	35.58	33.24	200	0	999	0.30	0.28	-0.02	0.03	-0.03	0.15	0.15	0.71	27.7
Misamfu	31.22	-10.17	1381	0	999	0.08	0.09	0.01	0.01	0.00	0.06	0.06	0.38	65.3
Weizmann_Institute	34.81	31.91	73	0	277	0.16	0.16	-0.00	0.04	-0.06	0.10	0.10	0.50	43.0
Iasi_LOASL	27.56	47.19	175	0	999	0.20	0.20	0.01	0.03	-0.03	0.12	0.12	0.48	28.9
IMAA_Potenza	15.72	40.60	770	0	141	0.10	0.19	0.09	0.09	0.00	0.16	0.14	0.43	29.1
Lamezia_Terme	16.23	38.88	8	1	999	0.17	0.21	0.04	0.04	0.04	0.08	0.07	0.78	42.6
Lecce_University	18.11	40.34	30	1	999	0.15	0.19	0.05	0.04	0.06	0.08	0.06	0.82	39.1
Magurele_Inoe	26.03	44.35	90	0	232	0.11	0.24	0.13	0.13	0.00	0.17	0.11	-0.18	24.6
Napoli_CeSMA	14.31	40.84	50	0	999	0.18	0.21	0.03	0.04	0.02	0.09	0.08	0.77	40.7
Aras_de_los_Olmos	-1.10	39.94	1280	0	660	0.08	0.12	0.04	0.04	0.00	0.09	0.08	0.29	55.3
Burjassot	-0.42	39.51	104	0	538	0.08	0.11	0.03	0.03	0.14	0.06	0.05	0.68	61.7
Izana	-16.50	28.31	2401	1	999	0.03	0.15	0.12	0.12	0.00	0.16	0.09	0.67	21.9
Madrid	-3.72	40.45	680	0	93	0.07	0.16	0.09	0.09	0.00	0.15	0.13	-0.17	28.0
Saada	-8.16	31.63	420	0	30	0.17	0.37	0.20	0.03	0.32	0.32	0.25	0.66	10.0
Valladolid	-4.71	41.66	705	0	38	0.06	0.29	0.23	0.23	0.00	0.26	0.13	-0.16	7.9
Arica	-70.31	-18.47	25	0	800	0.18	0.14	-0.04	-0.04	-0.04	0.08	0.07	0.36	44.2
Cape_San_Juan	-65.62	18.38	15	1	68	0.09	0.13	0.04	0.04	0.00	0.05	0.03	-0.62	69.1
La_Paz	-68.07	-16.54	3439	0	67	0.07	0.16	0.08	0.08	0.00	0.11	0.07	0.36	29.9
Tudor_Hill	-64.88	32.26	51	1	999	0.08	0.12	0.04	0.03	0.07	0.05	0.03	0.88	65.2
SP_Bayboro	-82.63	27.76	5	1	694	0.10	0.19	0.09	0.09	0.12	0.11	0.05	0.74	12.0
Tucson	-110.95	32.23	779	0	708	0.07	0.13	0.05	0.05	0.00	0.11	0.10	-0.08	37.1
White_Sands_HELSTF	-106.34	32.63	1207	0	999	0.08	0.19	0.11	0.11	0.00	0.18	0.14	-0.40	27.7
Saturn_Island	-123.13	48.78	193	0	840	0.07	0.11	0.04	0.04	0.00	0.07	0.05	0.52	64.0
Hankuk_UFS	127.27	37.34	167	0	571	0.28	0.34	0.06	0.06	0.06	0.18	0.17	0.52	21.7
Seoul_SNU	126.95	37.46	116	0	656	0.32	0.40	0.08	0.06	0.09	0.19	0.17	0.72	18.1
Taipei_CWB	121.54	25.01	26	1	222	0.74	0.63	-0.11	0.00	-0.11	0.21	0.17	0.55	17.6
Amsterdam_Island	77.57	-37.80	49	1	136	0.09	0.12	0.03	0.03	0.00	0.04	0.02	0.90	67.6
Chiang_Mai_Met_Sta	98.97	18.77	312	0	999	0.70	0.61	-0.09	-0.01	-0.10	0.28	0.26	0.82	26.4
Silpakorn_Univ	100.04	13.82	72	0	999	0.40	0.38	-0.02	0.07	-0.03	0.18	0.18	0.71	17.8
Gobabeb	15.04	-23.56	405	0	999	0.12	0.18	0.06	0.06	0.07	0.11	0.09	0.78	41.3
Kyiv	30.50	50.36	200	0	973	0.16	0.22	0.06	0.08	-0.04	0.14	0.13	0.18	23.7

Lubango	13.44	-14.96	2047	0	999	0.17	0.24	0.07	0.04	0.18	0.11	0.09	0.97	43.6
Barcelona	2.11	41.39	125	0	999	0.14	0.18	0.04	0.04	0.05	0.08	0.06	0.74	52.3
Coruna	-8.42	43.36	67	1	999	0.09	0.12	0.03	0.03	0.05	0.07	0.06	0.64	50.6
Loftus_MO	-0.86	54.56	159	0	453	0.11	0.17	0.06	0.06	0.09	0.09	0.07	0.87	35.1
OHP_OBSERVATOIRE	5.71	43.94	680	0	999	0.13	0.18	0.05	0.05	0.04	0.10	0.09	0.71	38.3
Tabernas_PSA-DLR	-2.36	37.09	500	0	984	0.11	0.17	0.05	0.05	0.04	0.09	0.08	0.63	33.5
Reykjavik	-21.90	64.13	51	1	999	0.06	0.11	0.05	0.05	0.00	0.07	0.06	0.55	55.0
Amazon_ATTO_Tower	-59.00	-2.14	210	0	417	0.09	0.23	0.14	0.14	0.10	0.17	0.10	0.16	21.1
ARM_Cordoba	-64.73	-32.13	1141	0	374	0.06	0.07	0.01	0.01	0.00	0.04	0.04	0.51	79.7
Lake_Okeechobee	-80.79	26.90	9	0	611	0.18	0.22	0.04	0.07	-0.01	0.13	0.12	0.47	29.6
Mauna_Loa	-155.58	19.54	3402	1	999	0.01	0.11	0.10	0.10	0.00	0.13	0.09	0.01	25.2
Hokkaido_University	141.34	43.08	59	0	537	0.12	0.19	0.06	0.06	0.07	0.10	0.08	0.63	41.7
Lake_Lefroy	121.71	-31.25	300	0	999	0.09	0.10	0.01	0.01	-0.02	0.05	0.04	0.65	81.5
Bac_Lieu	105.73	9.28	10	1	173	0.17	0.24	0.07	0.08	0.03	0.12	0.10	0.20	24.3
NGHIA_DO	105.80	21.05	40	0	13	1.54	1.04	-0.51	0.00	-0.51	0.53	0.17	0.86	0.0
Songkhla_Met_Sta	100.60	7.18	15	0	724	0.23	0.31	0.08	0.08	0.09	0.11	0.07	0.78	28.3
USM_Pe-g	100.30	5.36	51	1	855	0.33	0.37	0.04	0.08	0.03	0.09	0.09	0.75	37.2
Gandhi_College	84.13	25.87	60	0	502	0.51	0.64	0.13	0.00	0.13	0.35	0.33	0.78	2.8
MCO-Hanimaadhoo	73.18	6.78	13	1	969	0.36	0.40	0.04	0.00	0.04	0.07	0.06	0.79	36.6
Cairo_EMA_2	31.29	30.08	70	0	999	0.37	0.29	-0.07	0.00	-0.07	0.14	0.12	0.58	23.4
Galata_Platform	28.19	43.04	31	1	999	0.17	0.24	0.07	0.06	0.09	0.10	0.06	0.80	23.9
Gloria	29.36	44.60	30	1	999	0.14	0.21	0.07	0.08	0.03	0.10	0.07	0.64	23.2
Mongu_Inn	23.13	-15.27	1040	0	435	0.15	0.13	-0.02	-0.01	-0.03	0.05	0.05	0.76	67.1
SEDE_BOKER	34.78	30.85	480	0	260	0.08	0.40	0.32	0.32	0.00	0.42	0.28	0.08	14.6
Thessaloniki	22.96	40.63	60	0	64	0.11	0.16	0.05	0.05	0.00	0.06	0.03	0.84	51.6
AAOT	12.51	45.31	10	0	999	0.19	0.25	0.07	0.10	-0.01	0.14	0.13	0.51	22.9
Banizoumbou	2.67	13.55	274	0	100	0.54	0.62	0.08	0.00	0.08	0.10	0.07	0.00	35.0
Ben_Salem	9.91	35.55	130	0	64	0.06	0.52	0.46	0.46	0.00	0.47	0.12	-0.00	0.0
Ersa	9.36	43.00	80	1	999	0.12	0.17	0.04	0.04	0.08	0.07	0.05	0.90	55.7
Ilorin	4.67	8.48	400	0	168	0.56	0.50	-0.06	0.15	-0.11	0.17	0.16	0.78	14.3
Sirmione_Museo_GC	10.61	45.50	86	0	999	0.24	0.27	0.03	0.11	-0.03	0.15	0.15	0.35	21.7
Toulon	6.01	43.14	50	1	852	0.07	0.12	0.05	0.05	0.00	0.07	0.05	0.15	44.7
Venise	12.51	45.31	10	0	999	0.19	0.25	0.06	0.11	-0.01	0.15	0.13	0.49	18.2
CEILAP-BA	-58.51	-34.56	26	0	499	0.08	0.09	0.00	0.00	0.00	0.04	0.04	0.32	66.3
NASA_KSC	-80.66	28.46	1	0	175	0.12	0.20	0.09	0.09	0.00	0.16	0.13	-0.46	22.3
Bakersfield	-119.00	35.33	108	0	418	0.14	0.17	0.03	0.03	0.00	0.12	0.12	-0.24	25.6
Lake_Argyle	128.75	-16.11	150	0	91	0.07	0.05	-0.02	-0.02	0.00	0.03	0.02	0.00	79.1
Beijing	116.38	39.98	92	0	328	0.21	0.27	0.06	0.14	-0.04	0.22	0.22	0.14	15.2
NhaTrang	109.21	12.20	20	0	414	0.33	0.35	0.02	0.08	-0.01	0.11	0.11	0.81	27.8
AgiaMarina_Xyliatou	33.06	35.04	521	1	856	0.13	0.20	0.07	0.06	0.08	0.10	0.08	0.81	31.4
CUT-TEPAK	33.04	34.67	22	1	999	0.16	0.20	0.04	0.04	0.05	0.08	0.07	0.80	47.1

Messina	15.57	38.20	15	1	751	0.10	0.13	0.04	0.04	0.00	0.07	0.06	0.40	47.9
Dakar	-16.96	14.39	21	1	999	0.39	0.41	0.03	0.03	0.03	0.12	0.12	0.90	39.2
NEON_ONAQ	-112.45	40.18	1656	0	174	0.04	0.30	0.26	0.26	0.00	0.29	0.14	-0.19	3.4
Railroad_Valley	-115.69	38.50	1437	0	88	0.04	0.35	0.30	0.30	0.00	0.37	0.21	-0.21	5.7
USGS_Flagstaff_ROLO	-111.63	35.21	2179	0	992	0.06	0.17	0.11	0.11	0.00	0.16	0.12	-0.08	31.8
Chiba_University	140.10	35.62	60	0	591	0.15	0.22	0.06	0.06	0.07	0.13	0.11	0.55	19.0
EPA-NCU	121.19	24.97	144	1	971	0.32	0.36	0.04	0.09	-0.01	0.15	0.15	0.78	22.2
Dibrugarh_Univ	94.90	27.45	119	0	310	0.49	0.51	0.02	0.00	0.02	0.15	0.15	0.90	37.1
CATUC_Bamenda	10.16	5.95	1293	0	121	0.44	0.53	0.09	0.00	0.09	0.15	0.13	-0.21	21.5
Medenine-IRA	10.64	33.50	33	0	999	0.24	0.34	0.10	0.09	0.11	0.15	0.11	0.85	16.2
Poprad-Ganovce	20.32	49.03	706	0	707	0.16	0.26	0.10	0.10	0.09	0.16	0.13	0.50	23.3
Strzyzow	21.86	49.88	450	0	642	0.16	0.26	0.10	0.13	0.06	0.17	0.13	0.37	16.0
Bayfordbury	-0.10	51.78	75	0	66	0.12	0.10	-0.03	-0.03	0.00	0.07	0.07	0.36	43.9
Rhyl_MO	-3.51	53.26	77	0	186	0.08	0.13	0.05	0.05	0.00	0.09	0.07	-0.12	17.2
Stornoway_MO	-6.18	58.21	82	1	394	0.08	0.12	0.04	0.04	0.00	0.05	0.03	0.74	56.1
Toulouse_MF	1.37	43.57	160	0	164	0.13	0.12	-0.01	0.04	-0.25	0.13	0.13	-0.05	35.4
Appalachian_State	-81.69	36.21	1080	0	921	0.10	0.15	0.05	0.05	0.15	0.10	0.08	0.67	54.0
CCNY	-73.95	40.82	100	0	986	0.12	0.18	0.06	0.06	0.03	0.10	0.08	0.58	31.2
Easton-MDE	-76.08	38.79	4	0	395	0.20	0.27	0.07	0.06	0.08	0.13	0.11	0.71	27.1
Georgia_Tech	-84.40	33.78	294	0	654	0.10	0.17	0.07	0.07	0.00	0.11	0.09	0.73	47.4
MD_Science_Center	-76.61	39.28	15	0	372	0.16	0.26	0.10	0.08	0.15	0.14	0.10	0.81	26.6
NEON_SCBI	-78.14	38.89	354	0	494	0.10	0.14	0.03	0.04	0.01	0.11	0.11	0.30	49.6
NEON_SERC	-76.56	38.89	9	0	101	0.05	0.16	0.11	0.10	0.00	0.13	0.08	0.43	16.8
UMBC	-76.71	39.25	79	0	222	0.16	0.28	0.12	0.09	0.16	0.15	0.10	0.88	22.5
BMKG_GAW_PALU	120.18	-1.65	1370	0	666	0.07	0.15	0.08	0.08	0.00	0.11	0.07	0.55	32.7
Ussuriysk	132.16	43.70	280	0	274	0.23	0.26	0.04	0.06	-0.05	0.14	0.14	0.61	23.0
Doi_Ang_Khang	99.05	19.93	1536	0	697	0.41	0.87	0.45	0.39	0.47	0.52	0.26	0.81	1.3
Fang	99.21	19.91	480	0	718	0.95	0.90	-0.05	0.00	-0.05	0.24	0.24	0.85	31.1
Durban_UKZN	30.94	-29.82	205	0	43	0.12	0.14	0.02	0.02	0.00	0.02	0.02	0.00	86.0
LAMTO-STATION	-5.03	6.22	105	0	183	0.46	0.51	0.05	0.00	0.05	0.14	0.13	0.90	39.3
Billerica	-71.27	42.53	82	0	709	0.09	0.13	0.04	0.05	0.01	0.09	0.08	0.54	39.5
Brookhaven	-72.88	40.87	37	1	999	0.09	0.15	0.06	0.06	0.06	0.08	0.05	0.79	37.1
Hampton_University	-76.34	37.02	12	0	999	0.15	0.22	0.07	0.08	0.06	0.11	0.09	0.70	28.1
NASA_LaRC	-76.38	37.10	5	0	506	0.13	0.20	0.07	0.09	0.03	0.11	0.08	0.77	27.9
Tallahassee	-84.30	30.45	49	0	531	0.14	0.19	0.05	0.05	0.07	0.08	0.06	0.76	38.6
Wallops	-75.47	37.93	37	1	999	0.15	0.24	0.09	0.08	0.09	0.11	0.07	0.84	21.8
Yale_Coastal	-72.73	41.26	0	0	228	0.04	0.11	0.07	0.07	0.00	0.07	0.02	0.83	7.0
ARM_SGP	-97.49	36.61	319	0	734	0.15	0.10	-0.04	-0.04	-0.10	0.09	0.08	0.16	26.8
Modesto	-120.99	37.64	33	0	236	0.08	0.08	-0.00	-0.00	0.00	0.05	0.05	-0.03	61.0
Nong_Khai	102.72	17.88	175	0	729	0.50	0.53	0.03	0.04	0.03	0.15	0.14	0.94	26.6
Kanpur	80.23	26.51	123	0	980	0.53	0.51	-0.02	0.00	-0.02	0.17	0.17	0.75	23.6

DEWA_ResearchCentre	55.37	24.77	86	0	999	0.33	0.33	-0.00	-0.00	-0.00	0.21	0.21	0.58	13.3
Qena_SVU	32.75	26.20	75	0	999	0.24	0.24	0.00	0.04	-0.02	0.13	0.13	0.56	28.9
Leipzig	12.44	51.35	125	0	587	0.14	0.31	0.16	0.12	0.29	0.24	0.18	0.54	18.9
ARIAKE_TOWER	130.27	33.10	15	0	481	0.34	0.45	0.11	0.09	0.12	0.16	0.11	0.82	18.9
Pontianak	109.19	0.08	2	0	17	0.19	0.25	0.06	0.06	0.00	0.11	0.09	-0.00	47.1
Singapore	103.78	1.30	30	1	311	0.32	0.38	0.06	0.11	0.03	0.36	0.36	0.61	17.0
Bhola	90.76	22.23	7	1	230	0.53	0.58	0.06	0.00	0.06	0.17	0.16	0.75	27.0
Dhaka_University	90.40	23.73	34	0	312	0.74	0.67	-0.07	0.00	-0.07	0.18	0.17	0.61	34.0
Masdar_Institute	54.62	24.44	4	0	15	0.14	0.22	0.08	0.08	0.00	0.09	0.04	-	6.7
Nicosia	33.38	35.14	181	1	999	0.15	0.21	0.06	0.06	0.06	0.11	0.09	0.65	32.2
Technion_Haifa_IL	35.02	32.78	230	0	243	0.09	0.16	0.07	0.06	0.09	0.09	0.06	0.90	36.2
Welgegund	26.94	-26.57	1480	0	999	0.11	0.11	-0.00	-0.01	0.03	0.05	0.05	0.83	68.1
Minsk	27.60	53.92	235	0	481	0.17	0.20	0.03	0.03	0.07	0.12	0.11	0.63	27.2
Evora	-7.91	38.57	293	0	485	0.10	0.07	-0.03	-0.03	0.08	0.06	0.05	0.63	58.1
NEON_GUAN	-66.87	17.97	128	1	339	0.03	0.09	0.06	0.06	0.00	0.08	0.06	0.27	49.0
Toronto	-79.47	43.79	186	0	263	0.13	0.16	0.03	0.05	-0.05	0.12	0.12	0.13	38.4
WaveCIS_Site_CSI_6	-90.48	28.87	33	1	999	0.08	0.15	0.07	0.07	0.00	0.08	0.05	0.79	28.9
Monterey	-121.85	36.59	50	0	999	0.07	0.12	0.04	0.04	0.03	0.07	0.06	0.60	52.5
USC_SEAPRISM_2	-118.12	33.56	31	1	789	0.08	0.12	0.03	0.04	-0.01	0.07	0.06	0.69	62.9
Skukuza	31.59	-24.99	265	0	999	0.17	0.17	-0.00	-0.01	0.02	0.06	0.06	0.91	56.4
Granada	-3.61	37.16	680	0	701	0.10	0.15	0.05	0.06	-0.04	0.14	0.13	0.21	39.8
Portglenone_MO	-6.46	54.87	64	0	153	0.17	0.16	-0.02	0.02	-0.07	0.10	0.10	0.37	27.5
ARM_Graciosa	-28.03	39.09	15	1	593	0.07	0.11	0.03	0.03	0.00	0.04	0.03	0.56	67.3
Ragged_Point	-59.43	13.17	40	1	84	0.13	0.16	0.03	0.03	0.00	0.04	0.02	0.75	77.4
Denver_LaCasa	-105.01	39.78	1601	0	342	0.08	0.19	0.11	0.12	-0.16	0.17	0.13	0.15	19.6
MAXAR_FUTON	-104.89	40.04	1522	0	487	0.06	0.19	0.13	0.13	0.00	0.17	0.11	0.06	21.8
NEON-CPER	-104.74	40.81	1655	0	204	0.05	0.22	0.17	0.17	0.00	0.22	0.15	-0.12	20.1
NEON_CVALLA	-105.17	40.16	1539	0	488	0.06	0.17	0.12	0.12	0.00	0.16	0.10	0.12	23.6
NEON_RMNP	-105.55	40.28	2750	0	176	0.03	0.16	0.12	0.12	0.00	0.15	0.09	0.27	15.9
NEON_Sterling	-103.03	40.46	1372	0	332	0.03	0.27	0.24	0.24	0.00	0.27	0.12	0.01	0.3
Table_Mountain	-105.24	40.12	1689	0	487	0.06	0.18	0.11	0.12	-0.00	0.15	0.10	0.16	24.0
Dalanzadgad	104.42	43.58	1470	0	605	0.10	0.23	0.14	0.14	0.05	0.20	0.14	0.28	25.1
Palaiseau	2.21	48.71	156	0	41	0.12	0.11	-0.01	-0.01	0.00	0.06	0.06	0.09	29.3
SANTA_CRUZ_UTEPSA	-63.20	-17.77	432	0	7	0.07	0.11	0.04	0.04	0.00	0.05	0.04	0.00	42.9
Vienna_BOKU	16.33	48.24	266	0	933	0.16	0.22	0.07	0.06	0.09	0.14	0.12	0.46	30.3
Edinburgh	-3.18	55.92	97	0	114	0.06	0.12	0.06	0.06	0.00	0.07	0.04	0.08	36.8
Glasgow_MO	-4.53	55.91	59	0	346	0.10	0.11	0.01	0.01	0.00	0.07	0.07	0.38	48.6
Rame_Head	-4.22	50.32	105	1	866	0.15	0.19	0.04	0.03	0.08	0.09	0.08	0.86	41.8
UPC-GEAB-Valledupar	-73.33	9.56	157	0	66	0.43	0.50	0.08	0.00	0.08	0.15	0.12	-0.00	40.9

NEON_UKFS	-95.19	39.04	321	0	223	0.13	0.14	0.00	0.01	-0.06	0.10	0.10	0.09	41.3
Grizzly_Bay	-122.06	38.11	4	0	980	0.07	0.14	0.07	0.07	0.00	0.12	0.09	0.24	35.2
Rexburg_Idaho	-111.78	43.82	1501	0	319	0.06	0.19	0.12	0.12	0.20	0.19	0.14	0.20	29.8
Bujumbura	29.38	-3.38	863	0	177	0.25	0.21	-0.03	0.00	-0.03	0.09	0.08	0.02	31.1
Brno_Airport	16.68	49.16	238	0	55	0.22	0.21	-0.01	0.01	-0.02	0.10	0.10	0.14	40.0
LAQUILA_Coppito	13.35	42.37	656	0	14	0.05	0.25	0.20	0.20	0.00	0.21	0.08	-	0.0
Timisoara	21.23	45.75	122	0	14	0.12	0.19	0.07	0.07	0.00	0.08	0.05	-0.00	28.6
NEON_TALL	-87.39	32.95	165	0	999	0.14	0.20	0.06	0.06	0.09	0.09	0.07	0.73	35.9
CalTech	-118.13	34.14	260	0	980	0.11	0.16	0.05	0.05	0.00	0.10	0.09	0.31	36.1
EPA-Res_Triangle_Pk	-78.87	35.88	109	0	655	0.24	0.21	-0.02	-0.06	0.01	0.11	0.11	0.54	30.1
American_Samoa	-170.56	-14.25	76	1	290	0.05	0.06	0.02	0.02	0.00	0.04	0.03	0.61	72.8
Gwangju_GIST	126.84	35.23	52	0	187	0.33	0.38	0.06	0.00	0.06	0.21	0.20	0.89	6.4
Murcia	-1.17	38.00	69	0	46	0.10	0.15	0.05	0.03	0.15	0.08	0.06	0.98	65.2
Quito_USFQ	-78.44	-0.20	2414	0	312	0.08	0.17	0.08	0.08	0.08	0.12	0.09	0.56	29.8
NEON_OAES	-99.06	35.41	523	0	715	0.11	0.10	-0.01	-0.01	0.00	0.09	0.09	-0.01	33.3
Univ_of_Houston	-95.34	29.72	65	0	361	0.09	0.17	0.08	0.08	0.09	0.14	0.12	0.28	35.7
Fresno_2	-119.77	36.79	100	0	723	0.09	0.10	0.00	0.00	0.00	0.07	0.07	0.31	56.2
Bukit_Kototabang	100.32	-0.20	864	0	112	0.29	0.42	0.13	0.00	0.13	0.18	0.12	-0.01	17.9
Narsarsuaq	-45.42	61.16	75	0	19	0.06	0.16	0.10	0.10	0.00	0.13	0.08	0.45	21.1
Univ_of_Nevada-Reno	-119.81	39.54	1410	0	368	0.06	0.20	0.14	0.14	0.00	0.20	0.14	-0.00	21.7
Irkutsk	103.09	51.80	670	0	271	0.11	0.14	0.03	0.03	0.00	0.10	0.10	0.32	37.3
NEON_MOAB	-109.39	38.25	1799	0	115	0.03	0.33	0.30	0.30	0.00	0.32	0.11	0.05	0.0
NEON_SRER	-110.84	31.91	983	0	401	0.07	0.11	0.04	0.04	0.00	0.11	0.10	-0.00	47.4
NEON_MLBS	-80.52	37.38	1170	0	216	0.16	0.27	0.10	0.06	0.27	0.17	0.13	0.94	43.1
Sigma_Space_Corp	-76.84	38.95	44	0	230	0.18	0.28	0.10	0.09	0.12	0.14	0.09	0.88	25.7
NEON_KONZ	-96.56	39.10	415	0	126	0.06	0.22	0.17	0.17	0.00	0.17	0.05	-0.23	2.4
PNNL	-119.28	46.34	127	0	181	0.11	0.17	0.06	0.06	0.00	0.13	0.11	0.36	33.1
Ascension_Island	-14.41	-7.98	30	1	650	0.11	0.14	0.03	0.03	0.04	0.04	0.03	0.92	72.5
FZJ-JOYCE	6.41	50.91	111	0	562	0.16	0.24	0.07	0.05	0.12	0.12	0.10	0.82	34.9
NEON_CLBJ	-97.57	33.40	259	0	999	0.11	0.15	0.04	0.05	-0.02	0.10	0.09	0.40	34.3
St_Louis_University	-90.23	38.64	159	0	59	0.12	0.24	0.12	0.15	-0.13	0.19	0.15	0.15	1.7
NEON_SJER	-119.73	37.11	368	0	999	0.07	0.09	0.02	0.02	0.00	0.06	0.05	0.31	60.3
Jambi	103.64	-1.63	30	0	340	0.69	0.74	0.06	0.00	0.06	0.34	0.34	0.77	30.0
Huancayo-IGP	-75.32	-12.04	3313	0	254	0.09	0.11	0.02	0.02	0.00	0.08	0.07	0.56	48.0
IMPROVE-MammothCave	-86.15	37.13	235	0	737	0.19	0.23	0.04	0.02	0.11	0.14	0.13	0.75	34.7
Kellogg_LTER	-85.37	42.41	293	0	30	0.10	0.15	0.05	0.05	0.00	0.11	0.09	0.93	13.3
NEON_ORNL	-84.28	35.96	344	0	251	0.11	0.12	0.02	0.02	0.00	0.10	0.10	0.78	50.6
NEON_UNDE	-89.54	46.23	520	0	566	0.07	0.18	0.11	0.11	0.00	0.15	0.10	0.31	31.4
UAHuntsville	-86.64	34.73	223	0	39	0.06	0.05	-0.01	-0.01	0.00	0.03	0.03	0.66	82.1
Warsaw_UW	20.98	52.21	117	0	496	0.14	0.22	0.08	0.08	0.05	0.13	0.11	0.56	30.8
Aubiere_LAMP	3.11	45.76	423	0	835	0.12	0.13	0.01	0.02	-0.02	0.08	0.08	0.56	44.1

Brussels	4.35	50.78	120	0	260	0.18	0.21	0.03	0.02	0.06	0.13	0.13	0.80	49.6
Karlsruhe	8.43	49.09	140	0	764	0.12	0.17	0.05	0.05	0.05	0.10	0.08	0.57	30.9
Mainz	8.30	50.00	150	0	47	0.07	0.14	0.06	0.06	0.00	0.09	0.06	-0.06	31.9
Paris	2.36	48.85	50	0	79	0.23	0.11	-0.12	-0.06	-0.17	0.17	0.12	0.01	15.2
Ittoqqortoormiit	-21.95	70.48	68	1	50	0.02	0.18	0.16	0.16	0.00	0.18	0.07	0.34	2.0
HohenpeissenbergDWD	11.01	47.80	989	0	21	0.06	0.23	0.17	0.17	0.00	0.18	0.07	-	4.8
MetObs_Lindenberg	14.12	52.21	120	0	712	0.20	0.35	0.14	0.11	0.19	0.21	0.16	0.81	9.3
Brest_MF	-4.41	48.44	101	1	442	0.22	0.24	0.01	0.02	-0.00	0.14	0.14	0.66	40.0
Granite_Island	-87.41	46.72	183	0	164	0.12	0.19	0.07	0.03	0.23	0.12	0.10	0.89	42.1
Palangkaraya	113.95	-2.23	27	0	181	1.19	0.70	-0.50	0.14	-0.99	1.13	1.02	0.80	11.0
Gozo	14.26	36.03	111	1	999	0.21	0.25	0.04	0.03	0.05	0.07	0.06	0.91	46.4
Toravere	26.47	58.26	85	0	393	0.10	0.16	0.06	0.06	0.00	0.12	0.11	-0.11	33.3
Chilbolton	-1.44	51.14	88	0	489	0.13	0.15	0.02	0.01	0.09	0.09	0.09	0.62	38.9
Oxford	-1.26	51.76	87	0	257	0.16	0.18	0.02	-0.01	0.07	0.08	0.08	0.59	41.6
Dunkerque	2.37	51.04	5	0	999	0.11	0.18	0.07	0.07	0.08	0.09	0.06	0.69	30.4
Fort_McKay	-111.64	57.18	267	0	199	0.11	0.17	0.06	0.06	0.00	0.11	0.09	0.37	32.2
Shirahama	135.36	33.69	10	1	338	0.29	0.37	0.08	0.04	0.10	0.10	0.06	0.97	30.8
Watnall_MO	-1.25	53.01	120	0	270	0.16	0.13	-0.03	-0.02	-0.05	0.06	0.05	0.85	51.9
Amity_Univ_Gurgaon	76.92	28.32	285	0	114	0.39	0.47	0.08	0.00	0.08	0.30	0.29	0.75	6.1
Lille	3.14	50.61	60	0	524	0.14	0.20	0.06	0.05	0.10	0.10	0.08	0.84	34.5
Munich_University	11.57	48.15	533	0	19	0.09	0.20	0.11	0.11	0.00	0.17	0.12	-0.14	31.6
Palma_de_Mallorca	2.63	39.55	10	1	142	0.17	0.13	-0.05	-0.05	0.00	0.06	0.03	-0.11	31.7
San_Cristobal_USFQ	-89.61	-0.90	22	1	95	0.09	0.15	0.06	0.06	0.00	0.06	0.01	0.00	7.4
Martova	36.95	49.94	120	0	218	0.12	0.11	-0.01	-0.01	0.00	0.09	0.09	-0.41	36.7
Cabauw	4.93	51.97	0	0	48	0.11	0.18	0.08	0.07	0.16	0.10	0.07	0.71	27.1
St_Helena	-5.67	-15.94	434	1	110	0.05	0.08	0.03	0.03	0.00	0.04	0.02	-0.88	66.4
NEON_YELL	-110.54	44.95	2116	0	150	0.05	0.21	0.16	0.16	0.00	0.20	0.12	0.04	12.7
Maun_Tower	23.55	-19.90	951	0	999	0.13	0.15	0.02	0.01	0.07	0.06	0.06	0.92	67.6
Ny_Alesund_AWI	11.92	78.92	7	0	111	0.04	0.12	0.08	0.08	0.00	0.09	0.04	0.71	13.5
NEON_HEAL	-149.21	63.88	678	0	286	0.15	0.19	0.04	0.08	-0.04	0.12	0.12	0.52	24.8
Noto	137.14	37.33	200	1	792	0.12	0.17	0.05	0.04	0.06	0.07	0.06	0.71	53.4
Helsinki	24.96	60.20	52	0	415	0.16	0.19	0.04	0.06	-0.02	0.09	0.08	0.67	16.9
Dakar_Belair	-17.43	14.70	15	1	999	0.38	0.42	0.04	0.00	0.04	0.08	0.07	0.92	50.1
NEON_OSBS	-81.99	29.69	47	0	380	0.16	0.26	0.10	0.08	0.13	0.14	0.11	0.54	33.4
Dongsha_Island	116.73	20.70	5	1	779	0.14	0.19	0.04	0.04	0.11	0.07	0.06	0.47	58.2
ASI_Malindi	40.19	-3.00	12	0	340	0.19	0.27	0.08	0.07	0.10	0.11	0.07	0.77	26.2
Yekaterinburg	59.54	57.04	300	0	255	0.10	0.13	0.03	0.08	-0.17	0.13	0.12	-0.07	25.5
Gustav_Dalen_Tower	17.47	58.59	25	1	999	0.11	0.17	0.06	0.06	0.09	0.08	0.05	0.86	29.9
Casablanca_Platform	1.36	40.72	35	1	831	0.17	0.19	0.03	0.02	0.04	0.06	0.05	0.81	60.3
NEON_WOOD	-99.24	47.13	590	0	11	0.92	1.02	0.11	0.16	0.09	0.21	0.18	0.94	36.4
NEON_WREF	-121.95	45.82	407	0	493	0.05	0.11	0.07	0.07	0.00	0.10	0.07	0.26	45.8

Pune	73.81	18.54	595	0	125	0.49	0.60	0.11	0.00	0.11	0.14	0.09	0.67	24.0
Irbe_Lighthouse	21.72	57.75	38	1	999	0.12	0.20	0.08	0.08	0.08	0.10	0.06	0.74	22.0
KEMPTEN_UAS	10.31	47.72	718	0	486	0.13	0.18	0.05	0.05	0.05	0.11	0.10	0.46	41.4
Medellin	-75.58	6.26	1471	0	201	0.10	0.19	0.09	0.09	0.00	0.13	0.09	0.30	27.4
NEON_Bartlett	-71.29	44.06	273	0	265	0.08	0.14	0.06	0.06	0.00	0.11	0.09	0.04	35.8
NEON_Harvard	-72.17	42.54	348	0	500	0.08	0.14	0.07	0.07	0.00	0.12	0.09	0.32	49.4
Zvenigorod	36.78	55.69	200	0	432	0.13	0.16	0.03	0.06	-0.11	0.12	0.12	0.04	34.5
Modena	10.95	44.63	56	0	724	0.25	0.19	-0.06	-0.02	-0.09	0.12	0.10	0.47	26.0
South_Greenbay	-87.95	44.60	175	0	193	0.14	0.12	-0.02	-0.02	0.00	0.08	0.08	0.13	33.7
Pinehurst_Idaho	-116.24	47.54	680	0	457	0.09	0.13	0.03	0.03	0.00	0.08	0.07	0.15	38.9
Bo-za_Creek	-148.32	64.74	353	0	688	0.13	0.18	0.05	0.07	-0.00	0.12	0.11	0.45	38.8
NEON_NOGP	-100.92	46.77	578	0	63	0.07	0.13	0.06	0.06	0.00	0.17	0.16	-0.56	17.5
NEON_BONA	-147.50	65.15	263	0	528	0.11	0.16	0.06	0.07	-0.01	0.11	0.09	0.31	33.0
Xitun	120.62	24.16	91	0	620	0.18	0.22	0.04	0.07	-0.02	0.14	0.13	0.25	25.0
Ji_Parana_SE	-61.85	-10.93	218	0	619	0.02	0.59	0.56	0.56	0.00	0.77	0.53	-0.77	40.1
Sevilleta	-106.89	34.35	1477	0	52	0.04	0.10	0.06	0.06	0.00	0.09	0.06	-0.00	50.0
OPAL	-85.94	79.99	5	0	155	0.04	0.19	0.14	0.14	0.00	0.16	0.08	-0.48	16.1
NEON_DEJU	-145.75	63.88	529	0	57	0.06	0.20	0.14	0.14	0.00	0.17	0.09	0.22	17.5
NEON_PUUM	-155.32	19.55	1685	1	105	0.02	0.13	0.11	0.11	0.00	0.14	0.08	0.06	4.8
PEARL	-86.42	80.05	615	0	16	0.07	0.17	0.10	0.10	0.00	0.16	0.13	-0.72	50.0
Red_Mountain_Pass	-107.71	37.91	3376	0	388	0.04	0.21	0.17	0.17	0.00	0.20	0.10	0.32	8.5
Yellowknife_Aurora	-114.38	62.45	220	0	79	0.05	0.12	0.08	0.08	0.00	0.10	0.07	-0.23	35.4
Kluane_Lake	-138.41	61.03	773	0	211	0.15	0.22	0.06	0.09	-0.03	0.14	0.13	0.65	31.8
Tomsk	85.05	56.48	174	0	394	0.12	0.21	0.09	0.11	-0.14	0.15	0.12	-0.52	13.2
Davos	9.84	46.81	1589	0	257	0.10	0.20	0.10	0.10	0.00	0.15	0.10	0.32	25.3
NEON_BARR	-156.62	71.28	6	1	521	0.08	0.14	0.06	0.06	0.00	0.08	0.05	0.29	45.7
Helsinki_Lighthouse	24.93	59.95	20	0	817	0.09	0.15	0.06	0.06	0.06	0.07	0.04	0.84	29.0
NEON_TOOL	-149.37	68.66	843	0	137	0.15	0.17	0.03	0.04	-0.06	0.10	0.09	0.73	43.8
Caillouel_COBIACC	3.13	49.62	53	0	326	0.16	0.26	0.10	0.13	0.06	0.14	0.10	0.56	23.9
Palgrunden	13.15	58.76	49	0	95	0.13	0.26	0.13	0.12	0.17	0.17	0.11	0.49	14.7
UNC-Palmira	-76.31	3.51	1065	0	40	0.13	0.23	0.10	0.10	0.00	0.12	0.07	-0.00	20.0
Hyytiala	24.30	61.85	191	0	252	0.09	0.11	0.01	0.01	0.00	0.06	0.06	0.48	52.8
Bozeman	-111.05	45.66	1507	0	121	0.08	0.17	0.09	0.09	0.00	0.13	0.09	0.16	25.6
EastMalling_MO	0.44	51.29	33	0	99	0.24	0.28	0.03	0.00	0.03	0.09	0.08	-0.00	46.5
Eforie	28.63	44.08	40	0	201	0.09	0.15	0.06	0.06	0.08	0.07	0.04	0.94	34.3
Section-7_Platform	29.45	44.55	30	1	999	0.14	0.20	0.07	0.06	0.09	0.08	0.05	0.83	31.9
Cliff_Creek_1	-114.84	45.11	1351	0	100	0.04	0.15	0.10	0.10	0.00	0.14	0.09	-0.04	28.0
Cliff_Creek_2	-114.84	45.12	1552	0	100	0.04	0.15	0.11	0.11	0.00	0.14	0.09	0.01	24.0
Cliff_Creek_3	-114.84	45.12	1727	0	159	0.06	0.15	0.09	0.09	0.00	0.12	0.09	0.01	30.8
Cliff_Creek_4	-114.84	45.12	2024	0	162	0.06	0.15	0.09	0.09	0.00	0.12	0.08	0.05	28.4
Cliff_Creek_5	-114.85	45.13	2068	0	156	0.05	0.15	0.09	0.09	0.00	0.13	0.09	0.05	26.9
Cliff_Creek_6	-114.85	45.14	2232	0	179	0.06	0.14	0.09	0.09	0.00	0.12	0.08	0.08	31.3

McCall_AB_Standard	-116.12	44.87	1524	0	34	0.05	0.09	0.04	0.04	0.00	0.07	0.05	0.45	55.9
McCall_Dragon_1	-116.20	44.76	2247	0	24	0.03	0.07	0.04	0.04	0.00	0.06	0.05	0.00	62.5
McCall_Dragon_3	-116.29	45.04	1179	0	10	0.06	0.06	-0.00	-0.00	0.00	0.03	0.03	-	80.0
McCall_Dragon_4	-115.91	45.28	1865	0	11	0.05	0.11	0.05	0.05	0.00	0.09	0.07	0.24	63.6
McCall_Dragon_5	-115.68	45.27	1774	0	13	0.05	0.08	0.03	0.03	0.00	0.07	0.06	-0.00	76.9
McCall_Dragon_6	-116.03	45.41	1139	0	13	0.07	0.07	-0.00	-0.00	0.00	0.03	0.03	0.00	76.9
McCall_Dragon_7	-116.33	45.41	582	0	92	0.00	0.12	0.11	0.11	0.00	0.13	0.06	-0.24	9.8
McCall_Dragon_8	-115.85	45.27	1785	0	35	0.07	0.14	0.07	0.07	0.00	0.12	0.10	0.37	48.6
Missoula_Health_Dpt	-114.00	46.88	985	0	258	0.14	0.14	0.00	0.00	0.07	0.09	0.09	0.21	36.8
Missoula_Midslope	-114.03	47.00	1613	0	254	0.08	0.13	0.06	0.06	0.00	0.10	0.08	-0.29	40.6
Missoula_Waterworks	-113.99	46.88	1107	0	260	0.10	0.14	0.04	0.04	0.11	0.09	0.09	0.23	36.9
Lake_Erie	-83.19	41.83	173	0	188	0.18	0.17	-0.01	0.04	-0.06	0.09	0.09	0.47	29.8
Resolute_Bay	-94.97	74.71	35	0	208	0.09	0.12	0.03	0.03	0.00	0.04	0.02	0.49	72.1
Maldives_Gan	73.15	-0.69	4	1	435	0.07	0.10	0.03	0.03	0.00	0.04	0.03	0.78	72.4
KAUST_Campus	39.10	22.30	11	0	630	0.45	0.54	0.09	0.00	0.09	0.14	0.11	0.42	15.2
NSPO_Taiwan	121.00	24.78	99	1	57	0.11	0.32	0.22	0.22	0.00	0.24	0.10	0.00	0.0
Missoula_Pt_Six	-113.99	47.04	2420	0	24	0.06	0.09	0.03	0.03	0.00	0.05	0.04	-	62.5
Kanzelhohe_Obs	13.90	46.68	1526	0	7	0.05	0.09	0.04	0.04	0.00	0.06	0.04	-	57.1
McCall_AB_Polar	-116.12	44.87	1524	0	18	0.09	0.11	0.02	0.02	0.00	0.06	0.05	-0.00	50.0
McCall_Dragon_9	-115.85	45.27	1875	0	24	0.12	0.16	0.05	0.05	0.00	0.11	0.10	-0.00	33.3
Yakutsk	129.37	61.66	118	0	37	0.10	0.17	0.08	0.08	0.00	0.10	0.06	-0.21	24.3

Table 9.4 *Station statistics for SLSTR/SENTINEL-3B / 2019*

SLSTR / S3B 2019 (3, 6, 9, 12)														
station					AOD550									
station_name	**longitude**	**latitude**	**elevation**	**watermask**	**number**	**meanAeronet**	**meanSatellite**	**mean_bias**	**mean_bias(low)**	**mean_bias(high)**	**rmse**	**stdv**	**Pearson**	**gcos-fraction**
Bac_Lieu	105.73	9.28	10	1	101	0.21	0.26	0.05	0.06	0.04	0.10	0.08	0.37	33.7
Beijing	116.38	39.98	92	0	65	0.07	0.38	0.31	0.31	0.00	0.36	0.19	0.92	10.8
REUNION_ST_DENIS	55.48	-20.90	93	1	999	0.07	0.10	0.03	0.03	0.00	0.06	0.05	0.40	63.0
IMS-METU-ERDEMLI	34.26	36.56	3	0	138	0.15	0.22	0.07	0.06	0.10	0.09	0.05	0.91	27.5
Migal	35.58	33.24	200	0	999	0.27	0.25	-0.02	0.04	-0.05	0.14	0.14	0.36	23.6
Weizmann_Institute	34.81	31.91	73	0	134	0.31	0.27	-0.03	0.07	-0.06	0.11	0.11	0.43	33.6
AAOT	12.51	45.31	10	0	999	0.16	0.24	0.08	0.09	0.04	0.13	0.11	0.58	19.5
Ersa	9.36	43.00	80	1	999	0.14	0.20	0.06	0.05	0.10	0.08	0.06	0.87	46.4
Iasi_LOASL	27.56	47.19	175	0	968	0.18	0.19	0.01	0.03	-0.10	0.13	0.13	0.01	23.6
Lamezia_Terme	16.23	38.88	8	1	999	0.17	0.23	0.06	0.05	0.07	0.09	0.07	0.85	32.6
Magurele_Inoe	26.03	44.35	90	0	130	0.09	0.17	0.08	0.08	0.00	0.13	0.09	0.44	24.6
Messina	15.57	38.20	15	1	462	0.13	0.20	0.07	0.07	0.10	0.10	0.07	0.65	32.0
Poprad-Ganovce	20.32	49.03	706	0	459	0.16	0.26	0.10	0.09	0.13	0.16	0.12	0.54	28.8
Thessaloniki	22.96	40.63	60	0	56	0.10	0.20	0.10	0.10	0.00	0.15	0.11	0.04	32.1
Venise	12.51	45.31	10	0	999	0.17	0.24	0.07	0.09	0.01	0.13	0.11	0.53	20.3
Aras_de_los_Olmos	-1.10	39.94	1280	0	387	0.08	0.14	0.06	0.05	0.11	0.09	0.08	0.56	41.3
Bayfordbury	-0.10	51.78	75	0	8	0.29	0.21	-0.08	0.09	-0.14	0.15	0.13	0.42	25.0
Burjassot	-0.42	39.51	104	0	262	0.09	0.13	0.05	0.05	0.00	0.06	0.04	0.69	42.0
Chilbolton	-1.44	51.14	88	0	301	0.13	0.18	0.05	0.05	0.04	0.12	0.11	0.37	29.9
Coruna	-8.42	43.36	67	1	999	0.10	0.14	0.04	0.03	0.13	0.08	0.07	0.83	51.3
Dakar	-16.96	14.39	21	1	999	0.40	0.44	0.04	0.04	0.04	0.10	0.09	0.93	39.1
Edinburgh	-3.18	55.92	97	0	33	0.07	0.11	0.05	0.05	0.00	0.06	0.04	0.56	27.3
Evora	-7.91	38.57	293	0	310	0.08	0.09	0.01	0.01	0.00	0.10	0.10	-0.26	60.0
Glasgow_MO	-4.53	55.91	59	0	111	0.09	0.16	0.07	0.07	0.00	0.10	0.07	0.66	33.3
Granada	-3.61	37.16	680	0	647	0.12	0.17	0.05	0.06	-0.03	0.12	0.11	0.36	40.3
Izana	-16.50	28.31	2401	1	599	0.04	0.20	0.16	0.16	0.00	0.19	0.10	0.75	4.8
Loftus_MO	-0.86	54.56	159	0	385	0.09	0.15	0.06	0.07	0.01	0.08	0.05	0.82	33.0
Madrid	-3.72	40.45	680	0	102	0.10	0.20	0.10	0.10	0.00	0.17	0.13	0.03	28.4
Rame_Head	-4.22	50.32	105	1	681	0.17	0.23	0.06	0.05	0.09	0.11	0.09	0.86	34.7
Saada	-8.16	31.63	420	0	36	0.47	0.18	-0.28	0.10	-0.41	0.37	0.24	-0.26	5.6
Tabernas_PSA-DLR	-2.36	37.09	500	0	912	0.12	0.19	0.07	0.07	0.07	0.12	0.10	0.52	27.6
Valladolid	-4.71	41.66	705	0	5	0.04	0.45	0.41	0.41	0.00	0.45	0.19	-	0.0
La_Paz	-68.07	-16.54	3439	0	76	0.11	0.17	0.06	0.09	-0.05	0.11	0.09	0.49	32.9
NEON_GUAN	-66.87	17.97	128	1	36	0.04	0.10	0.06	0.06	0.00	0.06	0.02	-	19.4
Lake_Okeechobee	-80.79	26.90	9	0	737	0.13	0.19	0.06	0.06	0.00	0.14	0.12	0.23	32.3

NEON_MLBS	-80.52	37.38	1170	0	154	0.16	0.27	0.11	0.06	0.14	0.15	0.10	0.80	29.2
NEON_Sterling	-103.03	40.46	1372	0	91	0.06	0.22	0.17	0.17	0.00	0.18	0.07	-0.33	2.2
Tucson	-110.95	32.23	779	0	516	0.08	0.12	0.04	0.04	0.00	0.09	0.08	0.04	47.7
USGS_Flagstaff_RO LO	-111.63	35.21	2179	0	834	0.05	0.17	0.11	0.11	0.00	0.16	0.12	-0.05	29.0
American_Samoa	-170.56	-14.25	76	1	346	0.04	0.08	0.03	0.03	0.00	0.05	0.04	0.21	70.2
Anmyon	126.33	36.54	47	1	909	0.27	0.31	0.04	0.07	0.02	0.12	0.11	0.88	30.0
Kaohsiung	120.29	22.68	15	1	222	0.81	0.69	-0.13	0.00	-0.13	0.16	0.11	0.41	21.2
NhaTrang	109.21	12.20	20	0	173	0.45	0.53	0.08	0.10	0.07	0.18	0.16	0.89	16.2
Palangkaraya	113.95	-2.23	27	0	393	0.82	0.57	-0.25	0.11	-0.57	0.76	0.72	0.70	16.3
Bhola	90.76	22.23	7	1	148	0.67	0.68	0.01	0.00	0.01	0.19	0.19	0.70	22.3
Misamfu	31.22	-10.17	1381	0	939	0.06	0.09	0.04	0.04	0.00	0.07	0.06	0.43	77.0
Skukuza	31.59	-24.99	265	0	999	0.15	0.14	-0.01	-0.01	-0.02	0.05	0.05	0.90	67.1
Welgegund	26.94	-26.57	1480	0	999	0.09	0.09	-0.00	-0.00	0.00	0.05	0.05	0.62	75.3
CATUC_Bamenda	10.16	5.95	1293	0	201	0.53	0.63	0.10	0.00	0.10	0.17	0.13	0.87	18.4
Galata_Platform	28.19	43.04	31	1	999	0.19	0.28	0.09	0.08	0.10	0.11	0.07	0.82	15.5
Gloria	29.36	44.60	30	1	999	0.14	0.22	0.08	0.09	0.05	0.11	0.07	0.55	18.3
Ascension_Island	-14.41	-7.98	30	1	400	0.13	0.17	0.04	0.04	0.00	0.06	0.04	0.18	47.2
Barcelona	2.11	41.39	125	0	999	0.14	0.17	0.04	0.03	0.07	0.09	0.08	0.72	60.2
Brussels	4.35	50.78	120	0	227	0.16	0.11	-0.05	-0.01	-0.48	0.18	0.17	0.33	43.2
Dunkerque	2.37	51.04	5	0	785	0.14	0.22	0.09	0.08	0.10	0.12	0.08	0.72	16.8
FZJ-JOYCE	6.41	50.91	111	0	468	0.13	0.15	0.03	0.06	-0.39	0.15	0.15	0.22	34.6
Arica	-70.31	-18.47	25	0	486	0.14	0.12	-0.03	-0.03	0.00	0.07	0.06	0.23	42.2
Appalachian_State	-81.69	36.21	1080	0	668	0.09	0.17	0.07	0.07	0.32	0.13	0.11	0.78	47.6
Brookhaven	-72.88	40.87	37	1	999	0.08	0.14	0.06	0.06	-0.06	0.08	0.05	0.58	30.7
CCNY	-73.95	40.82	100	0	574	0.10	0.16	0.06	0.06	0.00	0.09	0.07	0.55	31.5
Easton-MDE	-76.08	38.79	4	0	136	0.20	0.34	0.14	0.11	0.21	0.16	0.08	0.98	4.4
Georgia_Tech	-84.40	33.78	294	0	331	0.25	0.30	0.05	0.02	0.10	0.12	0.11	0.89	51.1
MD_Science_Center	-76.61	39.28	15	0	191	0.16	0.23	0.07	0.06	0.21	0.12	0.10	0.67	39.8
NEON_SCBI	-78.14	38.89	354	0	467	0.16	0.19	0.03	0.04	-0.00	0.11	0.10	0.30	39.6
NEON_SERC	-76.56	38.89	9	0	65	0.05	0.15	0.10	0.10	0.00	0.12	0.05	0.37	16.9
Sigma_Space_Corp	-76.84	38.95	44	0	98	0.12	0.21	0.09	0.06	0.19	0.12	0.08	0.94	26.5
Toronto	-79.47	43.79	186	0	201	0.07	0.12	0.05	0.05	0.00	0.10	0.08	0.35	53.7
Wallops	-75.47	37.93	37	1	999	0.11	0.20	0.08	0.08	0.07	0.10	0.06	0.91	19.6
WaveCIS_Site_CSI_6	-90.48	28.87	33	1	999	0.11	0.18	0.07	0.07	0.04	0.08	0.05	0.85	32.7
Yale_Coastal	-72.73	41.26	0	0	131	0.08	0.14	0.06	0.06	0.00	0.08	0.06	-0.04	9.2
Denver_LaCasa	-105.01	39.78	1601	0	239	0.09	0.22	0.13	0.13	0.00	0.18	0.13	0.14	19.7
MAXAR_FUTON	-104.89	40.04	1522	0	322	0.08	0.21	0.13	0.13	0.00	0.19	0.14	-0.01	23.6
NEON-CPER	-104.74	40.81	1655	0	129	0.06	0.21	0.15	0.15	0.00	0.20	0.13	-0.01	18.6
NEON_CVALLA	-105.17	40.16	1539	0	366	0.07	0.21	0.14	0.14	0.00	0.19	0.13	0.11	21.0
NEON_MOAB	-109.39	38.25	1799	0	6	0.02	0.39	0.36	0.36	0.00	0.41	0.20	-	16.7
NEON_RMNP	-105.55	40.28	2750	0	137	0.04	0.17	0.13	0.13	0.00	0.15	0.08	0.27	12.4

NEON_SRER	-110.84	31.91	983	0	641	0.06	0.14	0.09	0.09	0.00	0.13	0.10	-0.13	31.7
Table_Mountain	-105.24	40.12	1689	0	310	0.07	0.21	0.13	0.13	0.00	0.18	0.12	0.14	19.0
White_Sands_HELSTF	-106.34	32.63	1207	0	999	0.09	0.15	0.07	0.07	0.00	0.11	0.09	0.09	35.2
Saturn_Island	-123.13	48.78	193	0	434	0.07	0.11	0.04	0.04	0.00	0.05	0.04	0.72	59.9
Mauna_Loa	-155.58	19.54	3402	1	999	0.01	0.13	0.11	0.11	0.00	0.15	0.10	0.09	20.0
BMKG_GAW_PALU	120.18	-1.65	1370	0	475	0.09	0.18	0.09	0.09	0.00	0.11	0.08	0.54	27.6
Taipei_CWB	121.54	25.01	26	1	125	0.80	0.71	-0.09	0.00	-0.09	0.26	0.24	-0.18	16.0
Chiang_Mai_Met_Sta	98.97	18.77	312	0	546	0.57	0.56	-0.01	0.06	-0.05	0.28	0.28	0.88	34.8
Doi_Ang_Khang	99.05	19.93	1536	0	210	0.45	0.97	0.52	0.00	0.52	0.64	0.37	0.75	3.8
Fang	99.21	19.91	480	0	211	1.04	1.00	-0.05	0.00	-0.05	0.32	0.31	0.85	27.0
Silpakorn_Univ	100.04	13.82	72	0	702	0.43	0.35	-0.07	0.08	-0.08	0.21	0.19	0.44	18.2
MCO-Hanimaadhoo	73.18	6.78	13	1	358	0.38	0.44	0.06	0.00	0.06	0.09	0.06	0.85	41.6
Gobabeb	15.04	-23.56	405	0	999	0.11	0.23	0.12	0.11	0.30	0.18	0.14	0.73	24.7
Aubiere_LAMP	3.11	45.76	423	0	568	0.11	0.15	0.04	0.04	0.13	0.10	0.09	0.61	47.2
HohenpeissenbergDWD	11.01	47.80	989	0	75	0.08	0.20	0.12	0.12	0.00	0.16	0.10	-0.31	21.3
Karlsruhe	8.43	49.09	140	0	719	0.13	0.17	0.04	0.06	-0.10	0.15	0.14	0.33	35.6
Leipzig	12.44	51.35	125	0	603	0.13	0.24	0.11	0.12	0.06	0.18	0.14	0.36	18.9
MetObs_Lindenberg	14.12	52.21	120	0	780	0.12	0.24	0.11	0.10	0.18	0.16	0.12	0.58	24.2
OHP_OBSERVATOIRE	5.71	43.94	680	0	999	0.12	0.17	0.04	0.05	0.02	0.10	0.09	0.57	41.8
Sirmione_Museo_GC	10.61	45.50	86	0	949	0.23	0.23	0.00	0.06	-0.07	0.16	0.16	0.30	26.3
Toulon	6.01	43.14	50	1	476	0.09	0.14	0.05	0.05	0.00	0.07	0.05	0.16	37.4
Toulouse_MF	1.37	43.57	160	0	27	0.06	0.41	0.35	0.35	0.00	0.39	0.16	0.74	11.1
Billerica	-71.27	42.53	82	0	384	0.07	0.13	0.06	0.06	0.14	0.11	0.09	0.43	33.6
Tallahassee	-84.30	30.45	49	0	417	0.14	0.21	0.07	0.07	0.07	0.13	0.11	0.65	38.6
ARM_SGP	-97.49	36.61	319	0	726	0.16	0.15	-0.01	-0.02	-0.00	0.12	0.12	0.08	21.9
NEON_KONZ	-96.56	39.10	415	0	69	0.07	0.20	0.13	0.13	0.00	0.14	0.05	0.10	2.9
NEON_OAES	-99.06	35.41	523	0	511	0.14	0.09	-0.05	-0.05	0.00	0.10	0.09	0.06	22.9
NEON_WREF	-121.95	45.82	407	0	446	0.06	0.10	0.05	0.05	0.00	0.07	0.05	0.05	51.6
PNNL	-119.28	46.34	127	0	223	0.11	0.17	0.05	0.11	-0.08	0.15	0.14	-0.22	24.7
NGHIA_DO	105.80	21.05	40	0	13	1.96	1.19	-0.78	0.00	-0.78	0.79	0.16	-0.00	0.0
Nong_Khai	102.72	17.88	175	0	512	0.46	0.44	-0.02	-0.01	-0.02	0.08	0.08	0.92	45.3
Singapore	103.78	1.30	30	1	157	0.37	0.48	0.10	0.14	0.08	0.14	0.10	0.92	17.2
Songkhla_Met_Sta	100.60	7.18	15	0	301	0.20	0.30	0.10	0.10	0.09	0.13	0.08	0.60	18.3
USM_Pe-g	100.30	5.36	51	1	300	0.28	0.34	0.06	0.07	0.05	0.13	0.12	0.79	33.3
Gandhi_College	84.13	25.87	60	0	293	0.53	0.91	0.37	0.00	0.37	0.41	0.18	0.57	2.0
Kanpur	80.23	26.51	123	0	914	0.59	0.56	-0.03	0.00	-0.03	0.19	0.18	0.75	23.3
DEWA_ResearchCentre	55.37	24.77	86	0	999	0.36	0.35	-0.00	0.03	-0.01	0.21	0.21	0.51	15.3
AgiaMarina_Xyliatou	33.06	35.04	521	1	521	0.17	0.25	0.08	0.06	0.11	0.12	0.09	0.83	19.4

CUT-TEPAK	33.04	34.67	22	1	999	0.20	0.26	0.06	0.05	0.07	0.10	0.07	0.85	28.5
Mongu_Inn	23.13	-15.27	1040	0	169	0.16	0.10	-0.06	-0.06	0.00	0.09	0.06	-0.63	50.3
Nicosia	33.38	35.14	181	1	999	0.17	0.24	0.07	0.06	0.07	0.12	0.09	0.71	26.9
Qena_SVU	32.75	26.20	75	0	999	0.25	0.27	0.03	0.05	0.00	0.15	0.15	0.59	25.6
SEDE_BOKER	34.78	30.85	480	0	93	0.23	0.29	0.05	0.01	0.05	0.12	0.11	0.34	32.3
Technion_Haifa_IL	35.02	32.78	230	0	181	0.18	0.25	0.07	0.08	0.04	0.10	0.07	0.77	22.7
Davos	9.84	46.81	1589	0	221	0.06	0.23	0.17	0.17	0.00	0.20	0.12	0.26	9.5
Mainz	8.30	50.00	150	0	12	0.06	0.09	0.03	0.03	0.00	0.07	0.07	-0.00	83.3
Medenine-IRA	10.64	33.50	33	0	999	0.19	0.30	0.11	0.11	0.11	0.15	0.10	0.65	15.1
Napoli_CeSMA	14.31	40.84	50	0	999	0.19	0.24	0.04	0.05	0.03	0.09	0.08	0.75	31.4
CEILAP-BA	-58.51	-34.56	26	0	135	0.10	0.05	-0.05	-0.05	0.00	0.07	0.04	0.07	23.0
Ittoqqortoormiit	-21.95	70.48	68	1	55	0.02	0.24	0.22	0.22	0.00	0.26	0.14	-0.11	0.0
Quito_USFQ	-78.44	-0.20	2414	0	287	0.09	0.17	0.08	0.10	-0.04	0.13	0.10	0.30	19.2
Granite_Island	-87.41	46.72	183	0	320	0.09	0.11	0.02	0.02	0.00	0.07	0.07	0.60	70.6
St_Louis_University	-90.23	38.64	159	0	79	0.49	0.43	-0.06	0.06	-0.27	0.30	0.29	0.81	32.9
Univ_of_Houston	-95.34	29.72	65	0	509	0.14	0.20	0.06	0.09	-0.07	0.13	0.12	0.04	25.1
Monterey	-121.85	36.59	50	0	999	0.07	0.13	0.06	0.06	-0.03	0.09	0.07	0.47	43.9
Lake_Lefroy	121.71	-31.25	300	0	999	0.08	0.09	0.01	0.01	0.00	0.05	0.05	0.58	77.7
Irkutsk	103.09	51.80	670	0	262	0.11	0.14	0.03	0.03	0.00	0.08	0.08	0.48	49.2
Bujumbura	29.38	-3.38	863	0	138	0.16	0.14	-0.02	0.01	-0.05	0.10	0.10	0.11	39.9
IMAA_Potenza	15.72	40.60	770	0	56	0.14	0.13	-0.02	-0.02	0.00	0.10	0.10	0.13	37.5
Lecce_University	18.11	40.34	30	1	890	0.19	0.24	0.05	0.05	0.07	0.10	0.08	0.80	34.2
Minsk	27.60	53.92	235	0	583	0.16	0.17	0.02	0.03	-0.01	0.10	0.10	0.47	29.7
Toravere	26.47	58.26	85	0	623	0.09	0.19	0.10	0.10	0.00	0.16	0.12	0.12	34.7
Tudor_Hill	-64.88	32.26	51	1	772	0.09	0.14	0.05	0.05	0.00	0.06	0.03	0.88	46.6
IMPROVE-MammothCave	-86.15	37.13	235	0	999	0.16	0.19	0.03	0.04	0.01	0.10	0.09	0.45	42.3
NEON_ORNL	-84.28	35.96	344	0	49	0.06	0.06	0.00	0.00	0.00	0.03	0.03	-0.00	73.5
NEON_TALL	-87.39	32.95	165	0	999	0.19	0.26	0.06	0.05	0.08	0.10	0.08	0.84	37.5
CalTech	-118.13	34.14	260	0	651	0.11	0.16	0.05	0.05	-0.01	0.10	0.09	0.42	36.9
Sevilleta	-106.89	34.35	1477	0	37	0.06	0.39	0.33	0.33	0.00	0.35	0.13	-0.00	5.4
USC_SEAPRISM_2	-118.12	33.56	31	1	368	0.10	0.15	0.05	0.05	0.13	0.07	0.05	0.78	34.5
Gwangju_GIST	126.84	35.23	52	0	217	0.38	0.37	-0.00	-0.00	-0.01	0.14	0.14	0.92	40.1
Kyiv	30.50	50.36	200	0	730	0.16	0.22	0.06	0.06	0.05	0.13	0.12	0.33	28.5
Lubango	13.44	-14.96	2047	0	992	0.17	0.23	0.06	0.05	0.11	0.09	0.06	0.95	39.9
Strzyzow	21.86	49.88	450	0	822	0.16	0.23	0.07	0.10	0.05	0.15	0.12	0.22	22.4
Brest_MF	-4.41	48.44	101	1	442	0.25	0.28	0.03	0.05	0.03	0.13	0.13	0.51	30.1
Stornoway_MO	-6.18	58.21	82	1	333	0.08	0.14	0.06	0.06	0.00	0.08	0.04	0.33	32.1
ARM_Graciosa	-28.03	39.09	15	1	351	0.08	0.13	0.04	0.04	0.00	0.05	0.03	0.66	42.5
EPA-Res_Triangle_Pk	-78.87	35.88	109	0	432	0.19	0.19	0.00	-0.02	0.02	0.09	0.09	0.54	47.2
Hampton_University	-76.34	37.02	12	0	768	0.14	0.22	0.09	0.10	0.05	0.12	0.08	0.74	17.1

NASA_LaRC	-76.38	37.10	5	0	346	0.16	0.24	0.08	0.10	0.04	0.11	0.08	0.84	20.2
SP_Bayboro	-82.63	27.76	5	1	749	0.10	0.18	0.08	0.08	0.16	0.11	0.07	0.67	23.1
ARIAKE_TOWER	130.27	33.10	15	0	389	0.24	0.32	0.07	0.05	0.10	0.13	0.10	0.87	27.2
Hankuk_UFS	127.27	37.34	167	0	482	0.22	0.29	0.08	0.06	0.09	0.15	0.13	0.70	29.7
Seoul_SNU	126.95	37.46	116	0	417	0.29	0.33	0.04	0.06	0.03	0.14	0.14	0.58	24.0
Rhyl_MO	-3.51	53.26	77	0	77	0.07	0.16	0.09	0.09	0.00	0.10	0.04	0.33	3.9
ARM_Cordoba	-64.73	-32.13	1141	0	78	0.05	0.04	-0.01	-0.01	0.00	0.04	0.03	0.00	79.5
Bakersfield	-119.00	35.33	108	0	586	0.16	0.20	0.03	0.05	-0.01	0.11	0.11	-0.00	32.4
Fresno_2	-119.77	36.79	100	0	725	0.12	0.13	0.01	0.01	-0.05	0.10	0.10	0.12	44.1
Modesto	-120.99	37.64	33	0	310	0.10	0.09	-0.01	-0.01	-0.11	0.05	0.05	0.01	56.5
NEON_SJER	-119.73	37.11	368	0	999	0.09	0.12	0.04	0.04	0.00	0.08	0.07	0.34	46.9
Univ_of_Nevada-Reno	-119.81	39.54	1410	0	340	0.07	0.23	0.16	0.16	0.00	0.22	0.15	-0.12	15.6
Shirahama	135.36	33.69	10	1	50	0.25	0.45	0.21	0.00	0.21	0.25	0.14	-	4.0
Bukit_Kototabang	100.32	-0.20	864	0	287	0.15	0.29	0.14	0.11	0.27	0.21	0.16	0.89	16.4
Jambi	103.64	-1.63	30	0	176	0.50	0.60	0.09	0.19	0.08	0.29	0.27	0.50	11.4
Martova	36.95	49.94	120	0	350	0.17	0.18	0.01	0.03	-0.05	0.09	0.09	0.25	36.9
NEON_ONAQ	-112.45	40.18	1656	0	5	0.07	0.11	0.04	0.04	0.00	0.08	0.07	-0.70	20.0
Dhaka_University	90.40	23.73	34	0	154	0.64	0.80	0.16	0.00	0.16	0.22	0.15	0.83	26.6
Gozo	14.26	36.03	111	1	999	0.18	0.25	0.06	0.04	0.10	0.09	0.06	0.94	41.4
Paris	2.36	48.85	50	0	50	0.23	0.12	-0.11	-0.01	-0.16	0.14	0.09	-0.50	14.0
EPA-NCU	121.19	24.97	144	1	692	0.27	0.31	0.04	0.09	-0.03	0.18	0.18	0.77	19.4
Dibrugarh_Univ	94.90	27.45	119	0	142	0.29	0.37	0.08	0.17	0.05	0.15	0.12	0.50	20.4
Dalanzadgad	104.42	43.58	1470	0	740	0.11	0.29	0.18	0.18	0.10	0.27	0.20	-0.26	17.2
Amity_Univ_Gurgaon	76.92	28.32	285	0	16	0.34	0.30	-0.04	0.00	-0.04	0.21	0.21	-	18.8
Cairo_EMA_2	31.29	30.08	70	0	726	0.35	0.32	-0.03	0.00	-0.03	0.12	0.11	0.40	28.4
Palma_de_Mallorca	2.63	39.55	10	1	140	0.16	0.13	-0.03	-0.03	0.00	0.04	0.03	0.43	75.7
Amazon_ATTO_Tower	-59.00	-2.14	210	0	458	0.07	0.21	0.14	0.14	0.00	0.17	0.10	0.04	14.8
NASA_KSC	-80.66	28.46	1	0	96	0.11	0.24	0.13	0.13	0.00	0.20	0.15	-0.21	30.2
Munich_University	11.57	48.15	533	0	44	0.11	0.24	0.14	0.14	0.00	0.19	0.13	0.00	11.4
Watnall_MO	-1.25	53.01	120	0	94	0.15	0.21	0.06	0.13	-0.23	0.18	0.17	-0.51	16.0
Railroad_Valley	-115.69	38.50	1437	0	40	0.06	0.23	0.17	0.17	0.00	0.27	0.21	-0.75	35.0
Hokkaido_University	141.34	43.08	59	0	586	0.14	0.21	0.07	0.07	0.10	0.12	0.09	0.51	32.9
Jabiru	132.89	-12.66	30	0	960	0.08	0.07	-0.01	0.00	-0.13	0.06	0.06	0.54	81.6
Cabauw	4.93	51.97	0	0	17	0.17	0.34	0.17	0.14	0.23	0.18	0.07	0.86	0.0
Lille	3.14	50.61	60	0	332	0.16	0.20	0.04	0.04	0.03	0.12	0.11	0.45	27.4
Oxford	-1.26	51.76	87	0	127	0.12	0.12	0.00	0.01	-0.16	0.08	0.08	-0.33	43.3
NEON_YELL	-110.54	44.95	2116	0	257	0.05	0.18	0.13	0.13	0.00	0.16	0.09	0.23	12.5
Xitun	120.62	24.16	91	0	835	0.30	0.30	0.00	0.08	-0.15	0.32	0.32	0.37	24.0
Kashi	75.93	39.50	1320	0	43	0.36	0.30	-0.05	0.00	-0.05	0.12	0.11	-0.00	23.3

ASI_Malindi	40.19	-3.00	12	0	397	0.20	0.29	0.10	0.08	0.12	0.12	0.07	0.78	18.6
Ny_Alesund_AWI	11.92	78.92	7	0	126	0.04	0.13	0.09	0.09	0.00	0.09	0.03	0.68	11.1
Portglenone_MO	-6.46	54.87	64	0	79	0.15	0.21	0.06	0.05	0.09	0.08	0.05	0.90	25.3
NEON_OSBS	-81.99	29.69	47	0	437	0.16	0.26	0.10	0.13	0.06	0.16	0.12	0.33	25.9
Fort_McKay	-111.64	57.18	267	0	246	0.12	0.22	0.09	0.09	0.00	0.14	0.11	0.39	19.1
Dongsha_Island	116.73	20.70	5	1	908	0.15	0.19	0.04	0.04	0.04	0.07	0.06	0.71	44.3
Pune	73.81	18.54	595	0	161	0.42	0.50	0.08	0.00	0.08	0.12	0.08	0.29	40.4
Helsinki	24.96	60.20	52	0	587	0.12	0.18	0.05	0.06	0.02	0.09	0.07	0.70	22.3
Casablanca_Platform	1.36	40.72	35	1	999	0.15	0.18	0.03	0.02	0.05	0.06	0.05	0.88	62.4
KEMPTEN_UAS	10.31	47.72	718	0	359	0.11	0.19	0.08	0.08	0.00	0.13	0.10	0.16	30.1
Reykjavik	-21.90	64.13	51	1	999	0.07	0.12	0.05	0.05	0.00	0.07	0.05	0.37	50.1
NEON_CLBJ	-97.57	33.40	259	0	999	0.11	0.13	0.01	0.02	-0.00	0.10	0.10	0.34	40.2
NEON_UKFS	-95.19	39.04	321	0	484	0.19	0.18	-0.00	-0.03	0.16	0.10	0.10	0.92	36.8
Pickle_Lake	-90.22	51.45	393	0	2	0.02	0.08	0.06	0.06	0.00	0.06	0.03	-	50.0
Grizzly_Bay	-122.06	38.11	4	0	927	0.07	0.15	0.07	0.07	0.00	0.12	0.09	0.17	37.5
Pinehurst_Idaho	-116.24	47.54	680	0	481	0.10	0.18	0.08	0.08	0.13	0.12	0.09	0.73	33.5
Yekaterinburg	59.54	57.04	300	0	150	0.13	0.21	0.08	0.13	-0.17	0.18	0.16	-0.25	23.3
Gustav_Dalen_Tower	17.47	58.59	25	1	999	0.11	0.17	0.06	0.06	0.06	0.08	0.05	0.79	26.1
Vienna_BOKU	16.33	48.24	266	0	772	0.14	0.23	0.09	0.09	0.09	0.15	0.12	0.52	32.0
UMBC	-76.71	39.25	79	0	37	0.18	0.36	0.18	0.13	0.23	0.19	0.07	0.96	2.7
NEON_UNDE	-89.54	46.23	520	0	589	0.07	0.14	0.07	0.07	0.00	0.11	0.08	0.34	43.0
South_Greenbay	-87.95	44.60	175	0	372	0.11	0.13	0.01	0.01	0.00	0.08	0.08	0.15	44.4
Rexburg_Idaho	-111.78	43.82	1501	0	212	0.07	0.21	0.14	0.14	0.00	0.19	0.13	-0.03	18.9
Noto	137.14	37.33	200	1	789	0.16	0.21	0.05	0.05	0.03	0.08	0.06	0.80	40.2
Maun_Tower	23.55	-19.90	951	0	999	0.14	0.15	0.01	0.00	0.02	0.06	0.06	0.90	69.6
Irbe_Lighthouse	21.72	57.75	38	1	999	0.12	0.20	0.08	0.08	0.09	0.10	0.05	0.76	14.4
Warsaw_UW	20.98	52.21	117	0	536	0.15	0.20	0.05	0.07	-0.07	0.13	0.12	0.51	33.2
Dakar_Belair	-17.43	14.70	15	1	965	0.39	0.45	0.06	0.04	0.06	0.10	0.08	0.93	39.3
Huancayo-IGP	-75.32	-12.04	3313	0	249	0.06	0.10	0.04	0.03	0.19	0.08	0.07	0.74	58.6
Kellogg_LTER	-85.37	42.41	293	0	165	0.11	0.08	-0.03	-0.03	0.00	0.06	0.05	0.01	40.0
UAHuntsville	-86.64	34.73	223	0	66	0.31	0.42	0.11	0.00	0.11	0.14	0.09	0.00	15.2
Bo-za_Creek	-148.32	64.74	353	0	624	0.16	0.24	0.08	0.09	0.06	0.18	0.16	0.54	34.6
NEON_HEAL	-149.21	63.88	678	0	220	0.13	0.24	0.11	0.11	0.13	0.17	0.13	0.65	19.1
SP-EACH	-46.50	-23.48	754	0	17	0.11	0.11	-0.00	-0.00	0.00	0.04	0.04	0.00	70.6
Narsarsuaq	-45.42	61.16	75	0	10	0.06	0.19	0.13	0.13	0.00	0.15	0.08	0.86	0.0
NEON_NOGP	-100.92	46.77	578	0	60	0.11	0.28	0.18	0.18	0.00	0.23	0.14	-0.04	15.0
Zvenigorod	36.78	55.69	200	0	535	0.12	0.18	0.06	0.07	0.03	0.15	0.14	0.64	28.6
NEON_BONA	-147.50	65.15	263	0	494	0.15	0.20	0.05	0.08	0.00	0.12	0.11	0.45	36.0
NEON_DEJU	-145.75	63.88	529	0	16	0.06	0.27	0.21	0.21	0.00	0.26	0.15	-0.04	18.8
NEON_Harvard	-72.17	42.54	348	0	332	0.07	0.13	0.06	0.06	0.00	0.12	0.10	0.18	48.8
Red_Mountain_Pass	-107.71	37.91	3376	0	242	0.04	0.20	0.16	0.16	0.00	0.19	0.11	0.09	11.2
OPAL	-85.94	79.99	5	0	173	0.04	0.19	0.15	0.15	0.00	0.17	0.08	-0.34	10.4

PEARL	-86.42	80.05	615	0	20	0.07	0.18	0.11	0.11	0.00	0.16	0.12	-0.67	45.0
Kluane_Lake	-138.41	61.03	773	0	257	0.14	0.25	0.12	0.12	0.07	0.17	0.13	0.68	20.2
Tomsk	85.05	56.48	174	0	453	0.17	0.20	0.03	0.09	-0.15	0.15	0.14	-0.44	19.6
Ji_Parana_SE	-61.85	-10.93	218	0	298	0.04	0.61	0.57	0.57	0.00	0.72	0.44	-0.90	30.9
NEON_Bartlett	-71.29	44.06	273	0	165	0.05	0.07	0.03	0.03	0.00	0.05	0.04	0.66	76.4
NEON_PUUM	-155.32	19.55	1685	1	139	0.02	0.13	0.11	0.11	0.00	0.13	0.07	-0.31	2.2
Yellowknife_Aurora	-114.38	62.45	220	0	28	0.07	0.16	0.09	0.09	0.00	0.11	0.07	0.00	32.1
Modena	10.95	44.63	56	0	536	0.23	0.19	-0.04	-0.03	-0.05	0.11	0.10	0.55	27.4
NEON_BARR	-156.62	71.28	6	1	457	0.08	0.14	0.07	0.07	0.00	0.09	0.05	0.53	28.7
Chiba_University	140.10	35.62	60	0	284	0.17	0.26	0.09	0.10	0.06	0.18	0.15	0.58	26.8
Medellin	-75.58	6.26	1471	0	108	0.07	0.15	0.08	0.08	0.06	0.10	0.07	0.73	35.2
Helsinki_Lighthouse	24.93	59.95	20	0	867	0.09	0.16	0.06	0.06	0.06	0.08	0.04	0.82	28.6
NEON_TOOL	-149.37	68.66	843	0	171	0.24	0.28	0.04	0.03	0.07	0.17	0.16	0.78	42.7
Palgrunden	13.15	58.76	49	0	124	0.15	0.23	0.08	0.11	0.06	0.12	0.09	0.54	25.8
Caillouel_COBIACC	3.13	49.62	53	0	213	0.21	0.34	0.13	0.11	0.16	0.15	0.07	0.72	5.2
EastMalling_MO	0.44	51.29	33	0	14	0.24	0.42	0.17	0.00	0.17	0.19	0.07	-0.00	0.0
Cliff_Creek_1	-114.84	45.11	1351	0	176	0.07	0.14	0.06	0.06	0.00	0.10	0.07	0.05	46.0
Cliff_Creek_2	-114.84	45.12	1552	0	176	0.07	0.14	0.07	0.07	0.00	0.10	0.07	0.15	40.3
Cliff_Creek_3	-114.84	45.12	1727	0	232	0.07	0.17	0.10	0.10	0.00	0.14	0.10	0.35	30.6
Cliff_Creek_4	-114.84	45.12	2024	0	229	0.07	0.18	0.11	0.11	0.00	0.15	0.10	0.42	32.8
Cliff_Creek_5	-114.85	45.13	2068	0	190	0.07	0.18	0.11	0.11	0.00	0.16	0.11	0.18	26.8
Hyytiala	24.30	61.85	191	0	99	0.04	0.11	0.07	0.07	0.00	0.09	0.05	-0.31	13.1
Eforie	28.63	44.08	40	0	354	0.11	0.21	0.09	0.09	0.00	0.11	0.06	0.60	16.7
Section-7_Platform	29.45	44.55	30	1	999	0.14	0.22	0.07	0.07	0.11	0.09	0.06	0.85	20.0
Resolute_Bay	-94.97	74.71	35	0	202	0.08	0.12	0.03	0.03	0.00	0.04	0.02	0.60	60.4
Cliff_Creek_6	-114.85	45.14	2232	0	167	0.06	0.18	0.12	0.12	0.00	0.15	0.10	0.50	21.0
McCall_Dragon_3	-116.29	45.04	1179	0	75	0.08	0.16	0.08	0.08	0.00	0.10	0.07	0.00	28.0
McCall_Dragon_4	-115.91	45.28	1865	0	132	0.09	0.15	0.07	0.07	0.00	0.10	0.07	0.19	25.8
McCall_Dragon_5	-115.68	45.27	1774	0	119	0.07	0.15	0.08	0.08	0.00	0.10	0.07	0.13	28.6
McCall_Dragon_6	-116.03	45.41	1139	0	159	0.11	0.17	0.06	0.06	0.00	0.10	0.08	0.31	38.4
McCall_Dragon_7	-116.33	45.41	582	0	149	0.10	0.16	0.06	0.06	0.00	0.10	0.07	0.42	36.2
McCall_Dragon_8	-115.85	45.27	1785	0	128	0.08	0.15	0.07	0.07	0.00	0.10	0.07	0.19	27.3
Missoula_Health_Dpt	-114.00	46.88	985	0	68	0.11	0.15	0.04	0.04	0.00	0.09	0.08	0.10	38.2
Missoula_Midslope	-114.03	47.00	1613	0	136	0.07	0.14	0.07	0.07	0.00	0.10	0.07	0.19	31.6
Missoula_Waterworks	-113.99	46.88	1107	0	135	0.09	0.14	0.05	0.05	0.00	0.09	0.07	0.12	40.7
Maldives_Gan	73.15	-0.69	4	1	748	0.08	0.10	0.02	0.02	0.00	0.04	0.03	0.62	75.0
Lake_Erie	-83.19	41.83	173	0	44	0.20	0.21	0.01	0.23	-0.02	0.14	0.14	-0.24	13.6
Bozeman	-111.05	45.66	1507	0	77	0.06	0.17	0.10	0.10	0.00	0.14	0.10	-0.18	26.0
KAUST_Campus	39.10	22.30	11	0	434	0.36	0.46	0.09	0.07	0.10	0.14	0.11	0.79	19.6
NSPO_Taiwan	121.00	24.78	99	1	22	0.11	0.27	0.16	0.16	0.00	0.18	0.07	0.00	0.0
La_Jolla	-117.25	32.87	80	0	57	0.05	0.14	0.09	0.09	0.00	0.12	0.09	-0.00	33.3

Missoula_Pt_Six	-113.99	47.04	2420	0	40	0.06	0.14	0.08	0.08	0.00	0.11	0.07	-	45.0
Eilat	34.92	29.50	15	0	95	0.09	0.31	0.21	0.21	0.00	0.25	0.13	0.00	7.4
Amsterdam_Island	77.57	-37.80	49	1	101	0.13	0.13	0.01	0.01	0.00	0.04	0.04	-0.87	63.4

End of the document